AD-A067 230 ILLINOIS UNIV AT URBANA-CHAMPAIGN ELECTROMAGNETICS LAB F/G 20/14
EXCITATION OF MODAL FIELDS IN PARALLEL-PLATE TRANSMISSION LINE.(U)
FEB 79 R MITTRA, S W LEE AFOSR-76-3066

UNCLASSIFIED UIEM-79-4 AFOSR-TR-79-0430 NL

1 OF 2
AD A067230

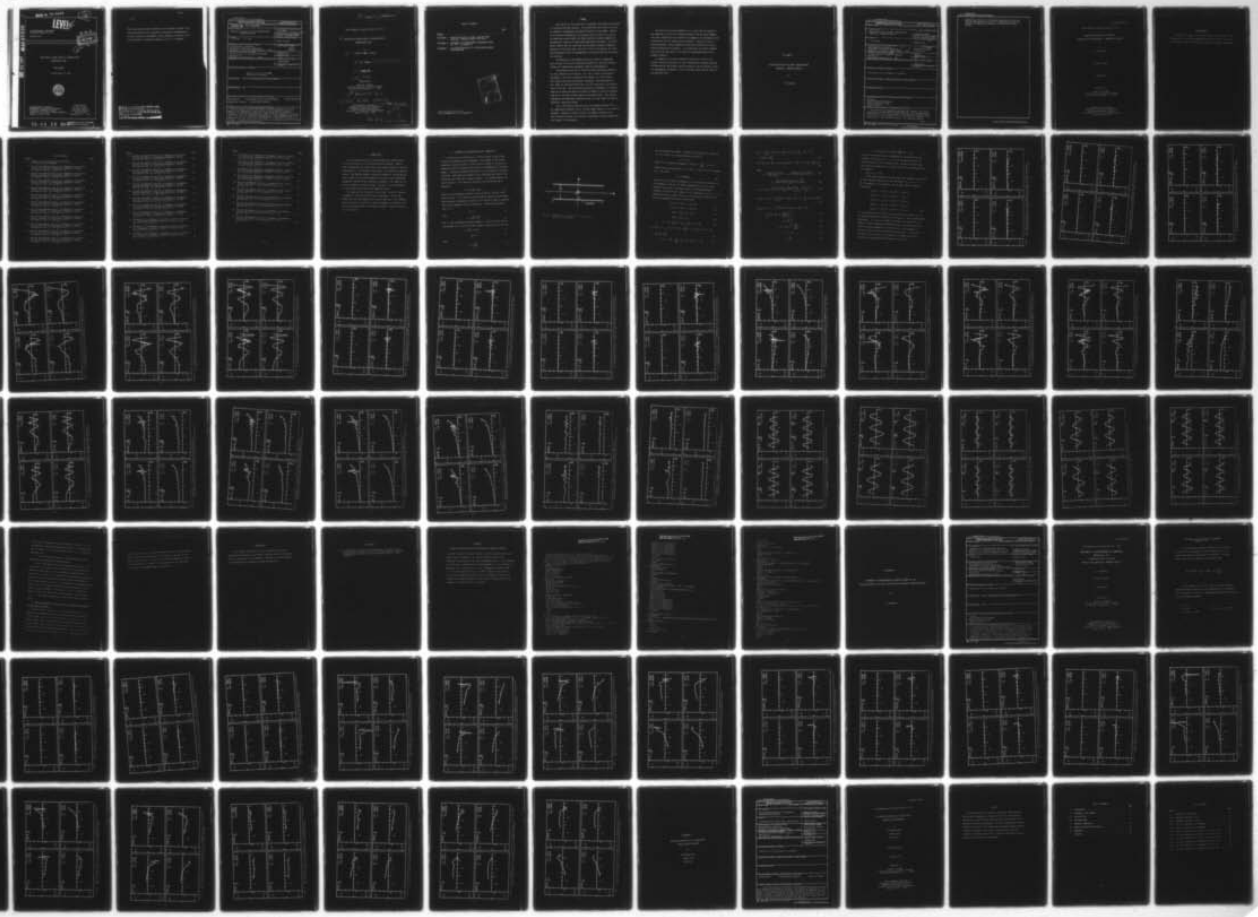

AFOSR-TR- 79-0430

LEVEL II

DDC FILE COPY, AD A067230

ELECTROMAGNETICS LABORATORY
SCIENTIFIC REPORT NO. 79-4

February 1979

DDC
RECEIVED
APR 12 1979
C

EXCITATION OF MODAL FIELDS IN PARALLEL-PLATE TRANSMISSION LINE

FINAL REPORT

R. Mittra and S. W. Lee

ELECTROMAGNETICS LABORATORY
DEPARTMENT OF ELECTRICAL ENGINEERING
ENGINEERING EXPERIMENT STATION
UNIVERSITY OF ILLINOIS AT URBANA-CHAMPAIGN
URBANA, ILLINOIS 61801

Supported by
Grant No. 76-3066
Air Force Office
of Scientific Research
Bolling AFB
Washington, D.C. 20332

79 04 12 058

Approved for public release;
Distribution unlimited.

"The views and conclusions contained in this document are those of the author and should not be interpreted as necessarily representing the official policies or endorsements, either expressed or implied, of the Air Force Office of Scientific Research or the U. S. Government."

AIR FORCE OFFICE OF SCIENTIFIC RESEARCH (AFSC)
NOTICE OF TRANSMITTAL TO DDC
This technical report has been reviewed and is approved for public release IAW AFR 190-12 (7b).
Distribution is unlimited.
A. D. BLOSE
Technical Information Officer

UNCLASSIFIED

SECURITY CLASSIFICATION OF THIS PAGE (When Data Entered)

REPORT DOCUMENTATION PAGE	READ INSTRUCTIONS BEFORE COMPLETING FORM
1. REPORT NUMBER: AFOSR-TR- 79-0430	2. GOVT ACCESSION NO. / 3. RECIPIENT'S CATALOG NUMBER
4. TITLE (and Subtitle): EXCITATION OF MODAL FIELDS IN PARALLEL-PLATE TRANSMISSION LINE	5. TYPE OF REPORT & PERIOD COVERED: Final Report 30 June 1976 - 31 December 1978
	6. PERFORMING ORG. REPORT NUMBER: EM 79-4; UIUL-ENG-79-2543
7. AUTHOR(s): R. Mittra S. W. Lee	8. CONTRACT OR GRANT NUMBER(s): AFOSR 76-3066
9. PERFORMING ORGANIZATION NAME AND ADDRESS: Electromagnetics Laboratory, Department of Electrical Engineering, University of Illinois, Urbana, Illinois 61801	10. PROGRAM ELEMENT, PROJECT, TASK AREA & WORK UNIT NUMBERS: 2301/A3, 61102F
11. CONTROLLING OFFICE NAME AND ADDRESS: Air Force Office of Scientific Research/NP, Building 410, Bolling AFB, Washington, D.C. 20332	12. REPORT DATE: February 1979 / 13. NUMBER OF PAGES: 133
14. MONITORING AGENCY NAME & ADDRESS(if different from Controlling Office)	15. SECURITY CLASS. (of this report): UNCLASSIFIED / 15a. DECLASSIFICATION/ DOWNGRADING SCHEDULE
16. DISTRIBUTION STATEMENT (of this Report): Approved for public release; distribution unlimited.	
17. DISTRIBUTION STATEMENT (of the abstract entered in Block 20, if different from Report)	
18. SUPPLEMENTARY NOTES	
19. KEY WORDS (Continue on reverse side if necessary and identify by block number): EMP Simulator; Finite-Width Parallel-Plate Waveguide; Source Excitation; Wiener-Hopf Technique; Moment Method Solution	

20. ABSTRACT (Continue on reverse side if necessary and identify by block number)

In this report we discuss the problem of source radiation in an open, parallel-plate waveguide of finite width. Such a structure is used as a simulator for testing EMP hardening of large systems such as aircrafts. A conventional approach to expanding the fields in an open waveguide of this type entails the use of the leaky-mode representation. Such a representation is an approximate one and, under certain situations, it is desirable to verify its accuracy. The solution derived in this report is a complete one and can be used to test the leaky mode representation.

DD FORM 1473

(14) UIEM-79-4, UILU-ENG-79-2543

Electromagnetics Laboratory Report No. 79-4

(6) EXCITATION OF MODAL FIELDS IN PARALLEL-PLATE TRANSMISSION LINE

by

(10) R. Mittra and S. W. Lee

(9) Final Report, 30 Jun 76-31 Dec 78,

(11) February 1979

(12) 32 p.

Supported by

Grant No. 76-3066
Air Force Office of Scientific Research
Bolling AFB, Washington, D.C. 20332

(15) AFOSR-76-3066

(16) 2301 (17) A3 (18) AFOSR

(19) TR-79-0430

Electromagnetics Laboratory
Department of Electrical Engineering
Engineering Experiment Station
University of Illinois at Urbana-Champaign
Urbana, Illinois 61801

408108

DD

79 04 12 058

TABLE OF CONTENTS

Page

SUMMARY 1

ATTACHMENT A: SOURCE EXCITATION OF AN OPEN, PARALLEL-PLATE WAVEGUIDE. NUMERICAL RESULTS (EM 78-4)*

ATTACHMENT B: SUPPLEMENT TO ELECTROMAGNETICS LABORATORY REPORT NO. 78-4 (Attachment A)

ATTACHMENT C: THE SOURCE EXCITATION OF A FINITE-WIDTH PARALLEL-PLATE WAVEGUIDE

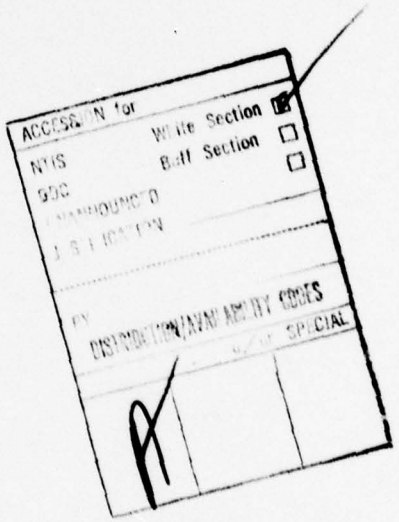

*Each ATTACHMENT has its own pagination.

SUMMARY

The objective of this grant was to investigate the problem of excitation of a parallel-plate EMP simulator. This problem has been studied in the past by a number of investigators including the authors of this report. However, in the previous investigations, the approach taken was based on the use of the leaky mode concept wherein the fields excited in an open waveguide are represented in terms of the leaky modes supported by the guide. It is well-known, however, that the leaky modes are not proper solutions of Maxwell's equations for the entire space, and that in order to be complete, the leaky mode representation must be supplemented by the contribution from the continuous spectrum.

The motivation of the present effort was to derive a numerically exact solution to the source excitation problem with a view to providing a standard for comparing the approximate leaky wave representation.

Two approaches were used to attack the source excitation problem in the open, parallel-plate waveguide. The first of these is described in Attachments A and B and is based upon the solution of a finite Wiener-Hopf equation using function-theoretic techniques. The above method is most useful for wide plate widths and is in fact restricted in its application to this case. The second method described in Attachment C is entirely numerical in nature and employs the method of moments to solve the integral equation for the plate current induced by the given source. This approach complements the Wiener-Hopf formulation since it is most useful for small to moderately large plate widths.

All of the results given here are for an assumed variation $e^{i\beta z}$ in the longitudinal direction, with β, the wave number along z, as the important parameter. Though not carried out here, the complete solution to the field excitation problem can be derived by performing a spectral integration with respect to the variable β.

The choice of the other parameters, e.g., plate width and separation was suggested by the Air Force Weapons Laboratory and the LuTech Company. The latter organization was collaboratively engaged in an experimental study on simulators with the research group at Harvard. During the course of these experiments, certain anomalous behaviors were observed for which no obvious explanation was available. It is hoped that the results presented here would shed some light on the problem of understanding some of the anomalous bahavior.

To summarize, this report presents the results of a study of the problem of source excitation of an open, parallel-plate waveguide modeling the EMP simulator and presents extensive numerical results derived by using two complementary approaches -- one for the small width, and the other for the wide-plate case.

Attachment A

SOURCE EXCITATION OF AN OPEN, PARALLEL-PLATE WAVEGUIDE. NUMERICAL RESULTS

by

V. Krichevsky

UNCLASSIFIED

SECURITY CLASSIFICATION OF THIS PAGE (When Data Entered)

REPORT DOCUMENTATION PAGE

READ INSTRUCTIONS BEFORE COMPLETING FORM

1. REPORT NUMBER

2. GOVT ACCESSION NO.

3. RECIPIENT'S CATALOG NUMBER

4. TITLE (and Subtitle)

SOURCE EXCITATION OF AN OPEN, PARALLEL-PLATE WAVEGUIDE. NUMERICAL RESULTS

5. TYPE OF REPORT & PERIOD COVERED

Scientific Report

6. PERFORMING ORG. REPORT NUMBER

EM 78-4; UILU-ENG-78-2546

7. AUTHOR(s)

V. Krichevsky

8. CONTRACT OR GRANT NUMBER(s)

AFOSR 76-3066

9. PERFORMING ORGANIZATION NAME AND ADDRESS

Electromagnetics Laboratory
Department of Electrical Engineering
University of Illinois, Urbana, Illinois 61801

10. PROGRAM ELEMENT, PROJECT, TASK AREA & WORK UNIT NUMBERS

Project-Task 2301/A3
P. R. No. N/A

11. CONTROLLING OFFICE NAME AND ADDRESS

Air Force Office of Scientific Research
Building 410
Bolling AFB, Washington, DC 20332

12. REPORT DATE

August 1978

13. NUMBER OF PAGES

56

14. MONITORING AGENCY NAME & ADDRESS (if different from Controlling Office)

15. SECURITY CLASS. (of this report)

Unclassified

15a. DECLASSIFICATION DOWNGRADING SCHEDULE

16. DISTRIBUTION STATEMENT (of this Report)

Distribution of this document is unlimited.

17. DISTRIBUTION STATEMENT (of the abstract entered in Block 20, if different from Report)

18. SUPPLEMENTARY NOTES

19. KEY WORDS (Continue on reverse side if necessary and identify by block number)

EM Field
Open Parallel-Plate Waveguide
Source Excitation Problem
Numerical Results

20. ABSTRACT (Continue on reverse side if necessary and identify by block number)

In this work we investigate numerically the problem of the source excitation of an open, parallel-plate waveguide. The following assumptions are made for the source current 1) the current is oriented in the y-direction, 2) it is located at $x = 0$, 3) there is no variation in the y-direction, 4) and the current has exp ($i\beta z$) behavior along the

(over)

DD FORM 1 JAN 73 1473 EDITION OF 1 NOV 65 IS OBSOLETE

UNCLASSIFIED

SECURITY CLASSIFICATION OF THIS PAGE (When Data Entered)

longitudinal z-direction. We provide graphical output for the EM-field components as functions of a longitudinal propagation constant and transverse coordinates and then discuss these results.

UILU-ENG-78-2546

Electromagnetics Laboratory Report No. 78-4

SOURCE EXCITATION OF AN OPEN, PARALLEL-PLATE WAVEGUIDE. NUMERICAL RESULTS

by

V. Krichevsky

Scientific Report

August 1978

Supported by

Grant No. 76-3066B
Air Force Office of Scientific Research
Bolling AFB, Washington, D.C. 20332

Electromagnetics Laboratory
Department of Electrical Engineering
Engineering Experiment Station
University of Illinois at Urbana-Champaign
Urbana, Illinois 61801

ACKNOWLEDGEMENT

The author is thankful to Professor R. Mittra for discussion of the problem and for the helpful suggestions during the course of this work. The financial support of AFOSR Grant-76-3066B is gratefully acknowledged.

ABSTRACT

In this work we investigate numerically the problem of the source excitation of an open, parallel-plate waveguide. The following assumptions are made for the source current 1) the current is oriented in the y-direction, 2) it is located at $x = 0$, 3) there is no variation in the y-direction, 4) and the current has $\exp(i\beta z)$ behavior along the longitudinal z-direction. We provide graphical output for the EM-field components as functions of a longitudinal propagation constant and transverse coordinates and then discuss these results.

TABLE OF CONTENTS

		Page
I.	INTRODUCTION	1
II.	STATEMENT OF THE PROBLEM AND BASIC FORMULATION	2
III.	NUMERICAL STUDY OF THE PROBLEM	39
	A. Field Components as Functions of a Longitudinal Propagation Constant	39
	B. Field Components as Functions of Transverse Coordinates. .	40
IV.	CONCLUSION	42
V.	REFERENCES	43
VI.	APPENDIX A (COMPUTER PROGRAM)	44

LIST OF FIGURES

Figure		Page
1.	Geometry of the problem of source excitation of a parallel-plate waveguide	3
2.	The real and imaginary parts of an x-component of the electric field as functions of a longitudinal propagation constant for points of view: $\frac{X}{L} = 0.1$; $\frac{Y}{H} = 0.0, 0.5$.	7
3.	The real and imaginary parts of an x-component of the electric field as functions of a logitudinal propagation constant for points of view: $\frac{X}{L} = 0.4$; $\frac{Y}{H} = 0.0, 0.5$.	8
4.	The real and imaginary parts of an x-component of the electric field as functions of a longitudinal propagation constant for points of view: $\frac{X}{L} = 0.6$; $\frac{Y}{H} = 0.0, 0.5$.	9
5.	The real and imaginary parts of an x-component of the electric field as functions of a longitudinal propagation constant for points of view: $\frac{X}{L} = 0.9$; $\frac{Y}{H} = 0.0, 0.5$.	10
6.	The real and imaginary parts of a y-component of the electric field as functions of a longitudinal propagation constant for points of view: $\frac{X}{L} = 0.1$; $\frac{Y}{H} = 0.0, 0.5$.	11
7.	The real and imaginary parts of a y-component of the electric field as functions of a longitudinal propagation constant for points of view: $\frac{X}{L} = 0.4$; $\frac{Y}{H} = 0.0, 0.5$.	12
8.	The real and imaginary parts of a y-component of the electric field as functions of a longitudinal propagation constant for points of view: $\frac{X}{L} = 0.6$; $\frac{Y}{H} = 0.0, 0.5$.	13
9.	The real and imaginary parts of a y-component of the electric field as functions of a longitudinal propagation constant for points of view: $\frac{X}{L} = 0.9$; $\frac{Y}{H} = 0.0, 0.5$.	14
10.	The real and imaginary parts of a z-component of the electric field as functions of a longitudinal propagation constant for points of view: $\frac{X}{L} = 0.1$; $\frac{Y}{H} = 0.0, 0.5$.	15
11.	The real and imaginary parts of a z-component of the electric field as functions of a longitudinal propagation constant for points of view: $\frac{X}{L} = 0.4$; $\frac{Y}{H} = 0.0, 0.5$.	16
12.	The real and imaginary parts of a z-component of the electric field as functions of a longitudinal propagation constant for points of view: $\frac{X}{L} = 0.6$; $\frac{Y}{H} = 0.0, 0.5$.	17

Figure Page

13. The real and imaginary parts of a z-component of the electric field as functions of a longitudinal propagation constant for points of view: $\frac{x}{L} = 0.9$; $\frac{Y}{H} = 0.0, 0.5$. 18

14. The real and imaginary parts of an x-component of the magnetic field as functions of a longitudinal propagation constant for points of view: $\frac{x}{L} = 0.1$; $\frac{Y}{H} = 0.0, 0.5$. 19

15. The real and imaginary parts of an x-component of the magnetic field as functions of a longitudinal propagation constant for points of view: $\frac{x}{L} = 0.4$; $\frac{Y}{H} = 0.0, 0.5$. 20

16. The real and imaginary parts of an x-component of the magnetic field as functions of a longitudinal propagation constant for points of view: $\frac{x}{L} = 0.6$; $\frac{Y}{H} = 0.0, 0.5$. 21

17. The real and imaginary parts of an x-component of the magnetic field as functions of a longitudinal propagation constant for points of view: $\frac{x}{L} = 0.9$; $\frac{Y}{H} = 0.0, 0.5$. 22

18. The real and imaginary parts of a z-component of the magnetic field as functions of a longitudinal propagation constant for points of view: $\frac{x}{L} = 0.1$; $\frac{Y}{H} = 0.0, 0.5$. 23

19. The real and imaginary parts of a z-component of the magnetic field as functions of a longitudinal propagation constant for points of view: $\frac{x}{L} = 0.4$; $\frac{Y}{H} = 0.0, 0.5$. 24

20. The real and imaginary parts of a z-component of the magnetic field as functions of a longitudinal propagation constant for points of view: $\frac{x}{L} = 0.6$; $\frac{Y}{H} = 0.0, 0.5$. 25

21. The real and imaginary parts of a z-component of the magnetic field as functions of a longitudinal propagation constant for points of view: $\frac{x}{L} = 0.9$; $\frac{Y}{H} = 0.0, 0.5$. 26

22. The module of a y-component of the electric field as a function of a longitudinal propagation constant for points of view: $\frac{x}{L} = 0.1, 0.4$; $\frac{Y}{H} = 0.0, 0.5$. 27

23. The module of a y-component of the electric field as a function of a longitudinal propagation constant for points of view: $\frac{x}{L} = 0.6, 0.9$; $\frac{Y}{H} = 0.0, 0.5$. 28

24. The module of an x-component of the magnetic field as a function of a longitudinal propagation constant for points of view: $\frac{x}{L} = 0.1, 0.4$; $\frac{Y}{H} = 0.0, 0.5$. 29

Figure Page

24. The module of an x-component of the magnetic field as a function of a longitudinal propagation constant for points of view: $\frac{X}{L} = 0.1, 0.4$; $\frac{Y}{H} = 0.0, 0.5$. 29

25. The module of an x-component of the magnetic field as a function of a longitudinal propagation constant for points of view: $\frac{X}{L} = 0.6, 0.9$; $\frac{Y}{H} = 0.0, 0.5$. 30

26. The module of a z-component of the magnetic field as a function of a longitudinal propagation constant for points of view: $\frac{X}{L} = 0.1, 0.4$; $\frac{Y}{H} = 0.0, 0.5$. 31

27. The module of a z-component of the magnetic field as a function of a longitudinal propagation constant for points of view: $\frac{X}{L} = 0.6, 0.9$; $\frac{Y}{H} = 0.0, 0.5$. 32

28. The real and imaginary parts of a y-component of the electric field as functions of an x-coordinate for $\tilde{\beta} = 0.4$; $\frac{Y}{H} = 0.0, 0.5$. 33

29. The real and imaginary parts of a y-component of the electric field as functions of an x-coordinate for $\tilde{\beta} = 0.75$; $\frac{Y}{H} = 0.0, 0.5$. 34

30. The real and imaginary parts of an x-component of the magnetic field as functions of an x-coordinate for $\tilde{\beta} = 0.4$; $\frac{Y}{H} = 0.0, 0.5$. 35

31. The real and imaginary parts of an x-component of the magnetic field as functions of an x-coordinate for $\tilde{\beta} = 0.75$; $\frac{Y}{H} = 0.0, 0.5$. 36

32. The real and imaginary parts of a z-component of the magnetic field as functions of an x-coordinate for $\tilde{\beta} = 0.4$; $\frac{Y}{H} = 0.0, 0.5$. 37

33. The real and imaginary parts of a z-component of the magnetic field as functions of an x-coordinate for $\tilde{\beta} = 0.75$; $\frac{Y}{H} = 0.0, 0.5$. 38

I. INTRODUCTION

In the previous report [1], we derived analytical expressions for the source excitation of an open parallel-plate waveguide. However, these formulas were very complicated, and it became necessary to evaluate them numerically. The purpose of this report is to present the numerical results. The computer program contained in Appendix A was written and used to obtain the field distribution as a function of the longitudinal propagation constant and the transverse coordinates. The numerical outputs are presented in graphical forms. The Cyber 175 at the University of Illinois was used for all of the numerical studies.

The organization of the report is as follows: Section II contains a statement of the problem and the basic formulation. Section III presents the real and imaginary parts and the amplitude of the component field distribution as functions of several parameters in graphical form and a detailed discussion of the numerical results. Finally, Section IV is the conclusion.

II. STATEMENT OF THE PROBLEM AND BASIC FORMULATION

In this section the fields due to a vertical current located inside an open, finite waveguide are investigated. The geometry of the problem considered is shown in Figure 1. This structure consists of two perfectly conducting plates with separation 2H located in a homogeneous and isotropic medium. A Cartesian coordinate system with its y-axis normal to the plates is erected. Both plates are infinite in the z-direction and finite in the x-direction with length 2L as shown in Figure 1. All figures appear at the end of Chapter II. The current is oriented in the y-direction and is defined as

$$J = \hat{y}\delta(x) \exp(i\beta z) \quad , \tag{1}$$

where β is the propagation constant in the z-direction, and $\delta(x)$ is the delta function. In [1] using the vector-potential approach and the Wiener-Hopf technique, we obtained a solution for the problem at hand in a general form for any parameters with one restriction: kL must be much greater than 1, i.e.,

$$kL >> 1 \quad , \tag{2}$$

where

$$k = \sqrt{\omega^2 \varepsilon \mu - \beta^2} \tag{3}$$

and ε, μ are the homogeneous media parameters. Using the solution which was obtained in [1], we will perform a numerical calculation for the case:

$$W = \frac{H}{L} = 0.16670 \quad , \tag{4}$$

$$\frac{L}{\lambda_0} = 5 \quad , \tag{5}$$

where

$$\lambda_0 = \frac{2\pi}{\omega\sqrt{\varepsilon\mu}} \tag{6}$$

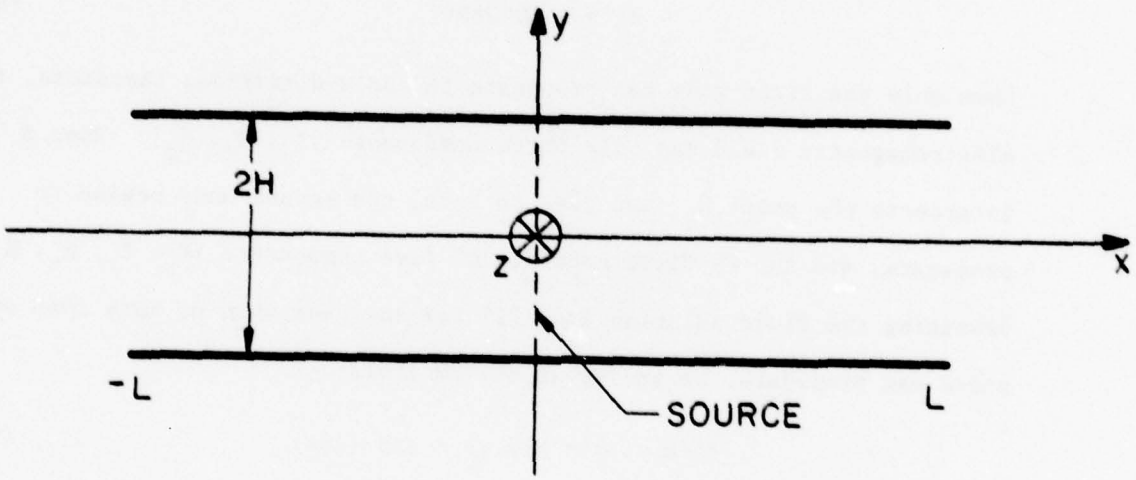

Figure 1. Geometry of the problem of source excitation of a parallel-plate waveguide.

is the free-space wave length. Because of the limitations of Equations (2), (3), and (5) we calculated numerical results for

$$0 < \tilde{\beta} < 0.93 \quad , \tag{7}$$

where $\tilde{\beta}$ is the normalized propagation constant $\tilde{\beta} = \frac{\beta}{\omega\sqrt{\varepsilon\mu}}$. It can be readily proved from Equations (3), (4), and (5) that if $\tilde{\beta}$ is in the region $[\tilde{\beta}_0, 0.93]$, where

$$\tilde{\beta}_0 = 0.80008997 \quad , \tag{8}$$

then only the first mode can propagate in the x-direction; therefore, the electromagnetic field has only three components $[E_y, H_x, H_z]$. When $\tilde{\beta}$ intersects the point $\tilde{\beta}_0$ and goes to zero, the second mode begins to propagate, and the EM-field consists of five components $[E_x, E_y, E_z, H_x, H_z]$. Rewriting the field solution from [1] for the case, when no more than two modes can propagate, we arrive at the EM field:

$$\bar{E}'(x,y,z) = \bar{E}(x,y) \cdot \exp(i\beta z) \tag{9}$$

$$\bar{H}'(x,y,z) = \bar{H}(x,y) \cdot \exp(i\beta z) \tag{10}$$

$$\bar{E}(x,y) = \hat{x}E_x + \hat{y}E_y + \hat{z}E_z \tag{11}$$

$$\bar{H}(x,y) = \hat{x}H_x + \hat{z}H_z \tag{12}$$

$$E_y = \sqrt{\frac{\mu}{\varepsilon}} \cdot \frac{0.1 \cdot \theta}{w} \cdot F_2 \sin\left(\frac{\pi}{H}y\right) \sin\left(\theta \cdot \frac{x}{L}\right) \tag{13}$$

$$E_y = \sqrt{\frac{\mu}{\varepsilon}} \cdot 10\pi \left(F_1 \cos\left(a \cdot \frac{x}{L}\right) + \left(1 - \frac{0.01}{w^2}\right) \cdot F_2 \cos\left(\frac{\pi}{H}y\right) \cos\left(\theta \cdot \frac{x}{L}\right) - \frac{1}{2a} \exp\left(ia\left|\frac{x}{L}\right|\right) \right) \tag{14}$$

$$E_z = -i\sqrt{\frac{\mu}{\varepsilon}} \cdot \frac{\beta}{\omega\sqrt{\varepsilon\mu}} \cdot \frac{\pi}{w} F_2 \sin\left(\pi\frac{y}{H}\right) \cos\left(\theta \cdot \frac{x}{L}\right) \quad , \tag{15}$$

$$H_x = -\mu \frac{\delta}{\omega\sqrt{\varepsilon\mu}} \cdot 10\pi \left\{ F_1 \cos\left(a\frac{x}{L}\right) + F_2 \cos\left(\pi \cdot \frac{y}{H}\right) \cdot \cos\left(\theta \cdot \frac{x}{L}\right) - \frac{1}{2a} \exp\left(ia\left|\frac{x}{L}\right|\right) \right\} , \quad (16)$$

$$H_z = i\mu a F_1 \sin\left(a\frac{x}{L}\right) + i\theta F_2 \cos\left(\pi\frac{y}{H}\right) \sin\left(\theta \cdot \frac{x}{L}\right) - 0.5 \cdot \exp\left(ia\left|\frac{x}{L}\right|\right) \cdot \frac{x}{|x|} , \quad (17)$$

where

$$F_1 = \frac{[M_{1+}(k)]^2 \exp(i2a)}{(1 + T_1)a} \cdot \left\{ 1 + \frac{2b[M_{1+}(\alpha_1)]^2 \exp\left(i2\frac{a}{b}\alpha_1\right)}{\theta} \right\} , \quad (18)$$

$$F_2 = \frac{2bM_{1+}(k)M_{1+}(\alpha_1) \exp\left[ia\left(1 + \frac{\alpha_1}{b}\right)\right]}{a \cdot Q} , \quad (19)$$

$$Q = (1 + T_1)\alpha_1 \cdot \left\{ \frac{[M_{1+}(\alpha_1)]^2 \exp\left(i2\frac{a}{b}\alpha_1\right)}{2\alpha_1} \left[\frac{4T_1 b}{1 + T_1} - \frac{(\alpha_1 + b)^2}{\alpha_1} \right] - 1 \right. , \quad (20)$$

$$M_{+1}(k) = (\alpha_1 + b) \cdot \exp\left\{ i\left[b\left(2 - C + \ln\left(\frac{2}{b}\right) + i\frac{\pi}{2}\right) - \frac{\pi}{2} + \sum_{n=2}^{\infty} \left(\frac{b}{n} - \arcsin\frac{b}{n}\right) \right] \right. , \quad (21)$$

$$M_{1+}(\alpha_1) = \sqrt{2} \cdot \alpha_1 \cdot \frac{1 - i\alpha_1}{b} \exp\left\{ i\left[\alpha_1\left(2 - C + \ln\left(\frac{2}{b}\right) + i\frac{\pi}{2}\right) + \sum_{n=2}^{\infty} \left(\frac{\alpha_1}{n} - \arcsin\frac{\alpha_1}{\sqrt{n^2 - 1}} \right) \right] \right\} , \quad (22)$$

$$\alpha_1 = \sqrt{b^2 - 1} , \quad (23)$$

$$a = kL = 10\pi \sqrt{1 - \left(\frac{\delta}{\omega\sqrt{\varepsilon\mu}}\right)^2} , \quad (24)$$

$$b = a \cdot \frac{W}{\pi} , \quad (25)$$

$$\theta = \frac{\pi\alpha_1}{W} , \quad (26)$$

$$T_1 = [M_{1+}(k)]^2 \exp(i2a)\left[1 + \frac{b\sqrt{\pi}}{\sqrt{a}} \exp\left(-i\frac{\pi}{4}\right)\right] \quad . \qquad (27)$$

It should be mentioned that we investigated the lossless medium case; therefore, in the region $\tilde{\beta}_0 < \tilde{\beta} < 0.93$, the propagation constant for the second mode has only an imaginary part. Because we neglect terms which decrease exponentially, our results for the above mentioned region of $\tilde{\beta}$ reduce to:

1) $E_x = E_z = 0$ and

2) more simple expressions for the other three components of the field.

We apply numerical analysis only over the regions $0 \leq y < H$, $0 < x < L$. For the remainder of the waveguide, one can obtain results using the correlations:

$$\begin{aligned}
E_x(x,y) &= -E_x(-x,y) \; ; \; E_x(x,y) = -E_x(x,-y) \\
E_y(x,y) &= E_y(-x,y) \; ; \; E_y(x,y) = E_y(x,-y) \\
E_z(x,y) &= E_z(-x,y) \; ; \; E_z(x,y) = -E_z(x,-y) \\
H_x(x,y) &= H_x(-x,y) \; ; \; H_x(x,y) = H_x(x,-y) \\
H_z(x,y) &= -H_z(-x,y) \; ; \; H_z(x,y) = H_z(x,-y) \quad . \qquad (28)
\end{aligned}$$

It is interesting to note that E_x, H_z are continuous and that E_y, E_z, H_x are discontinuous when $\tilde{\beta}$ crosses $\tilde{\beta}_0$ (or more exactly: they are exponentially decreasing). It is also of interest to determine the character of the behavior of the x-component of Poynting's vector. As one can easily see from the previous expressions for the EM fields, the x-component of Poynting's vector for the second mode is proportional to α_1 and goes to zero when $\tilde{\beta} \to \tilde{\beta}_0$. From this, one finds that the energy flow in the x-direction is continuous when $\tilde{\beta}$ intersects the point $\tilde{\beta}_0$.

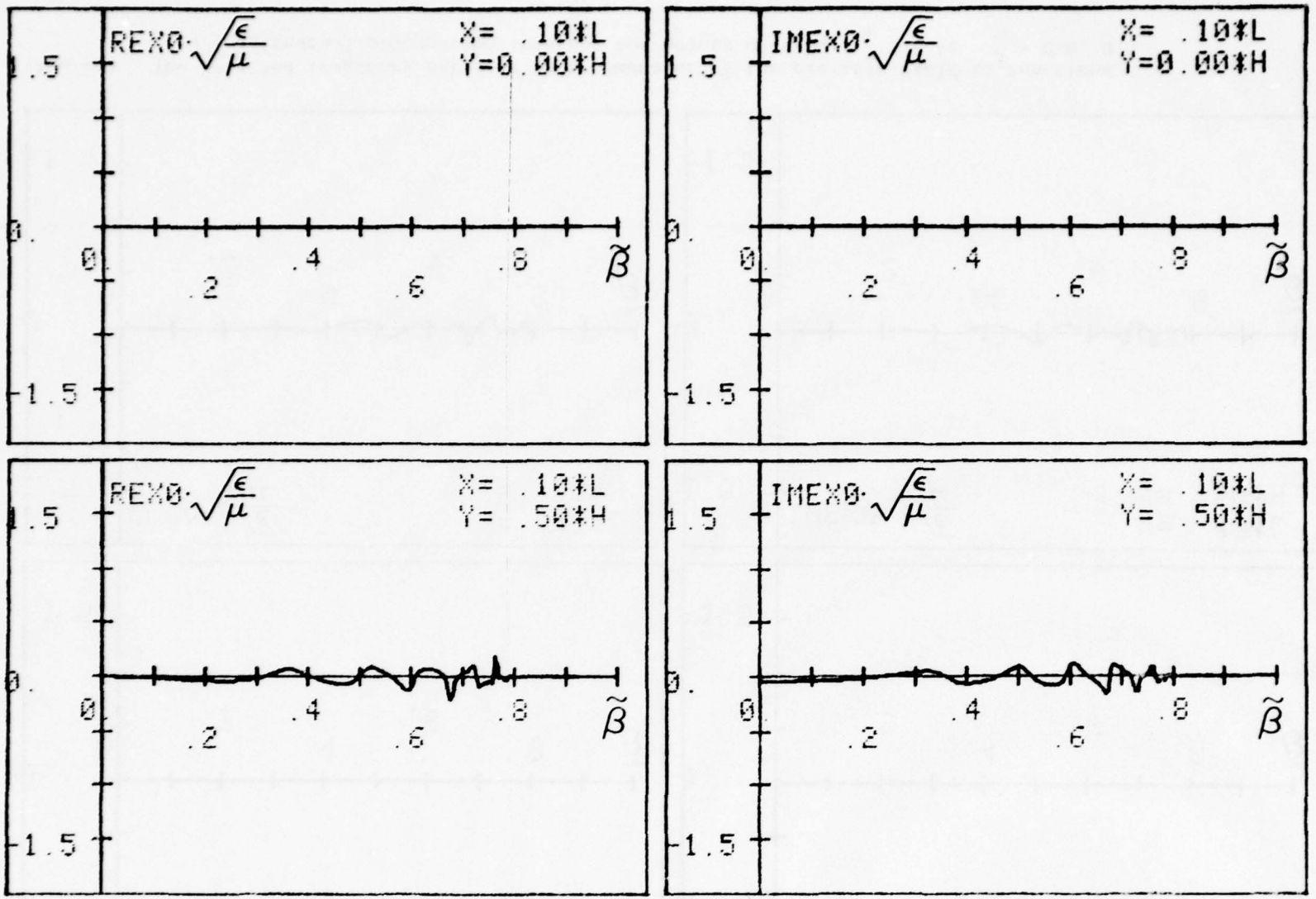

Figure 2. The real and imaginary parts of an x-component of the electric field as functions of a longitudinal propagation constant for points of view: $\frac{X}{L} = 0.1$; $\frac{Y}{H} = 0.0, 0.5$.

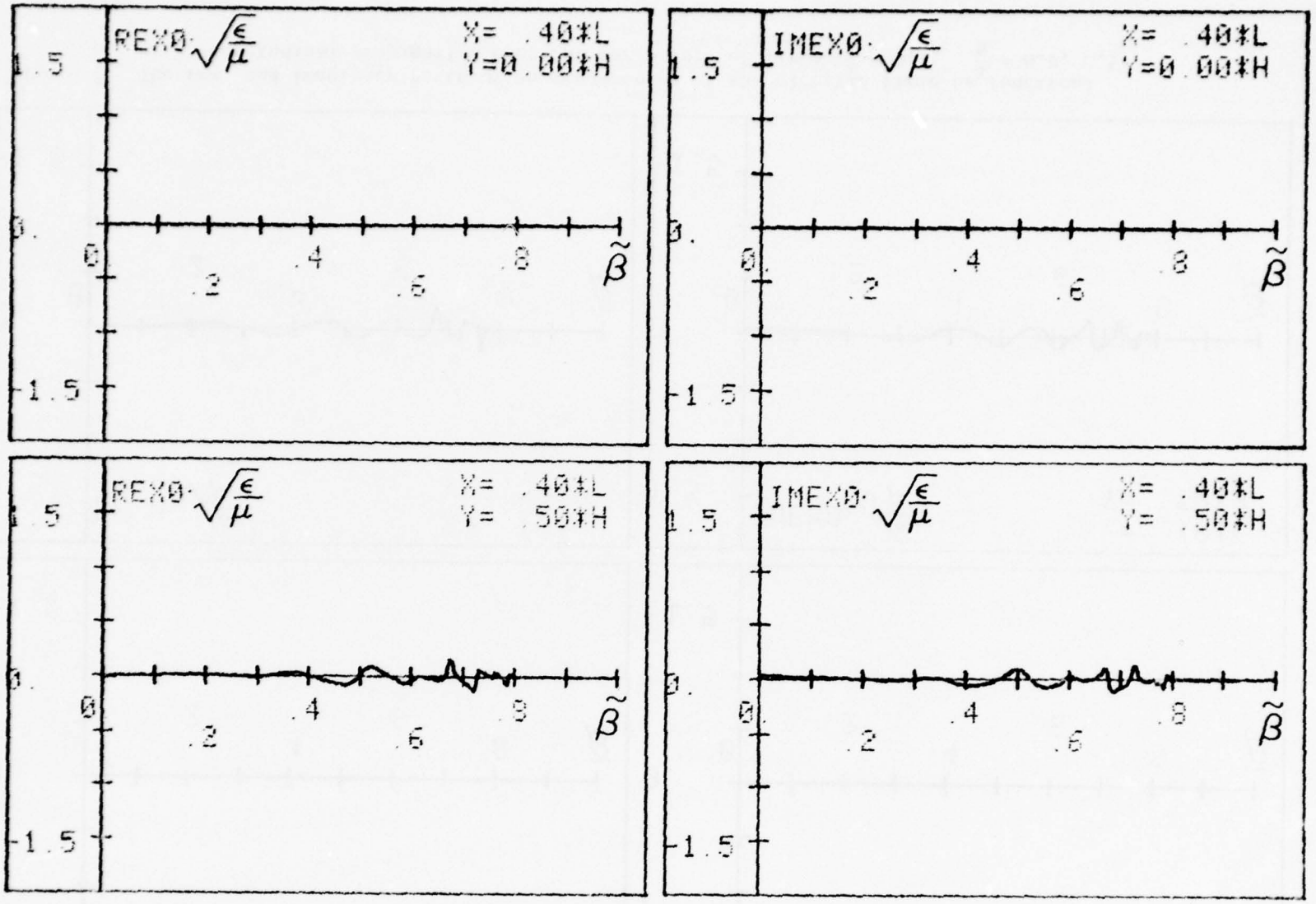

Figure 3. The real and imaginary parts of an x-component of the electric field as functions of a longitudinal propagation constant for points of view: $\frac{x}{L} = 0.4$; $\frac{y}{H} = 0.0, 0.5$.

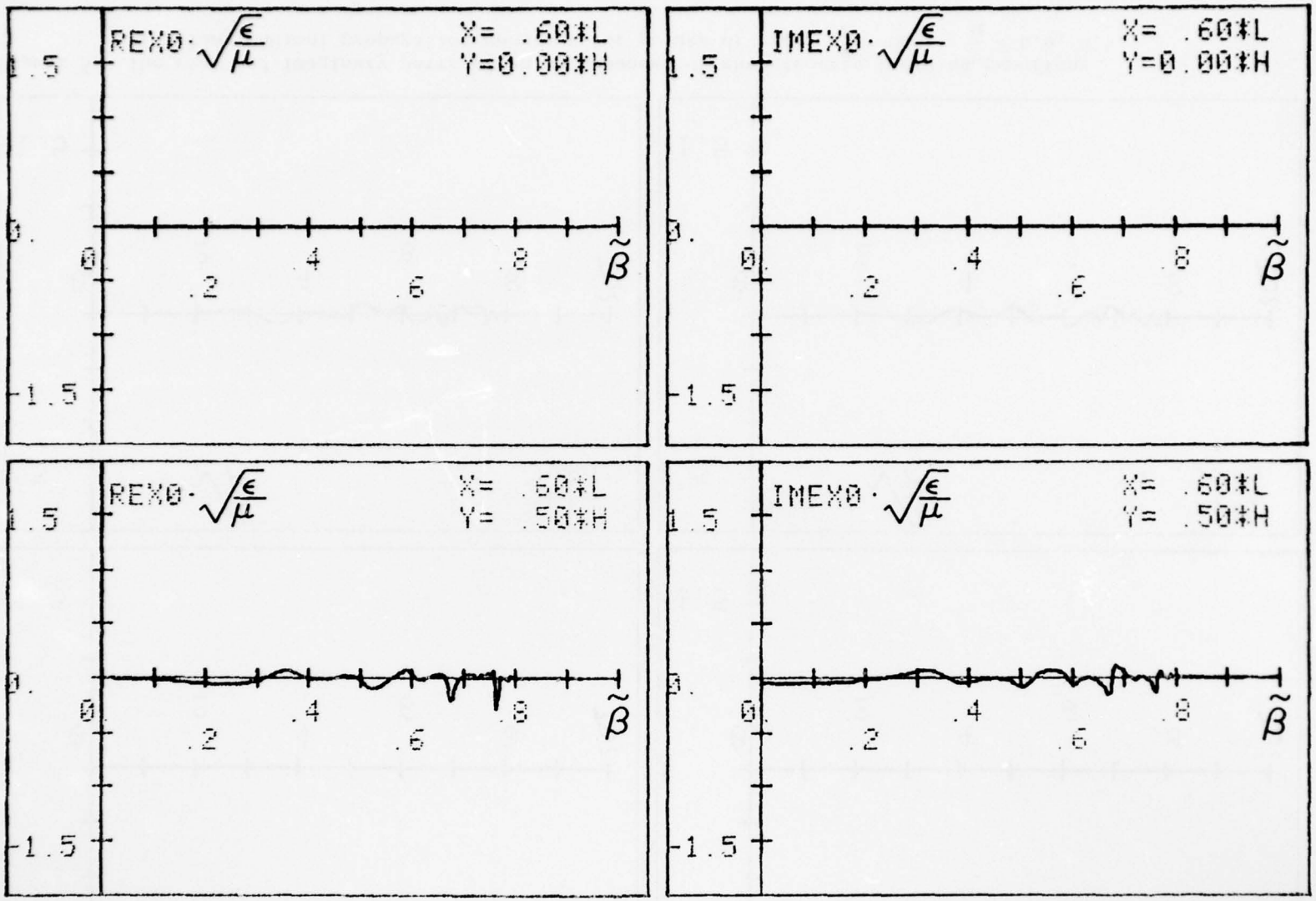

Figure 4. The real and imaginary parts of an x-component of the electric field as functions of a longitudinal propagation constant for points of view: $\frac{x}{L} = 0.6$; $\frac{Y}{H} = 0.0, 0.5$.

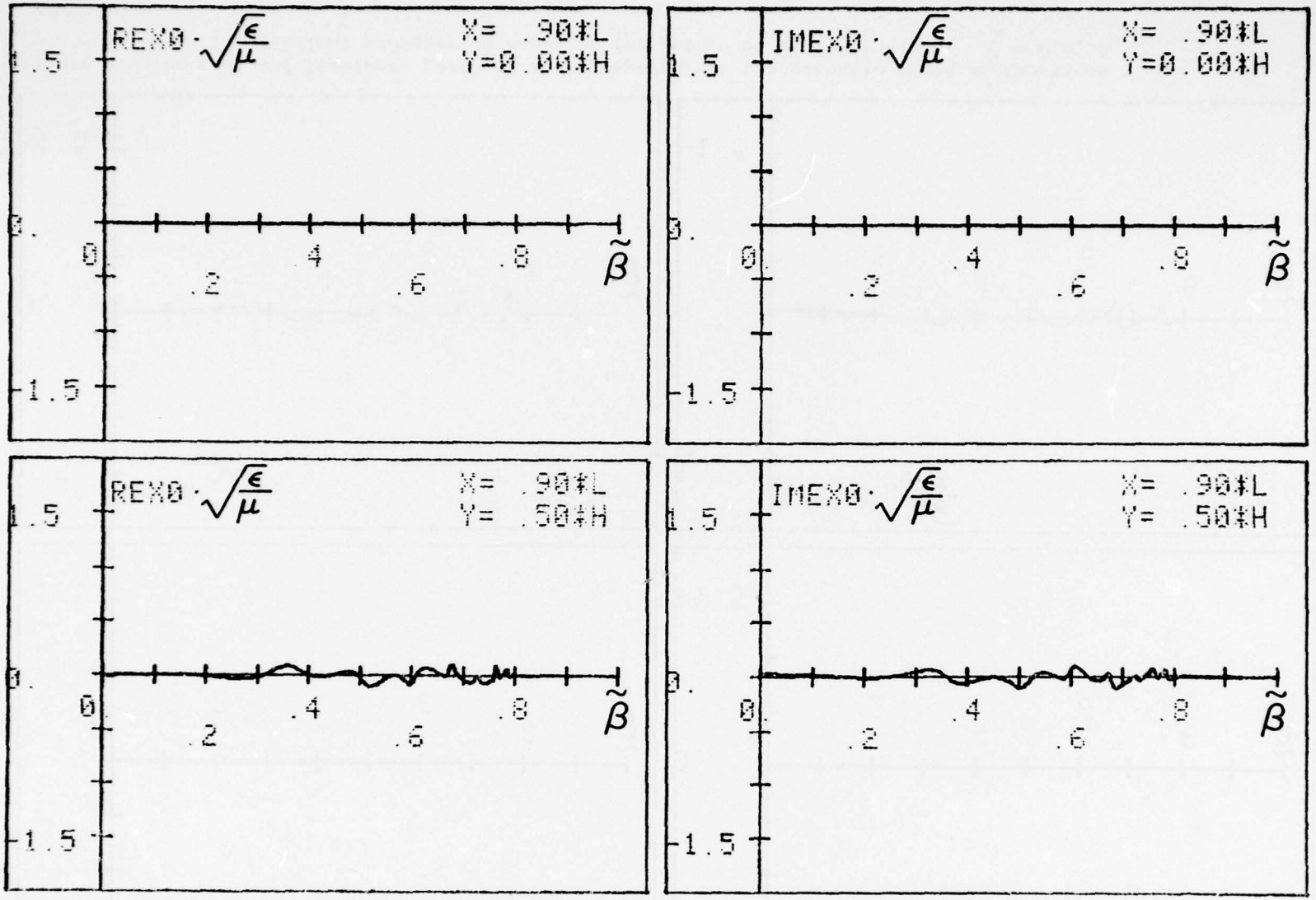

Figure 5. The real and imaginary parts of an x-component of the electric field as functions of a longitudinal propagation constant for points of view: $\frac{x}{L} = 0.9$; $\frac{Y}{H} = 0.0, 0.5$.

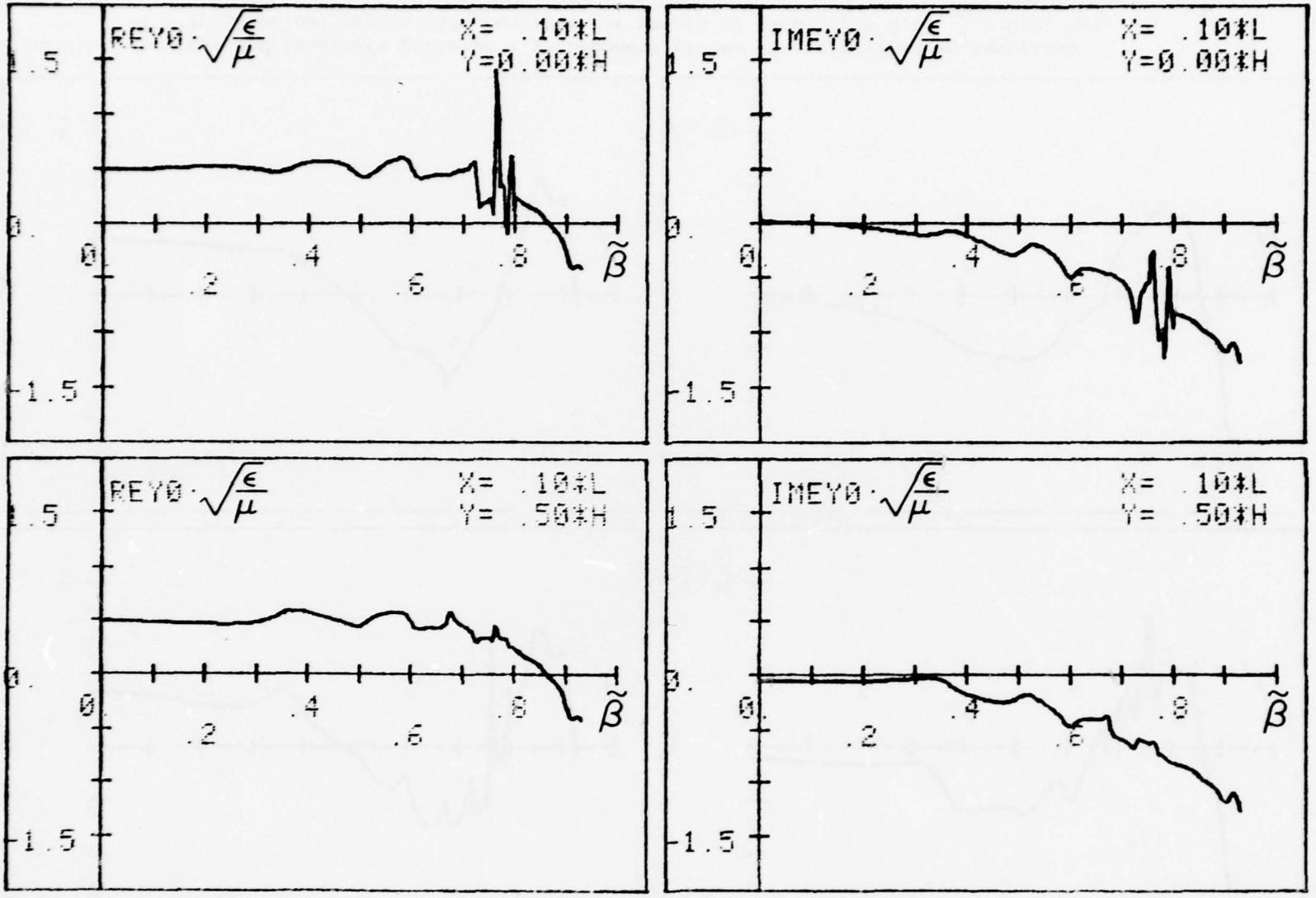

Figure 6. The real and imaginary parts of a y-component of the electric field as functions of a longitudinal propagation constant for points of view: $\frac{x}{L} = 0.1$; $\frac{y}{H} = 0.0, 0.5$.

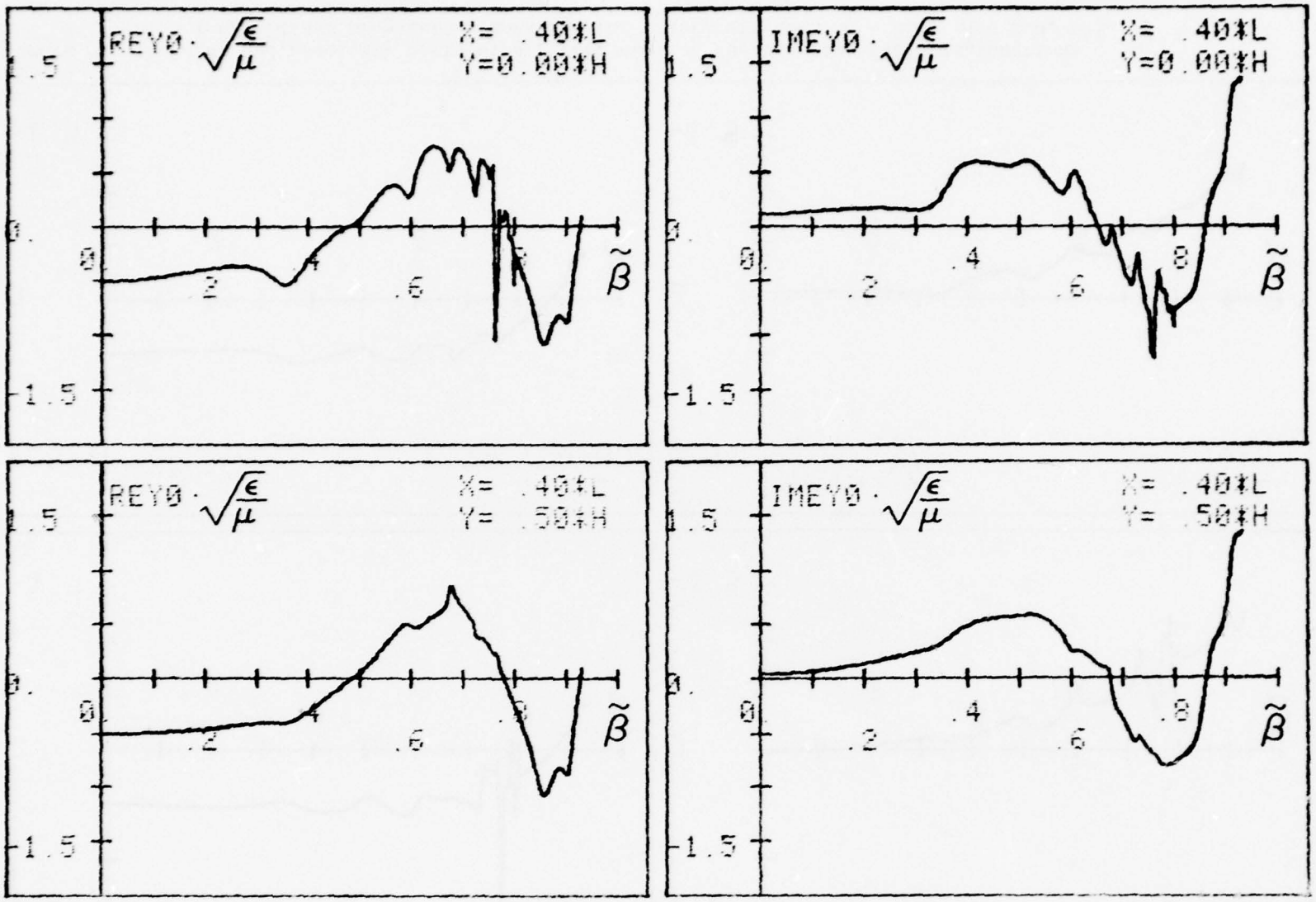

Figure 7. The real and imaginary parts of a y-component of the electric field as functions of a longitudinal propagation constant for points of view: $\frac{X}{L} = 0.4$; $\frac{Y}{H} = 0.0, 0.5$.

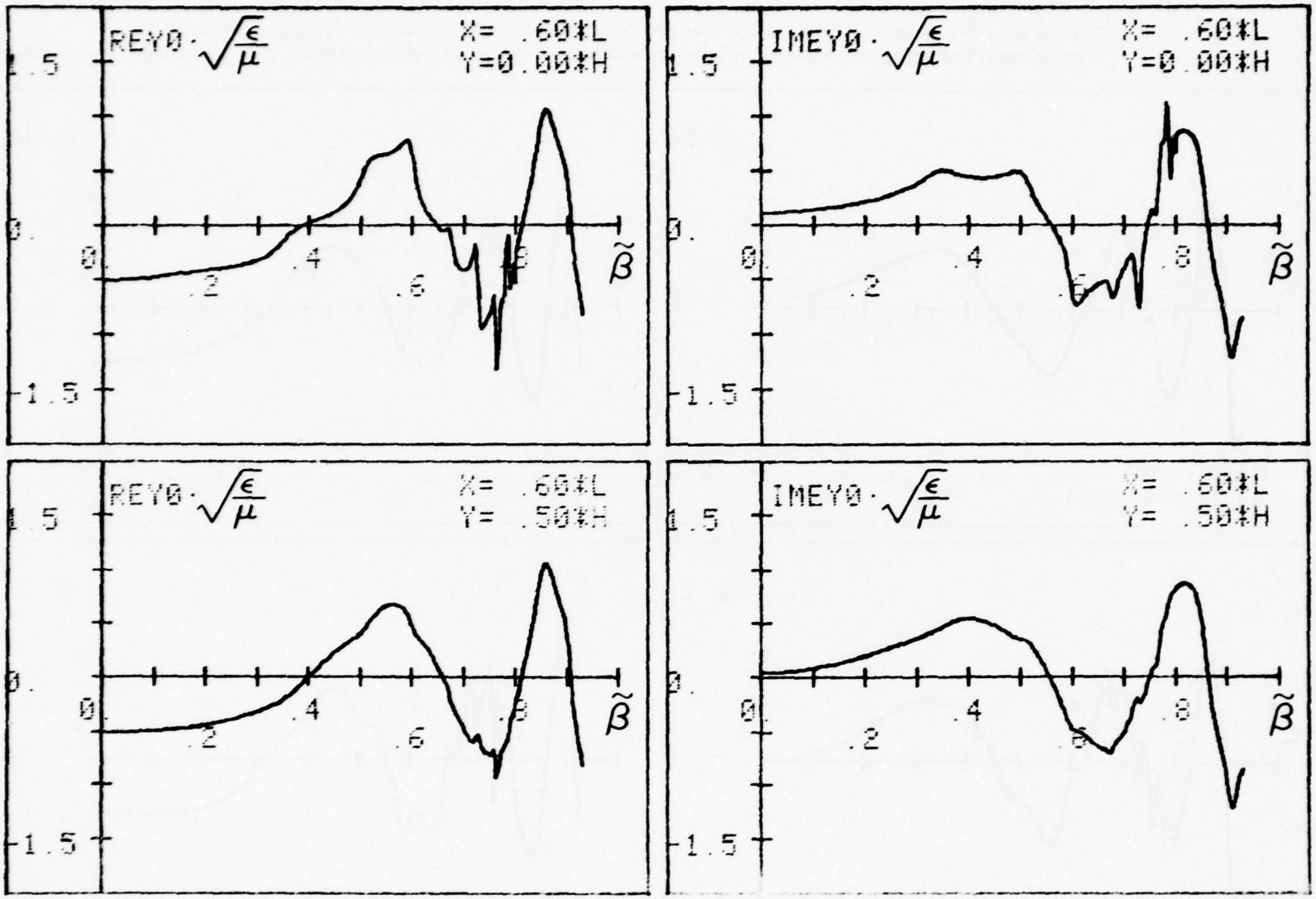

Figure 8. The real and imaginary parts of a y-component of the electric field as functions of a longitudinal propagation constant for points of view: $\frac{x}{L} = 0.6$; $\frac{Y}{H} = 0.0, 0.5$.

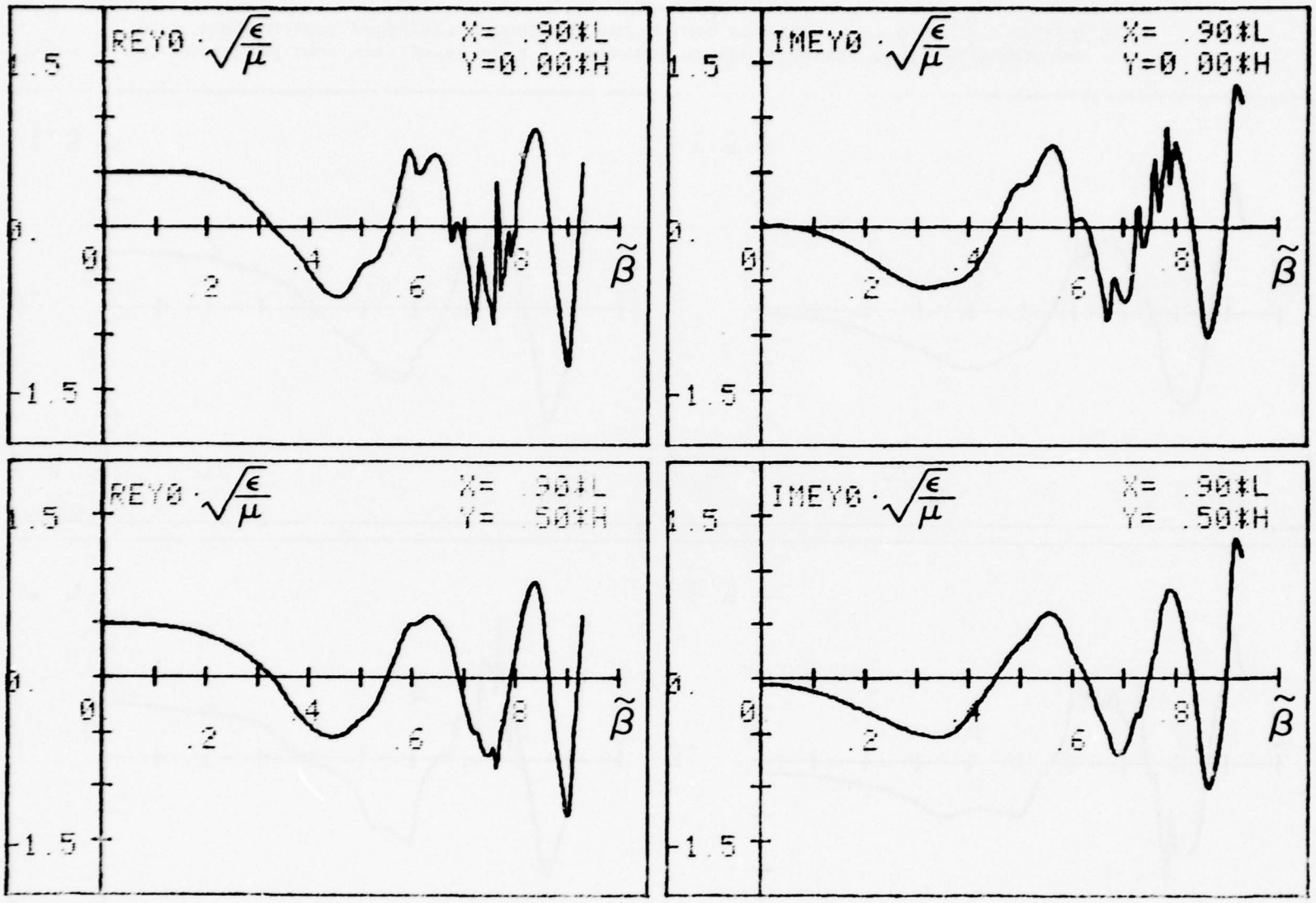

Figure 9. The real and imaginary parts of a y-component of the electric field as functions of a longitudinal propagation constant for points of view: $\frac{x}{L} = 0.9$; $\frac{Y}{H} = 0.0, 0.5$.

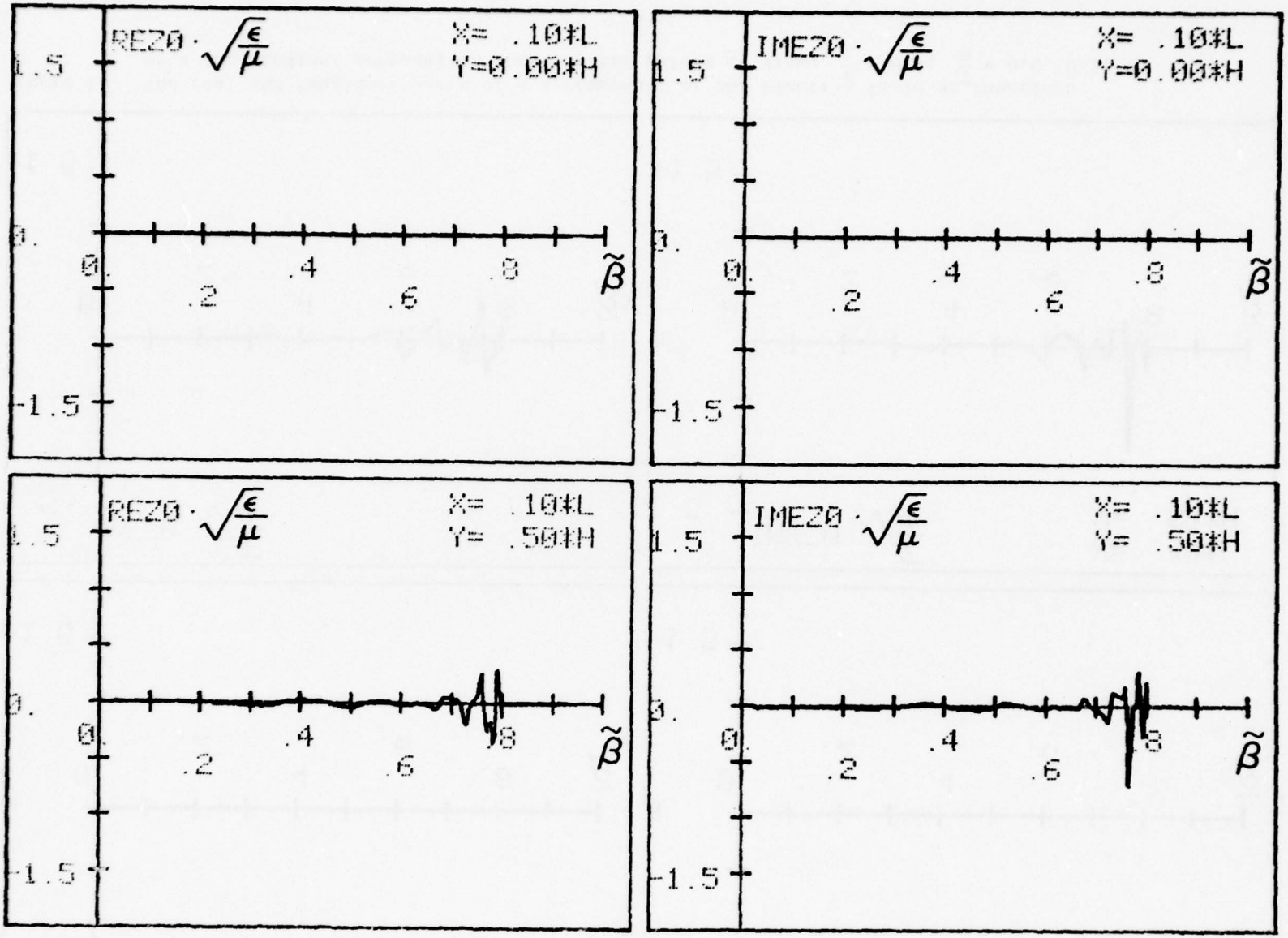

Figure 10. The real and imaginary parts of a z-component of the electric field as functions of a longitudinal propagation constant for points of view: $\frac{x}{L} = 0.1$; $\frac{y}{H} = 0.0, 0.5$.

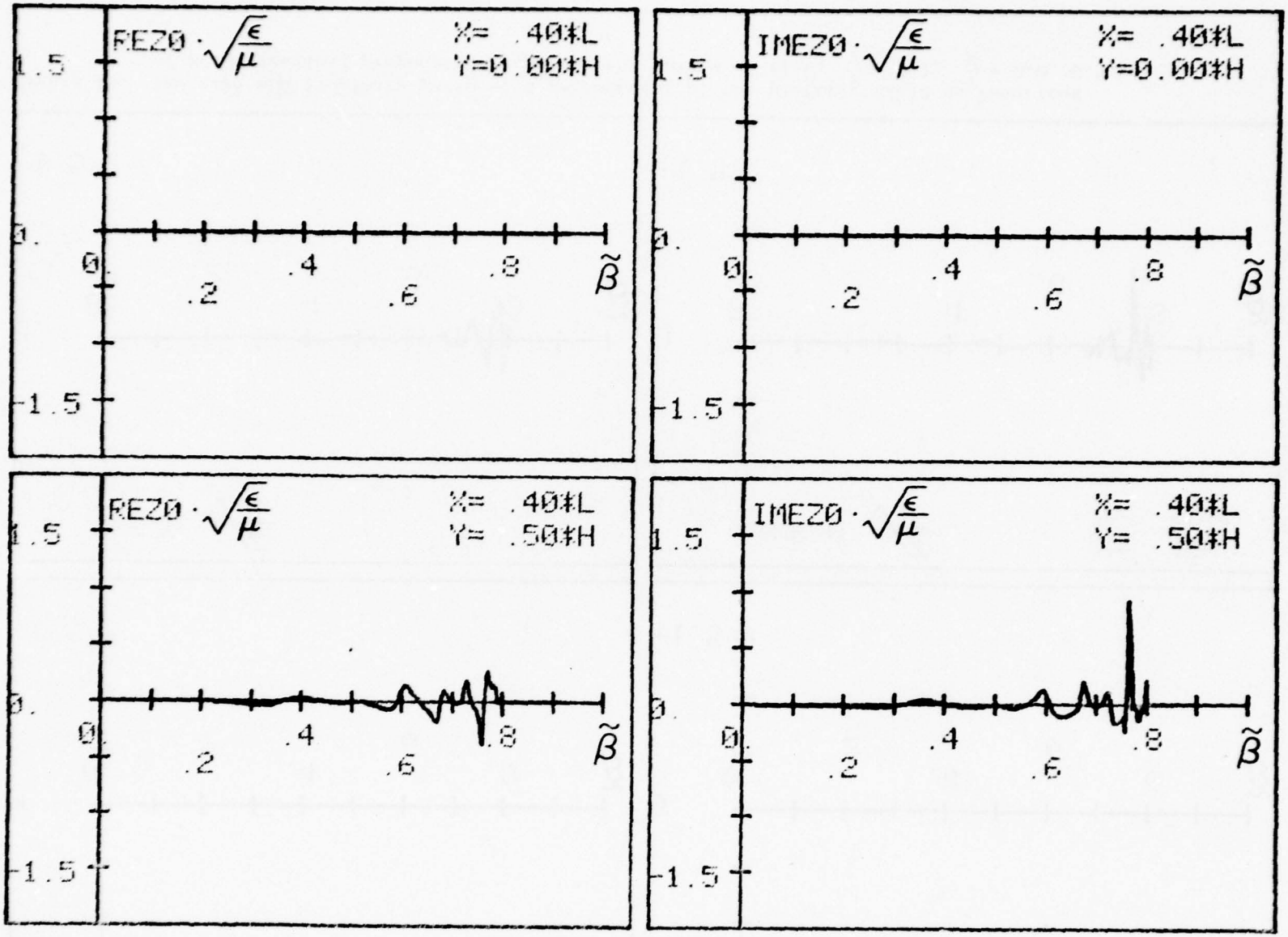

Figure 11. The real and imaginary parts of a z-component of the electric field as functions of a longitudinal propagation constant for points of view: $\frac{X}{L} = 0.4$; $\frac{Y}{H} = 0.0, 0.5$.

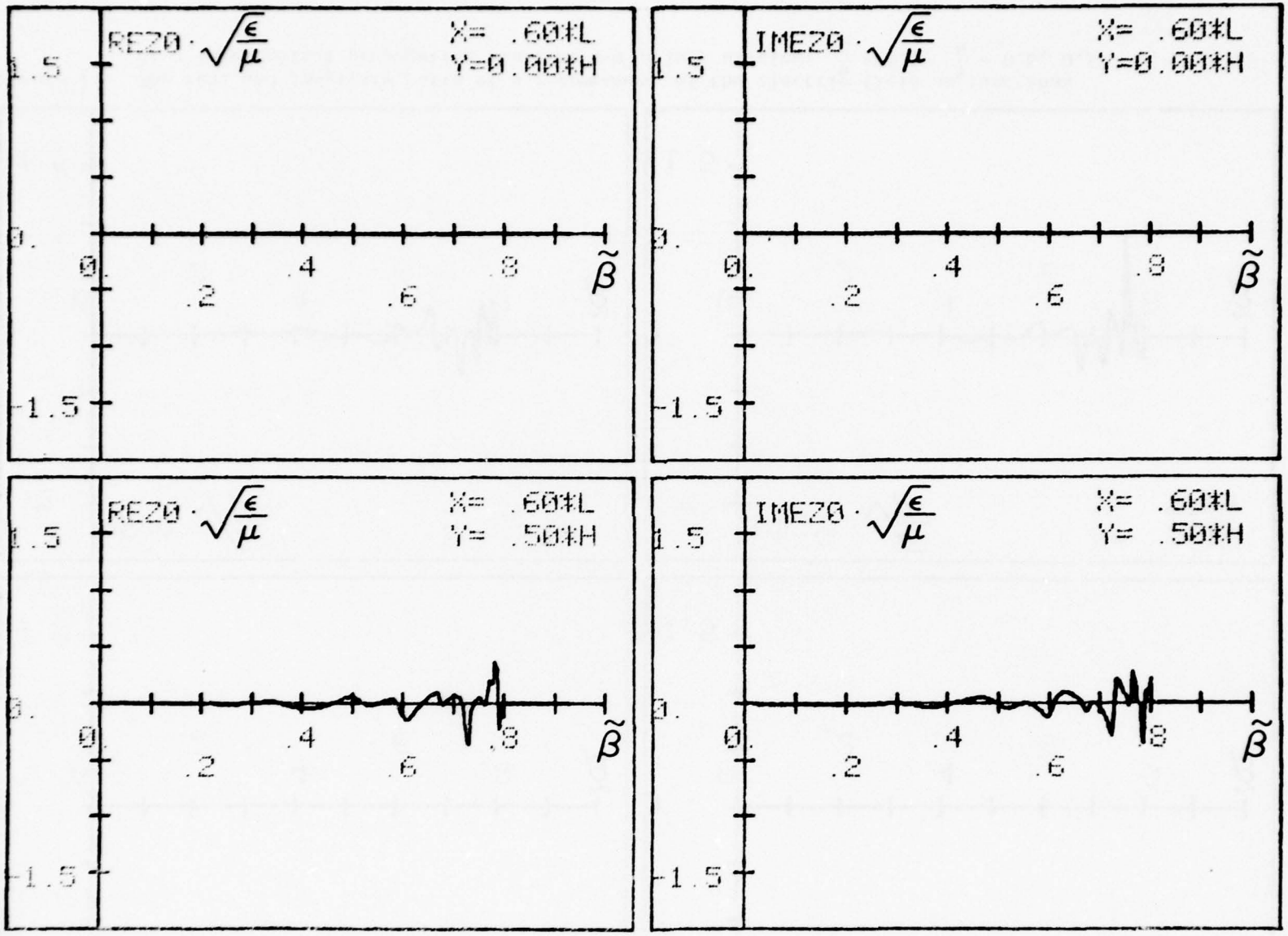

Figure 12. The real and imaginary parts of a z-component of the electric field as functions of a longitudinal propagation constant for points of view: $\frac{X}{L} = 0.6$; $\frac{Y}{H} = 0.0, 0.5$.

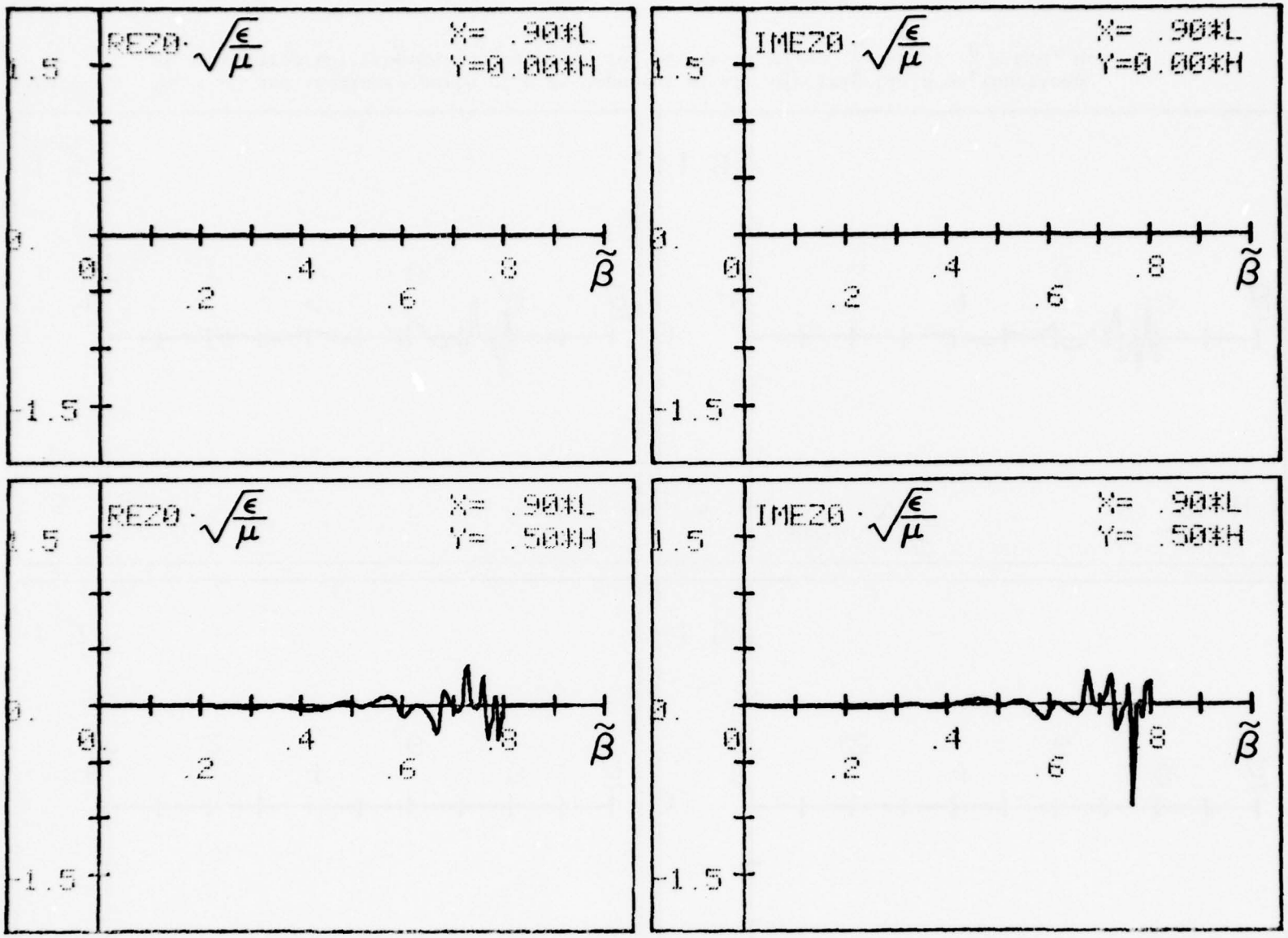

Figure 13. The real and imaginary parts of a z-component of the electric field as functions of a longitudinal propagation constant for points of view: $\frac{x}{L} = 0.9$; $\frac{Y}{H} = 0.0, 0.5$.

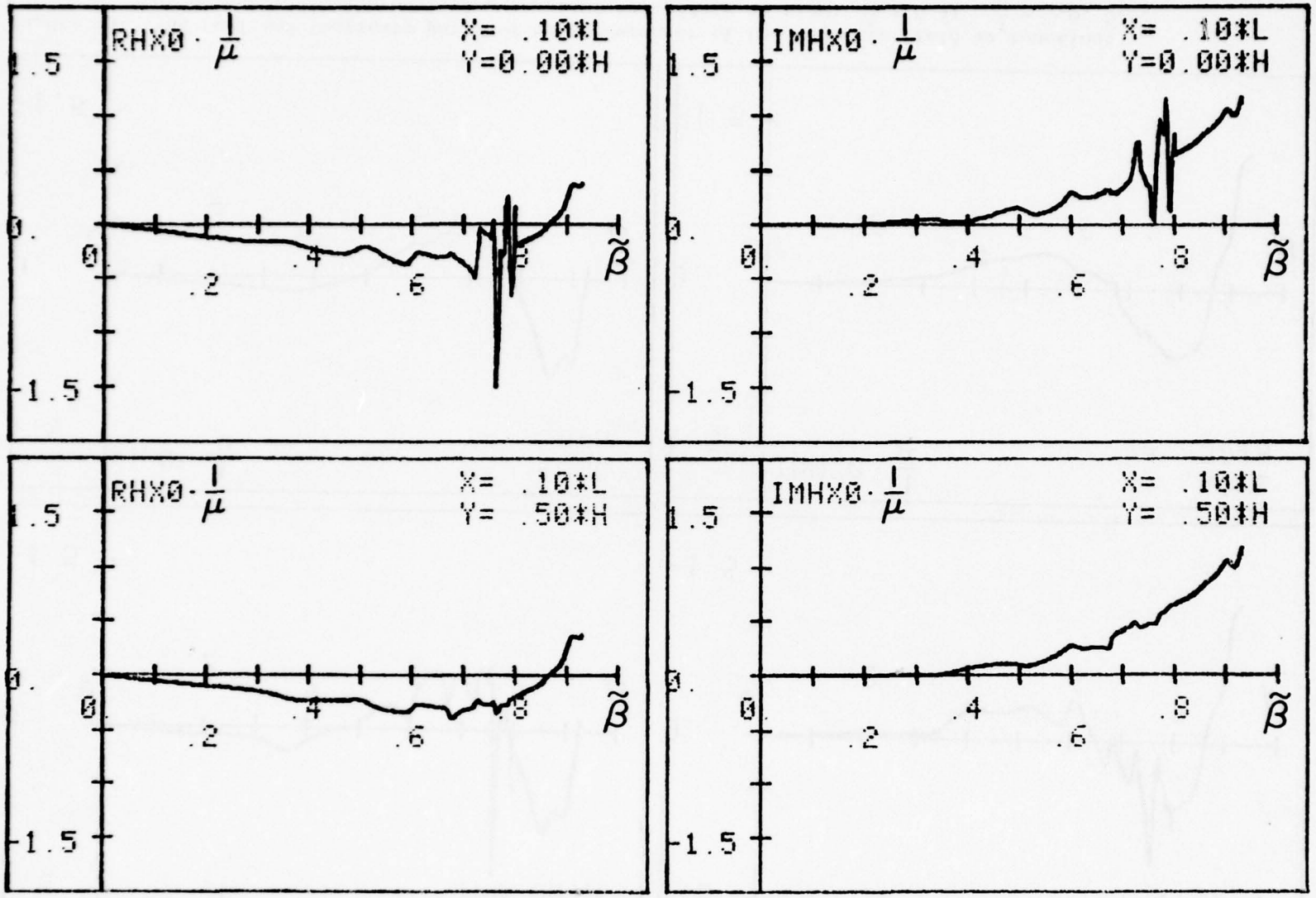

Figure 14. The real and imaginary parts of an x-component of the magnetic field as functions of a longitudinal propagation constant for points of view: $\frac{X}{L} = 0.1$; $\frac{Y}{H} = 0.0, 0.5$.

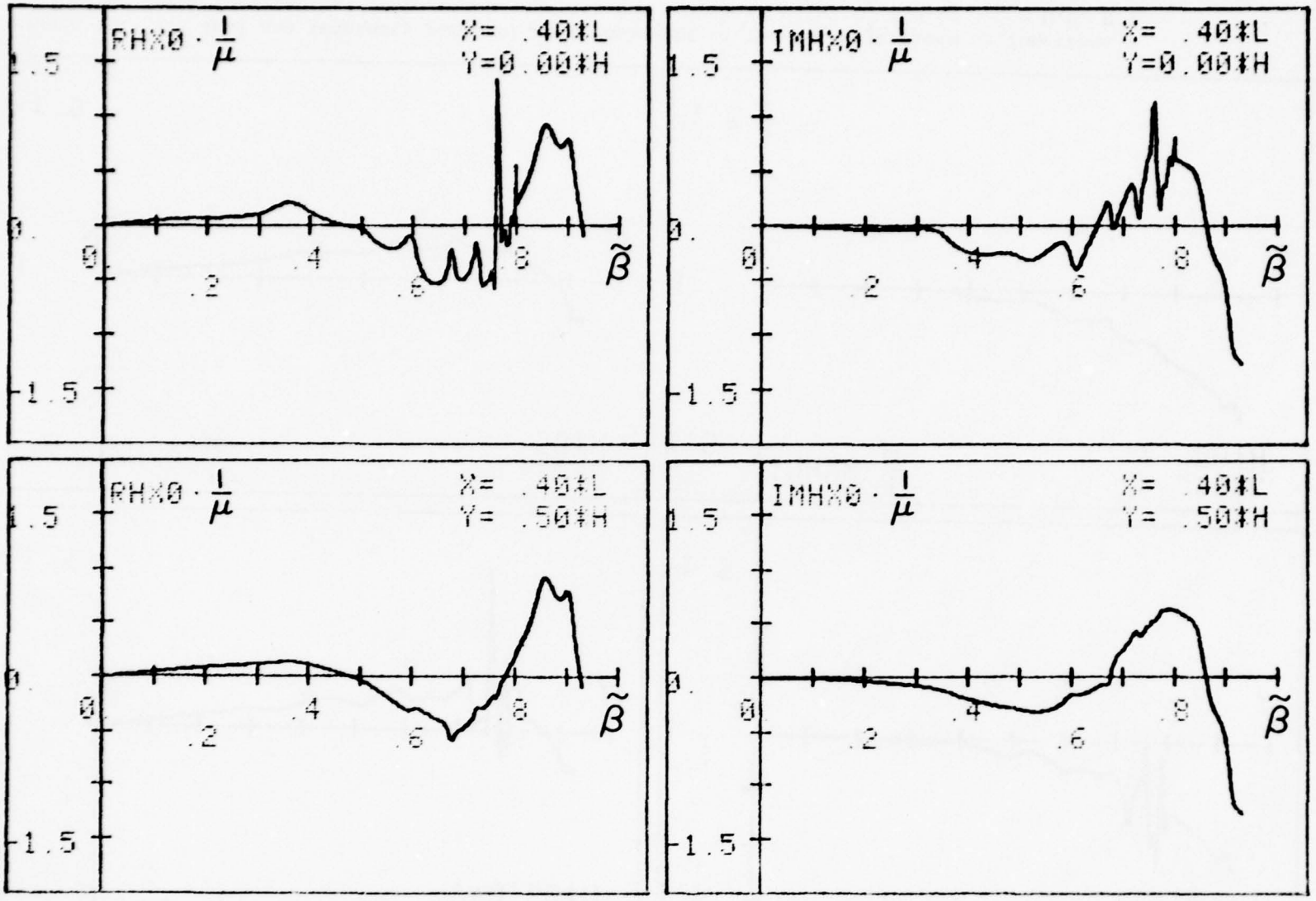

Figure 15. The real and imaginary parts of an x-component of the magnetic field as functions of a longitudinal propagation constant for points of view: $\frac{X}{L} = 0.4$; $\frac{Y}{H} = 0.0, 0.5$.

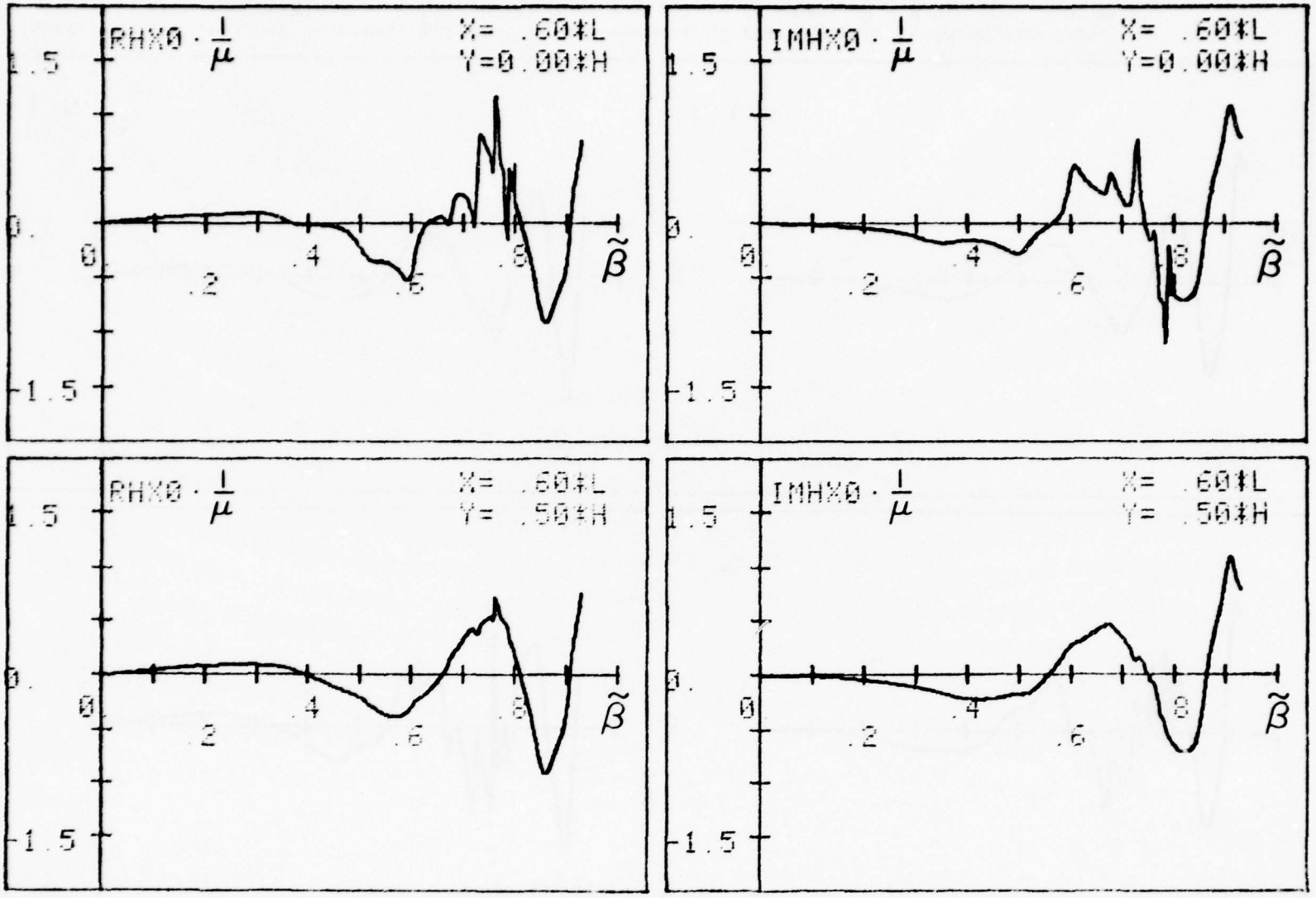

Figure 16. The real and imaginary parts of an x-component of the magnetic field as functions of a longitudinal propagation constant for points of view: $\frac{x}{L} = 0.6$; $\frac{Y}{H} = 0.0, 0.5$.

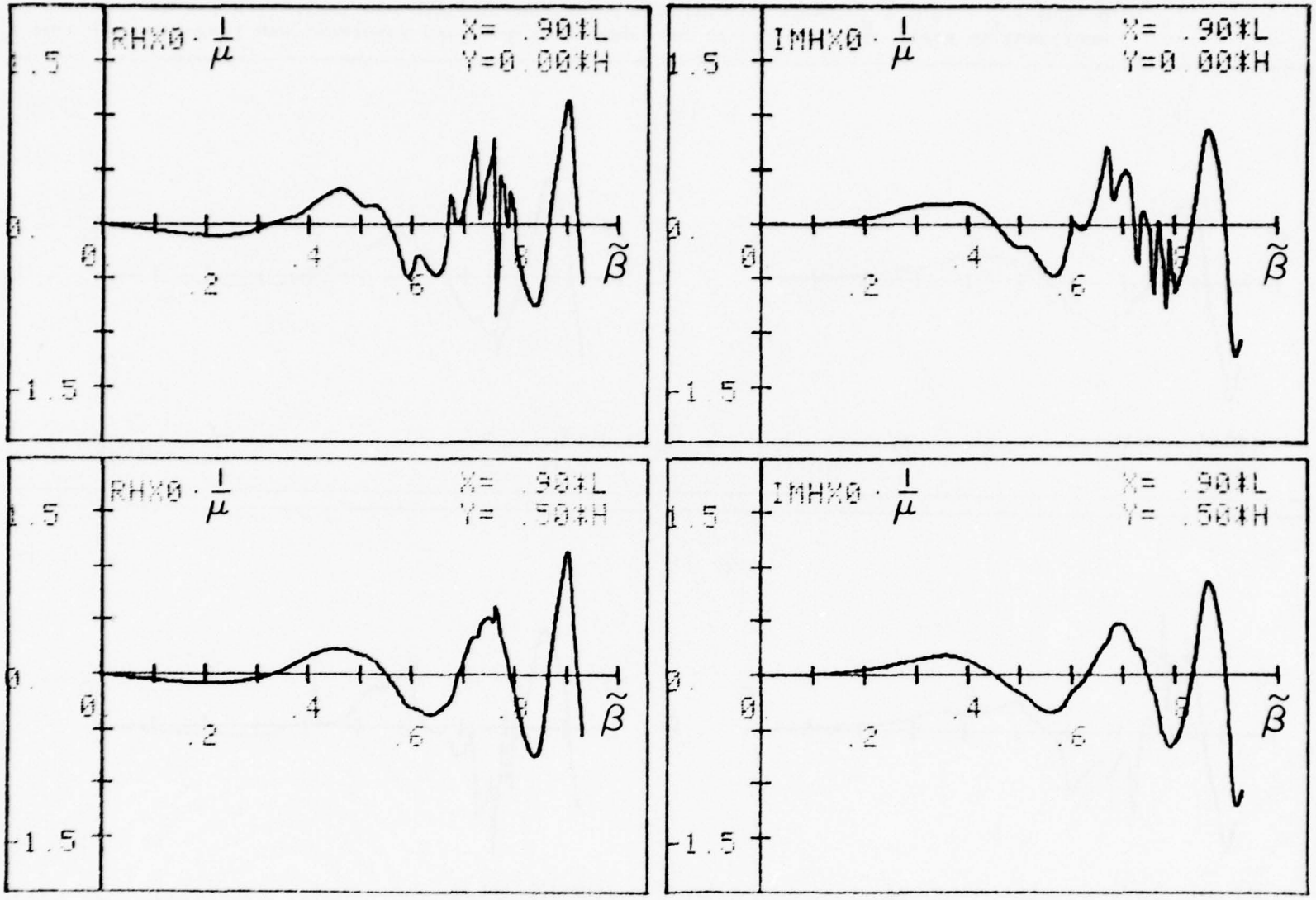

Figure 17. The real and imaginary parts of an x-component of the magnetic field as functions of a longitudinal propagation constant for points of view: $\frac{X}{L} = 0.9$; $\frac{Y}{H} = 0.0, 0.5$.

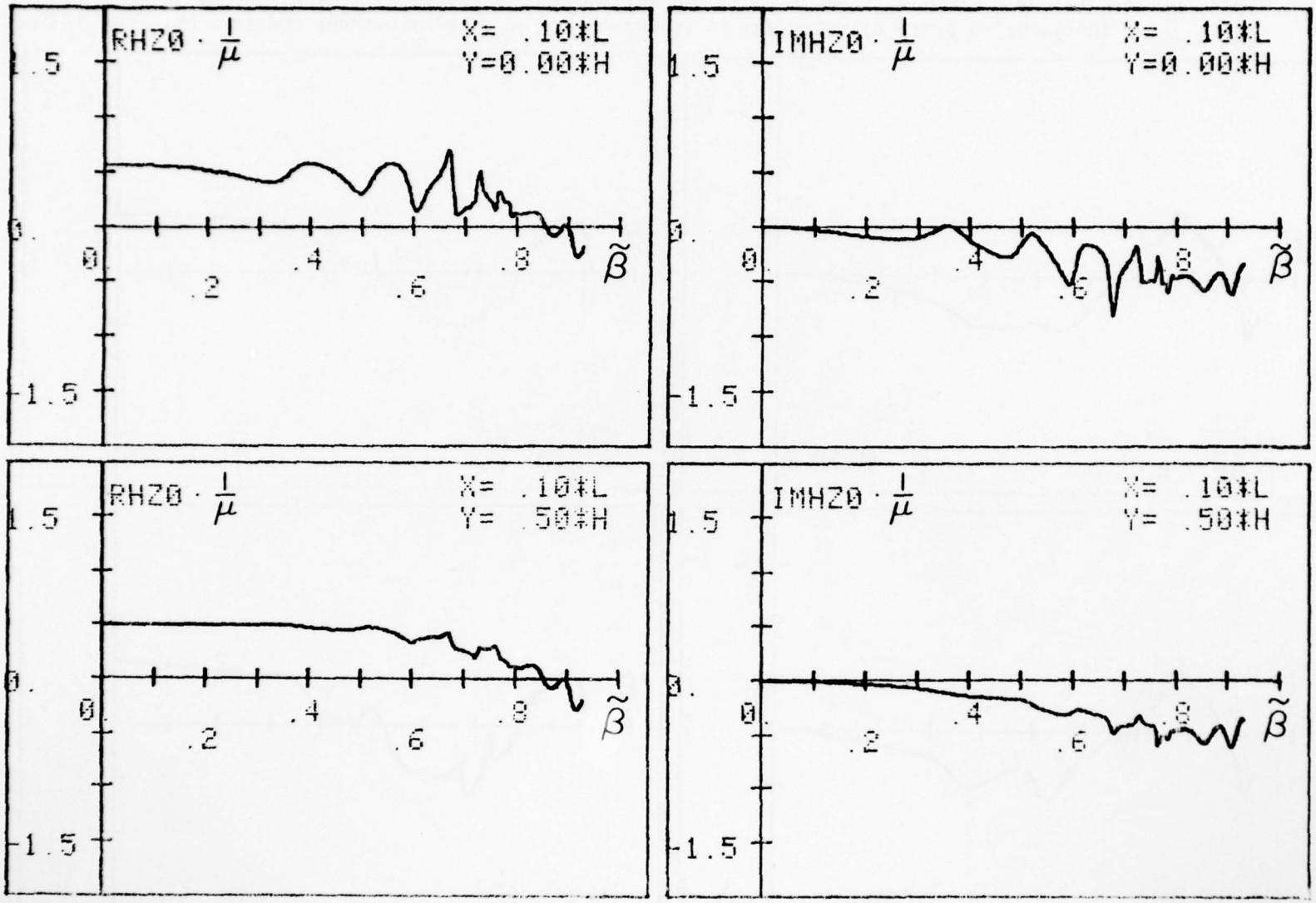

Figure 18. The real and imaginary parts of a z-component of the magnetic field as functions of a longitudinal propagation constant for points of view: $\frac{X}{L} = 0.1$; $\frac{Y}{H} = 0.0, 0.5$.

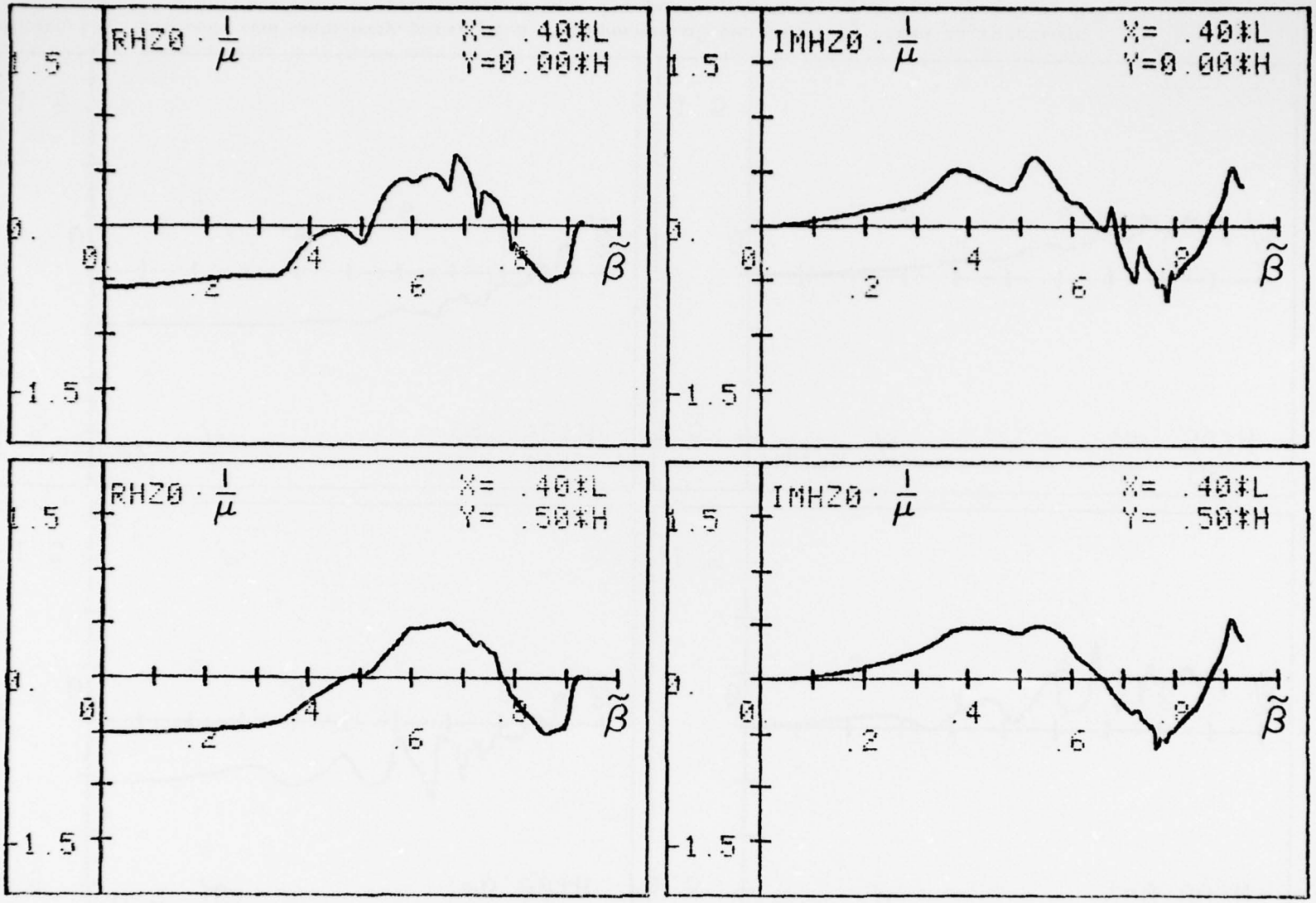

Figure 19. The real and imaginary parts of a z-component of the magnetic field as functions of a longitudinal propagation constant for points of view: $\frac{X}{L} = 0.4$; $\frac{Y}{H} = 0.0, 0.5$.

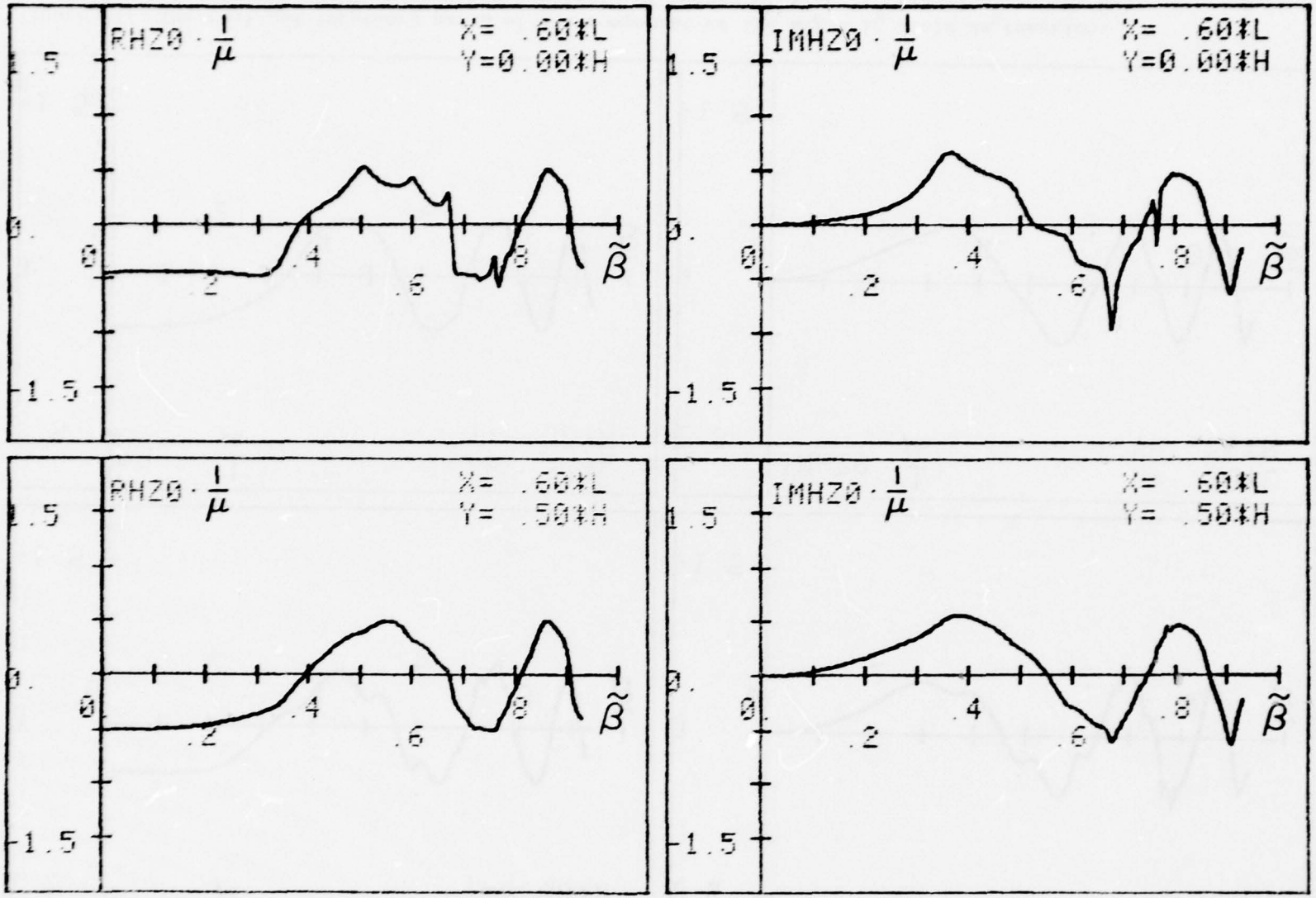

Figure 20. The real and imaginary parts of a z-component of the magnetic field as functions of a longitudinal propagation constant for points of view: $\frac{X}{L} = 0.6$; $\frac{Y}{H} = 0.0, 0.5$.

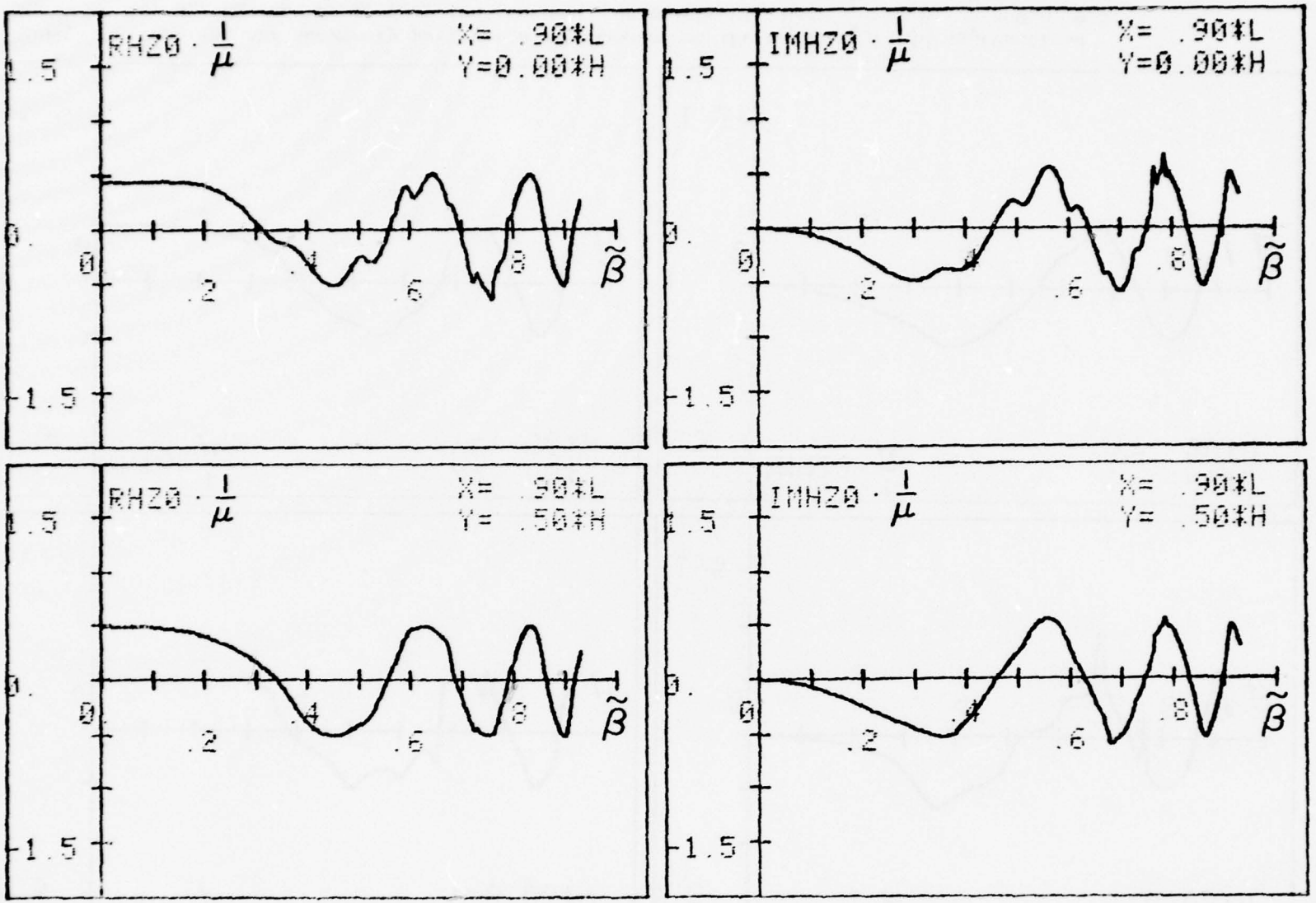

Figure 21. The real and imaginary parts of a z-component of the magnetic field as functions of a longitudinal propagation constant for points of view: $\frac{x}{L} = 0.9$; $\frac{y}{H} = 0.0, 0.5$.

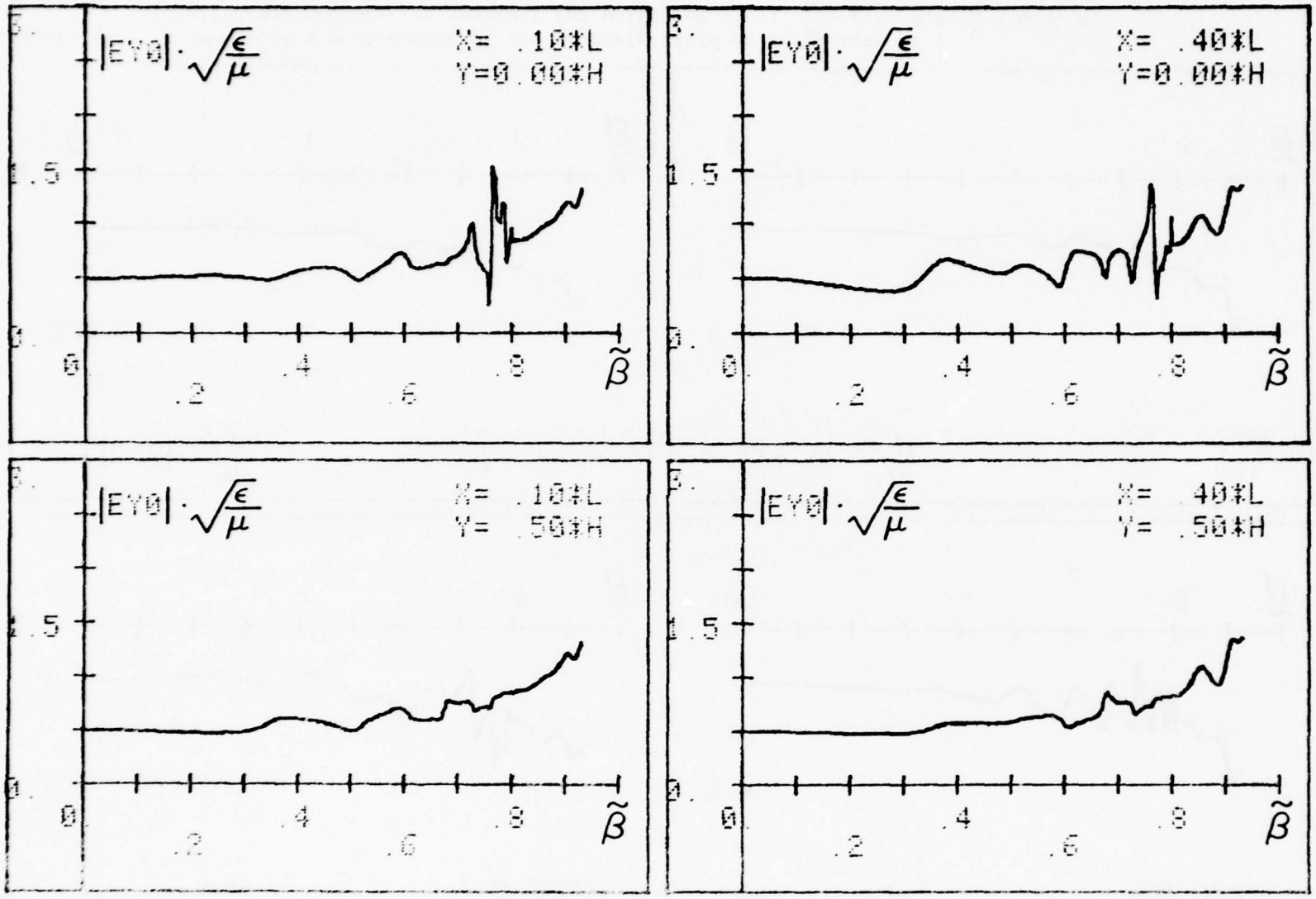

Figure 22. The moduleof a y-component of the electric field as a function of a longitudinal propagation constant for points of view: $\frac{X}{L}$ = 0.1, 0.4; $\frac{Y}{H}$ = 0.0, 0.5.

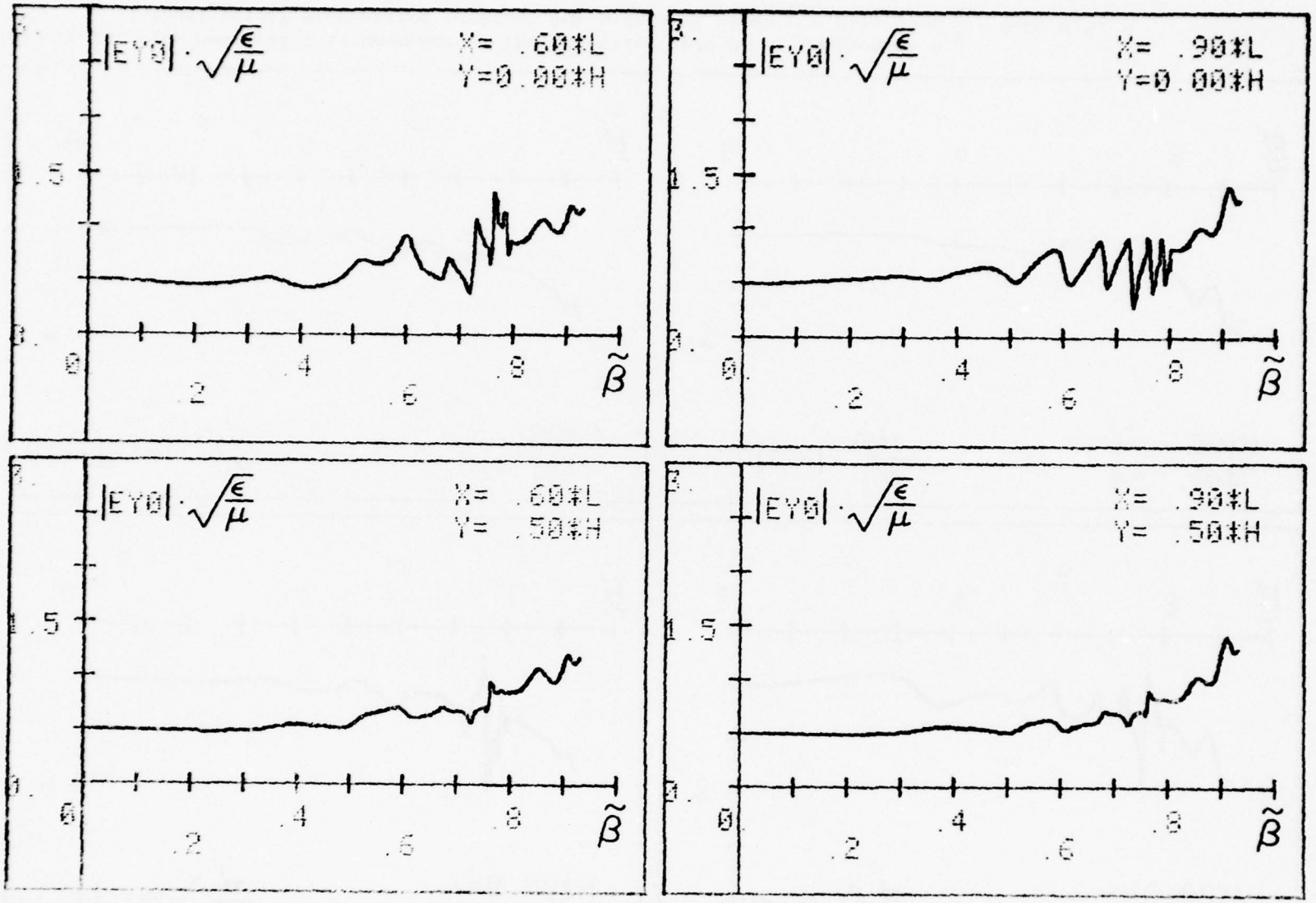

Figure 23. The module of a y-component of the electric field as a function of a longitudinal propagation constant for points of view: $\frac{X}{L}$ = 0.6, 0.9; $\frac{Y}{H}$ = 0.0, 0.5.

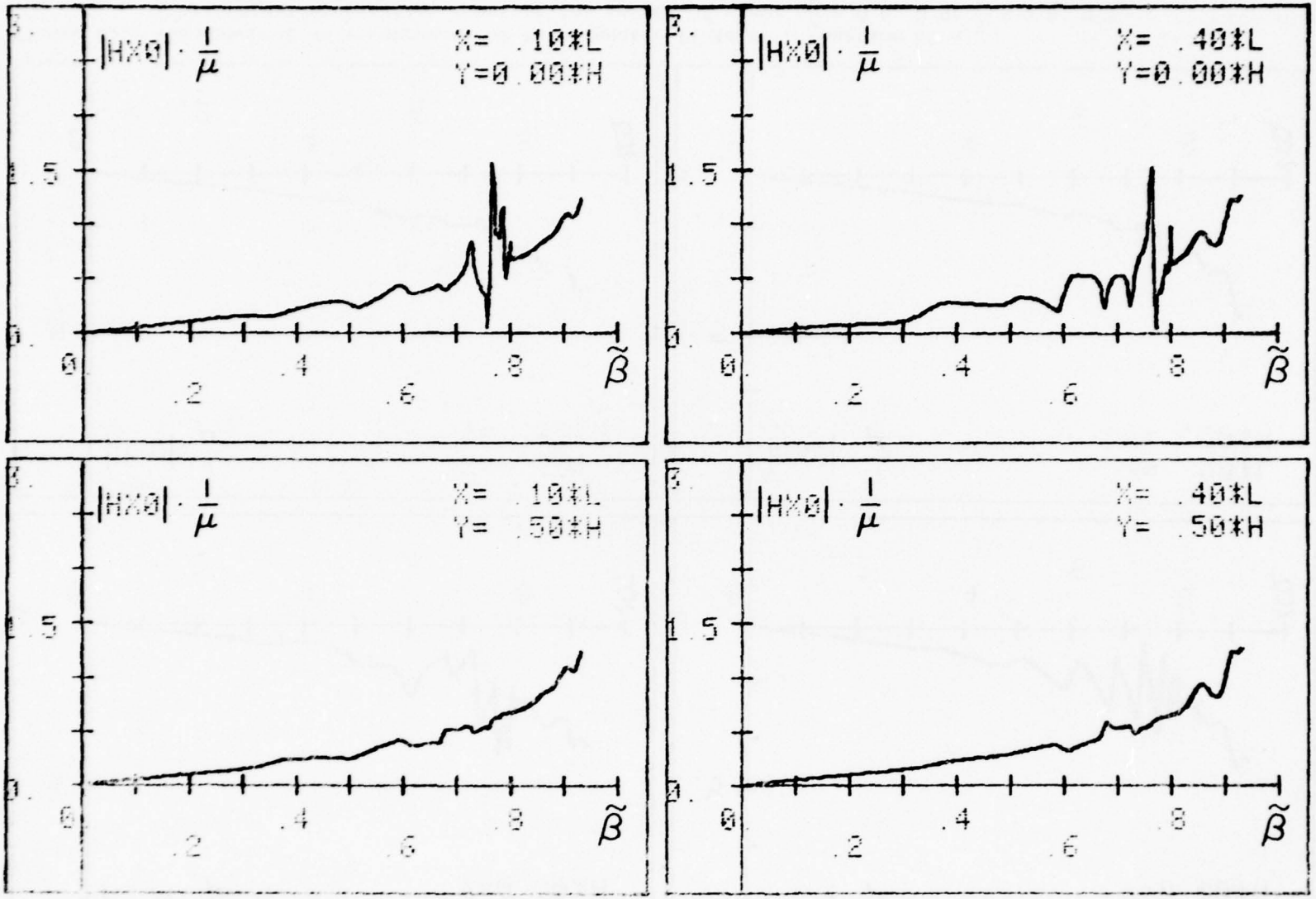

Figure 24. The module of an x-component of the magnetic field as a function of a longitudinal propagation constant for points of view: $\frac{X}{L}$ = 0.1, 0.4; $\frac{Y}{H}$ = 0.0, 0.5.

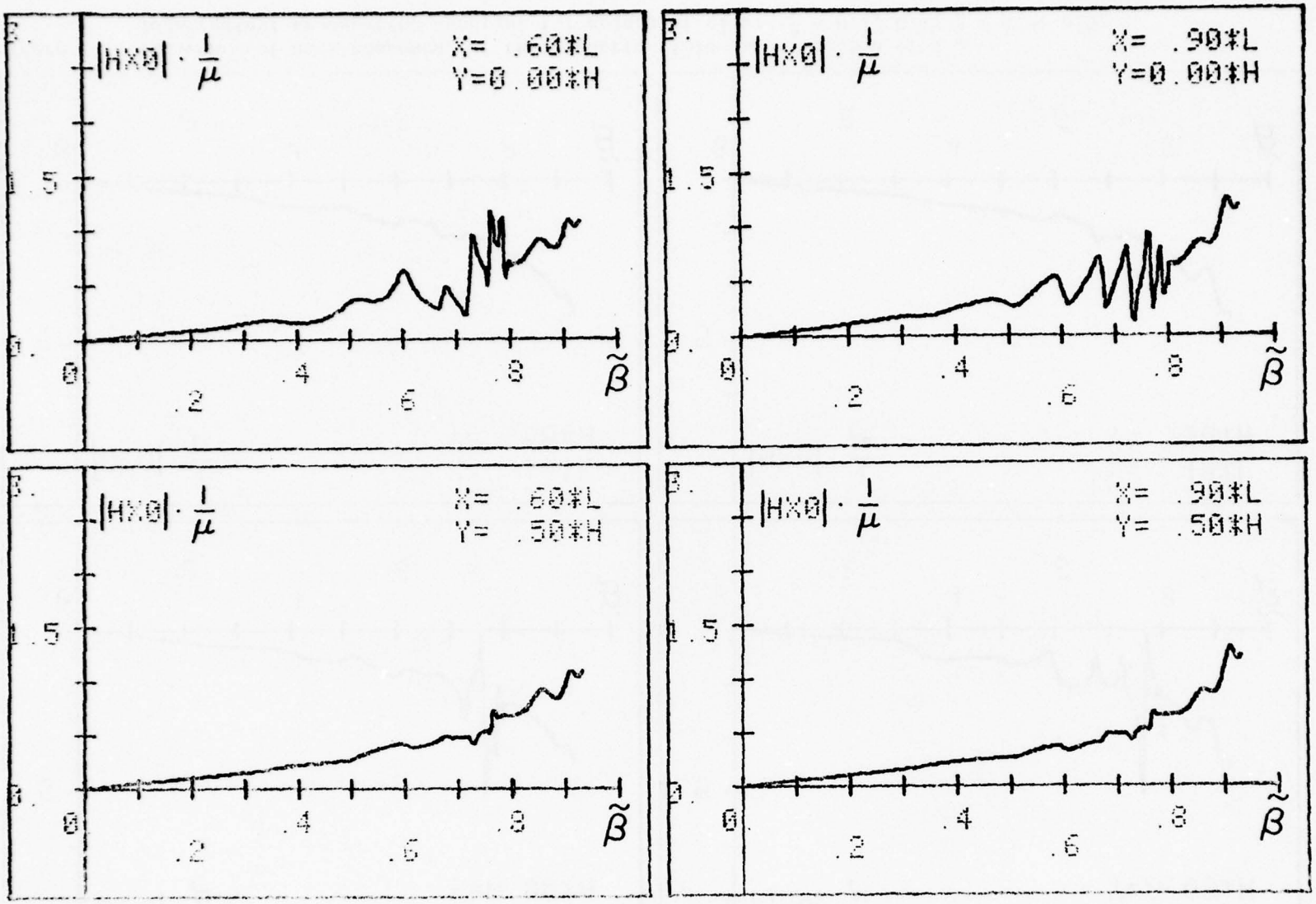

Figure 25. The module of an x-component of the magnetic field as a function of a longitudinal propagation constant for points of view: $\frac{X}{L}$ = 0.6, 0.9; $\frac{Y}{H}$ = 0.0, 0.5.

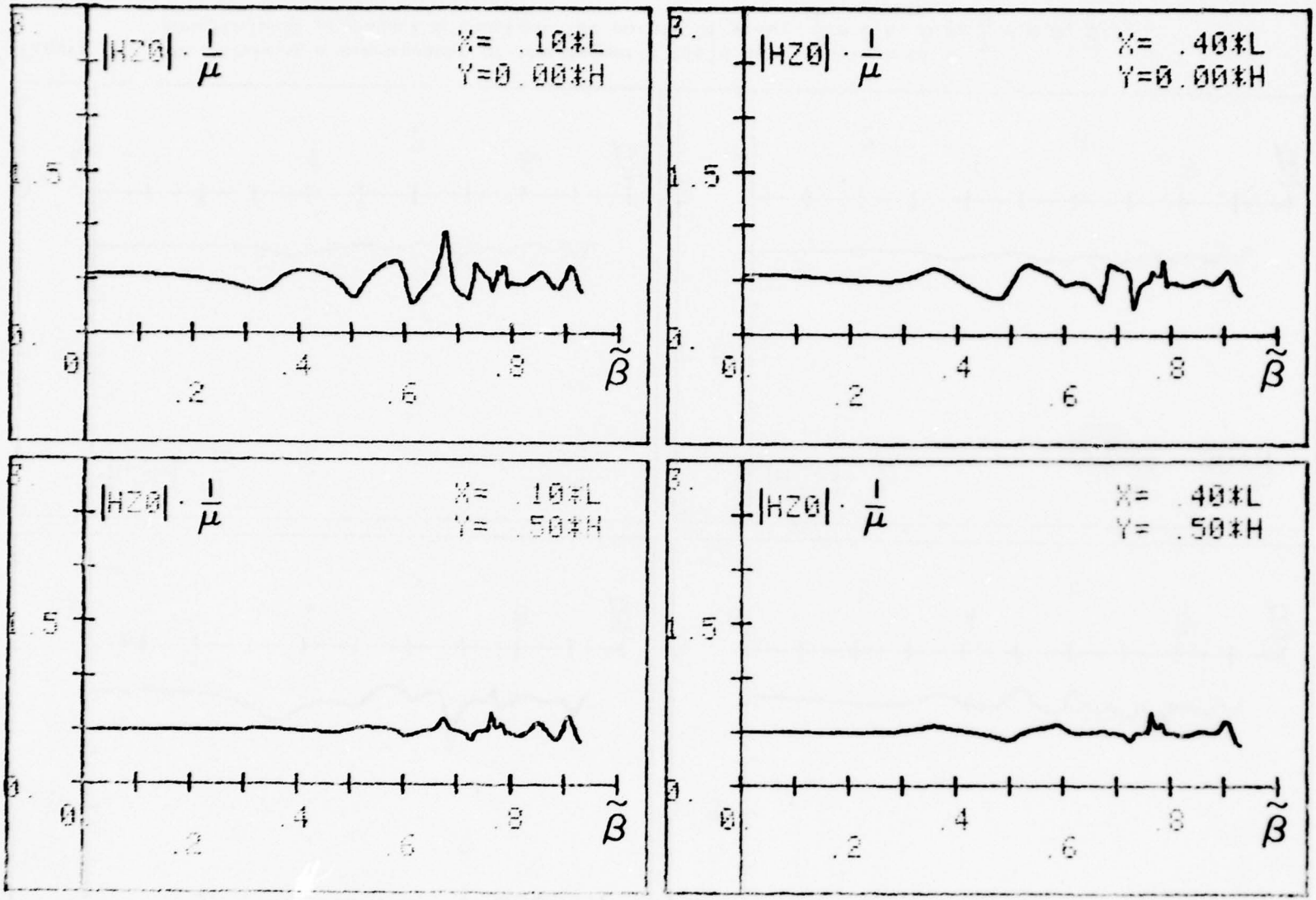

Figure 26. The module of a z-component of the magnetic field as a function of a longitudinal propagation constant for points of view: $\frac{X}{L}$ = 0.1, 0.4; $\frac{Y}{H}$ = 0.0, 0.5.

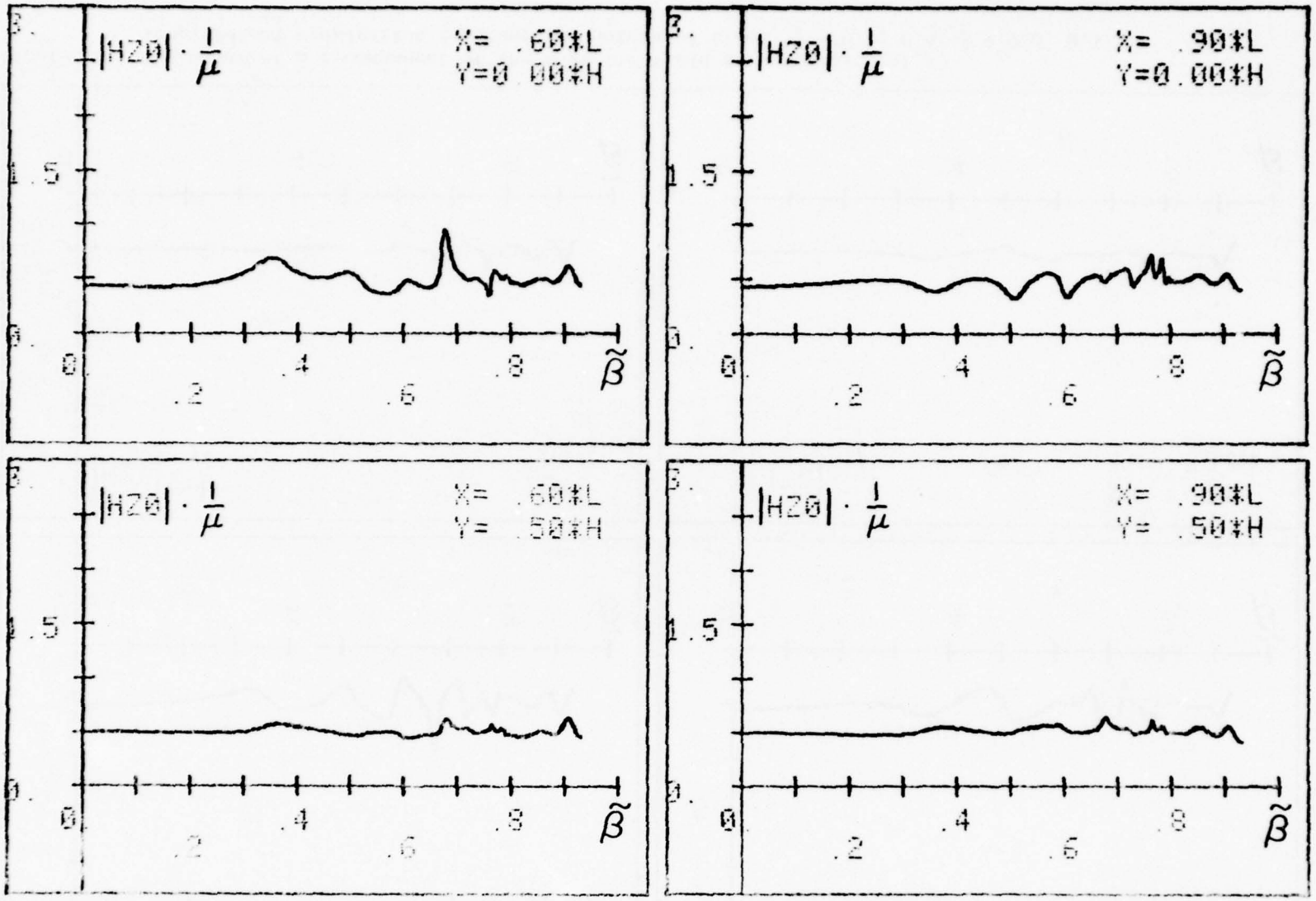

Figure 27. The module of a z-component of the magnetic field as a function of a longitudinal propagation constant for points of view: $\frac{X}{L}$ = 0.6, 0.9; $\frac{Y}{H}$ = 0.0, 0.5.

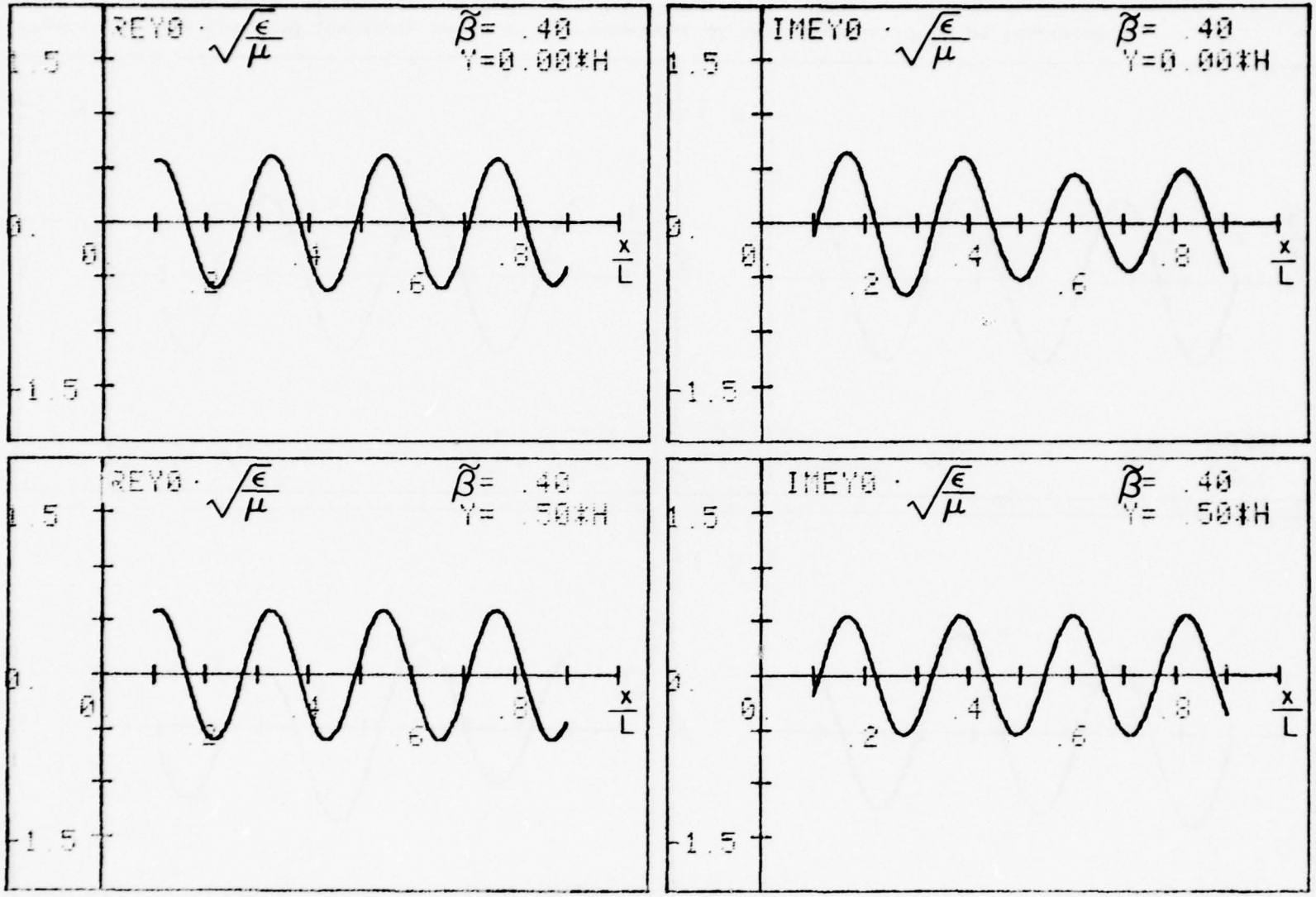

Figure 28. The real and imaginary parts of a $\frac{Y}{H}$ y-component of the electric field as functions of an x-coordinate for $\tilde{\beta}$ = 0.4; $\frac{Y}{H}$ = 0.0, 0.5.

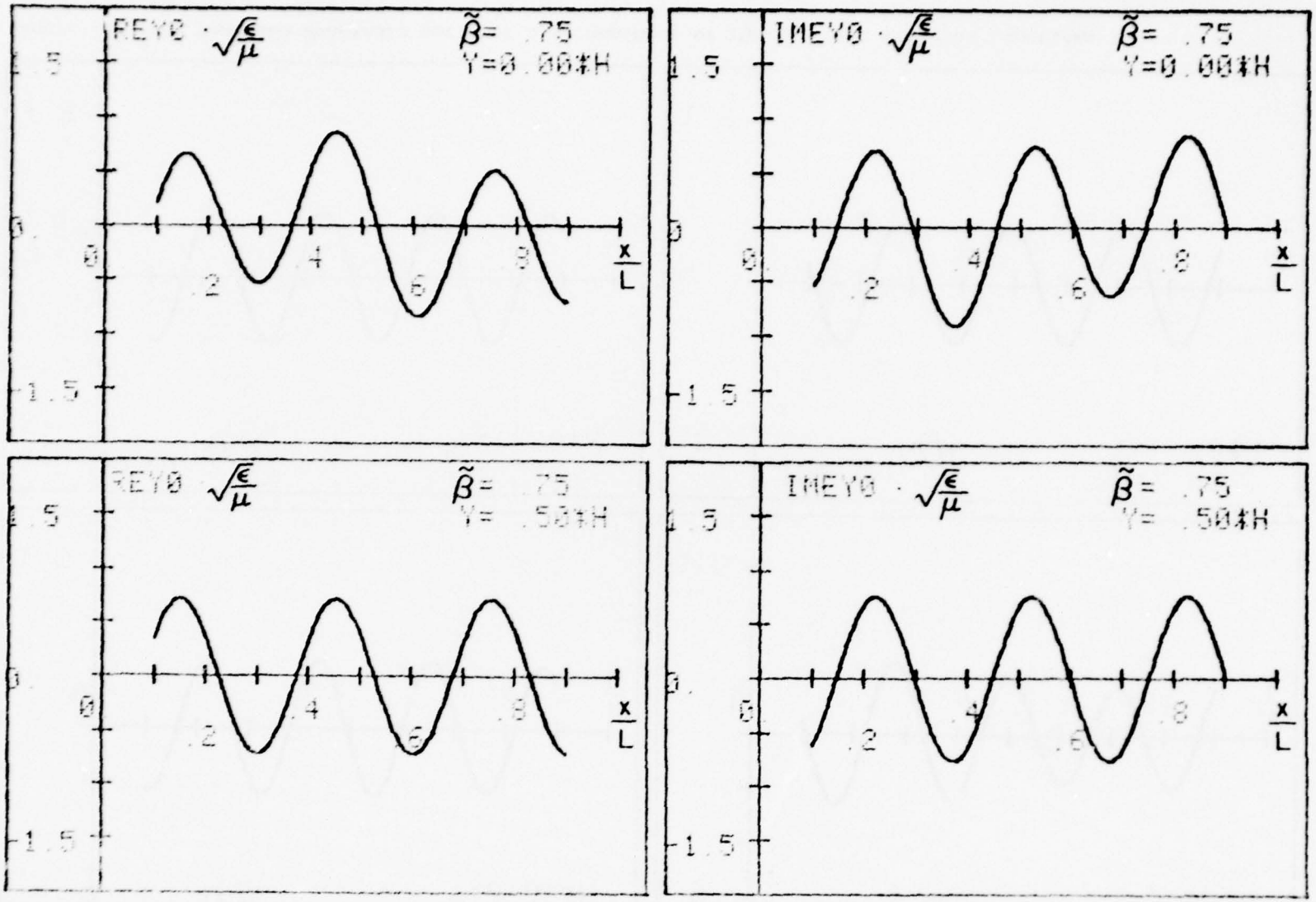

Figure 29. The real and imaginary parts of a_y y-component of the electric field as functions of an x-coordinate for $\tilde{\beta}$ = 0.75; $\frac{Y}{H}$ = 0.0, 0.5.

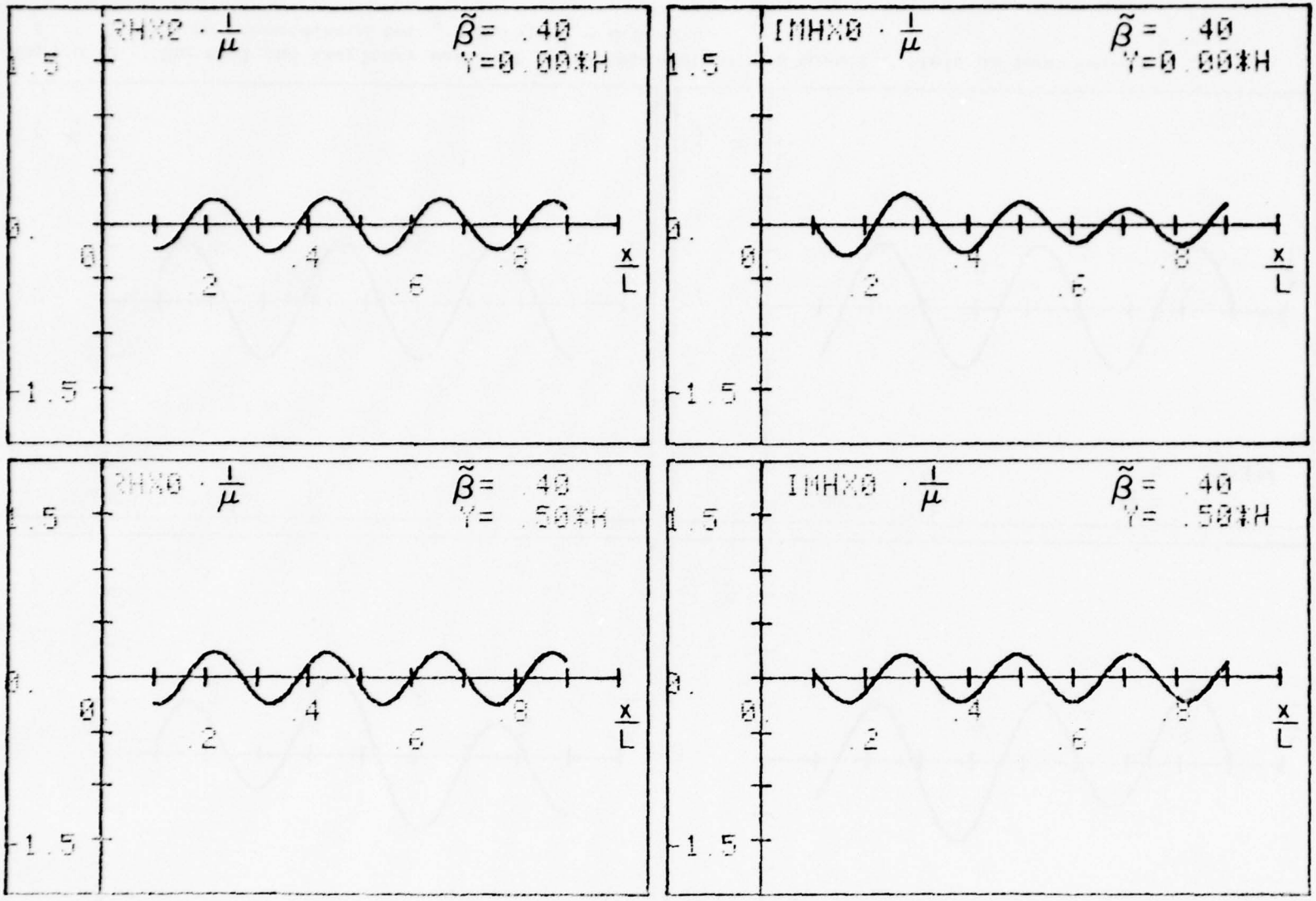

Figure 30. The real and imaginary parts of an x-component of the magnetic field as functions of an x-coordinate for $\tilde{\beta} = 0.4$; $\frac{Y}{H} = 0.0, 0.5$.

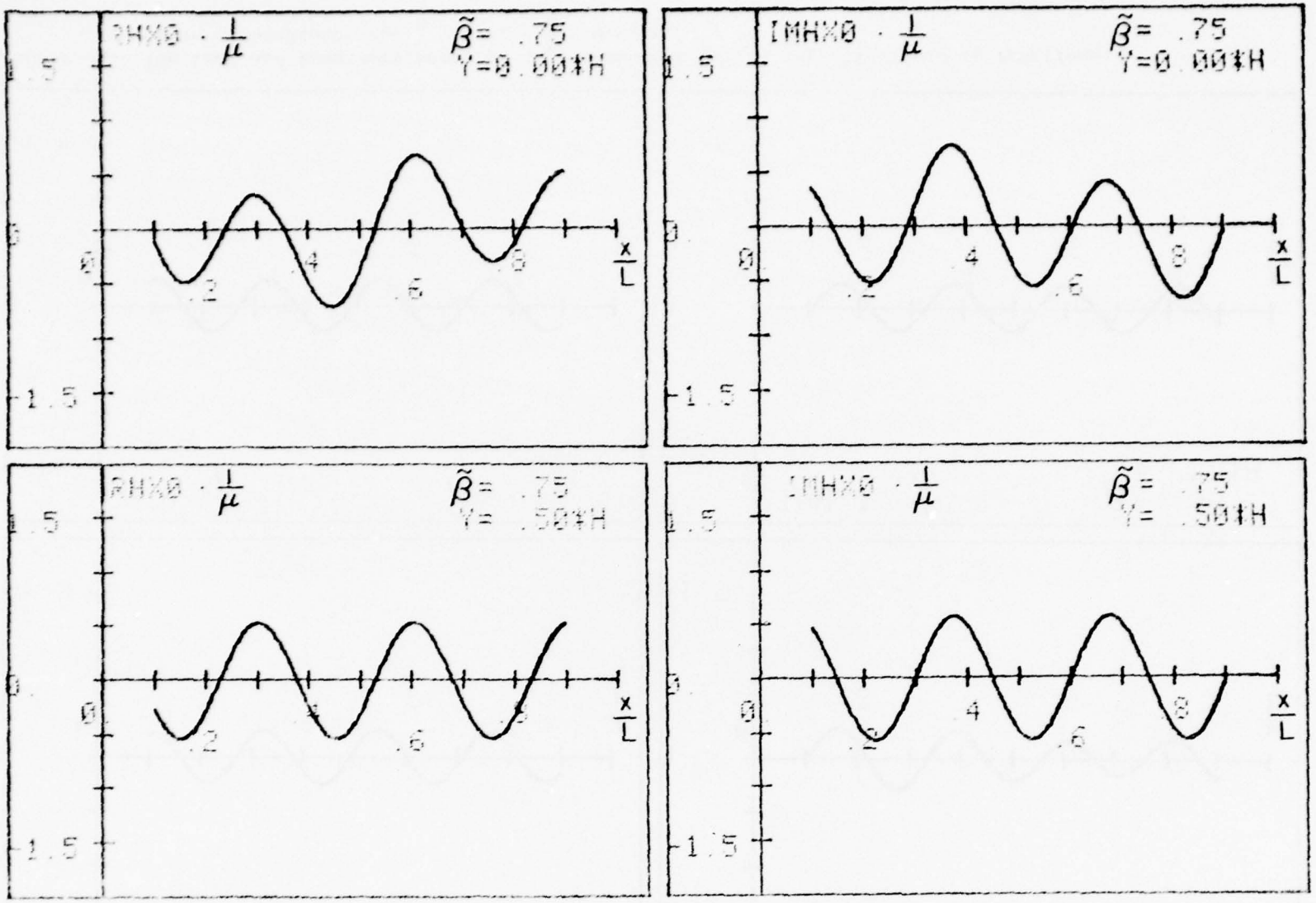

Figure 31. The real and imaginary parts of an x-component of the magnetic field as functions of an x-coordinate for $\tilde{\beta} = 0.75$; $\frac{Y}{H} = 0.0, 0.5$.

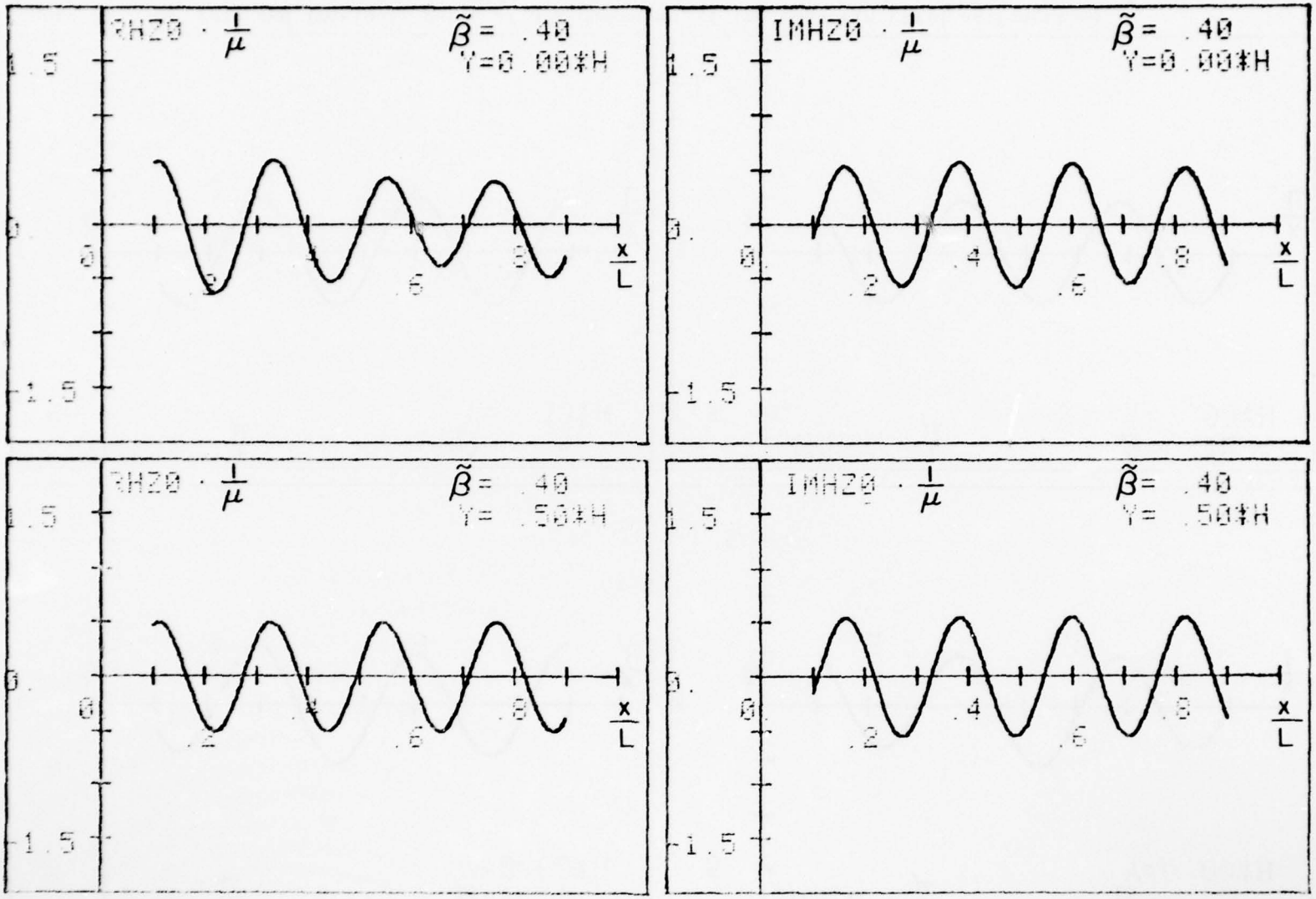

Figure 32. The real and imaginary parts of a $_{Y}$z-component of the magnetic field as functions of an x-coordinate for $\tilde{\beta}$ = 0.4; $\frac{Y}{H}$ = 0.0, 0.5.

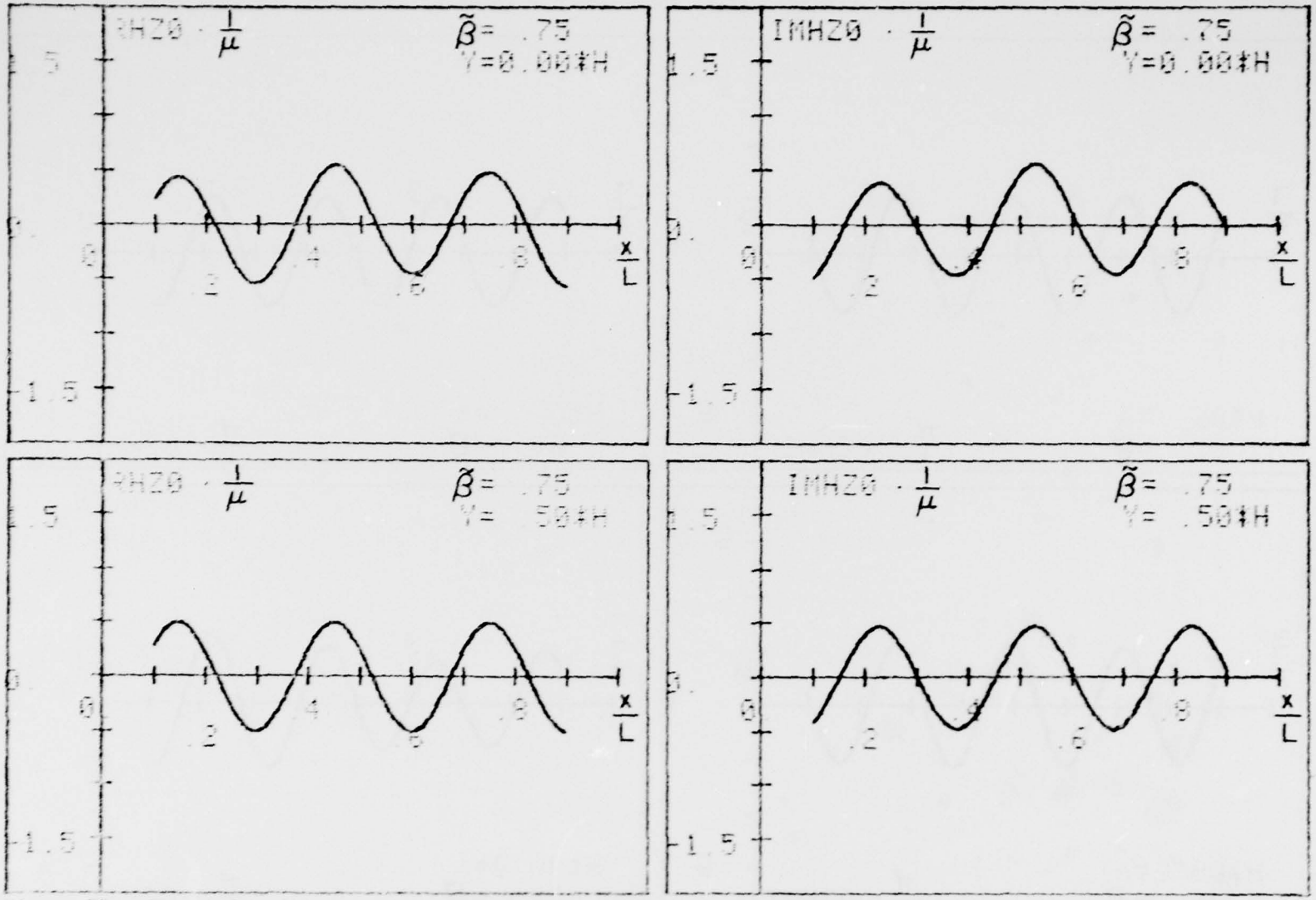

Figure 33. The real and imaginary parts of a $_{Y}$ z-component of the magnetic field as functions of an x-coordinate for $\tilde{\beta}$ = 0.75; $\frac{Y}{H}$ = 0.0, 0.5.

III. NUMERICAL STUDY OF THE PROBLEM

Because the analytical expressions derived in the second section are rather complicated and difficult to analyze, we numerically evaluated the solutions using a digital computer. The results are presented in this section in graphical form. This section consists of two parts: in the first we discuss the field components as functions of the longitudinal propagation constant; in the second - as functions of the transverse coordinates.

A. Real and Imaginary Parts and Amplitudes of the Field Components As Functions of the Longitudinal Propagation Constant

The graphics that are supplied in this section were plotted with a step for $\tilde{\beta}$ equal to 0.005. The point, $\tilde{\beta} = 0.80009$, also was used. The figures were plotted using 188 points. The output for the real and imaginary parts and the amplitudes of all five field components for eight observation points: $\frac{X}{L} = 0.1, 0.4, 0.6, 0.9$ and $\frac{Y}{H} = 0.0, 0.5$ are presented. From the figures it is observed that E_y, H_x, H_z are dominant components. In Figures 6-9 the real and imaginary parts of E_y are given. By comparing these results, one can observe for points $\frac{Y}{H} = 0.0$ and $\frac{Y}{H} = 0.5$ that the E_y, H_x, H_z - field behaviors as functions of $\tilde{\beta}$ are more complicated in the middle of the waveguide. This is hardly surprising in view of the largest contribution of the second mode for the above-mentioned components for $\frac{Y}{H} = 0.0$. When the point of observation approaches $\frac{Y}{H} = 0.5$, the contribution of the second mode for those components decreases and has a limiting value equal to zero. In Figures 6-9, 14-17, 22-25 we observe the step changing for the E_y, H_x components at $\tilde{\beta} = \tilde{\beta}_0$. The

second mode is responsible for this misbehavior. When $\frac{y}{H} \to 0.5$, the contribution of that step decreases, and for $\frac{y}{H} = 0.5$, it equals zero. One can observe that the curves are smooth at $\tilde{\beta} = \tilde{\beta}_0$. It should be mentioned that:

(a) The discontinuous behavior is observed because we have neglected the exponentially decreasing terms;

(b) In a lossy medium, the rate of decrease would be less. The H_z-component (see Figures 18-21, 26) doesn't have the step behavior because the contribution of the second mode is proportional to α_1, which goes to 0, when $\tilde{\beta} \to \tilde{\beta}_0$. The other two components, E_x and E_z, are equal to zero on the x-axis and have their largest contribution for $\frac{y}{H} = 0.5$ (see Figures 2-5, 10-13). E_x is smooth and E_z exhibits the step behavior at $\tilde{\beta}_0$. The figures demonstrate that the complexity of the curves occurs approximately in the region $0.7 < \tilde{\beta} < 0.8$, where we observe a sharp peak, which is due to the resonance. In the region $0 < \tilde{\beta} < 0.5$ the figures demonstrate the very smooth character of the curves.

B. Real and Imaginary Parts of the Field Components as Functions of Transverse Coordinates

In this section we present the real and imaginary parts of the dominant field components E_y, H_x, H_z as functions of the x-coordinate for two values of $\frac{y}{H} = 0.0;\ 0.5$ and two values of $\tilde{\beta} = 0.4;\ 0.75$. The graphic output, shown in Figures 28-33, was obtained using the results of calculations for 81 points of $\frac{x}{L}$ in the region [0.1, 0.9] (step = 0.010). All the graphs have very smooth characteristics. For $\tilde{\beta} = 0.75$ they have slightly more complicated form than for $\tilde{\beta} = 0.4$. As mentioned in the

previous section, for $\frac{y}{H} = 0.5$ the contribution of the second mode equals zero. We see that the amplitudes of the curves are constant for the entire region of view. For the $\frac{y}{H} = 0.0$, the field components are sums of the contributions of two modes. One can observe that the amplitudes of the curves are changing along the x-direction.

IV. CONCLUSIONS

In this report the problem of a source excitation of an open parallel-plate waveguide was developed. Extensive numerical results for the field components in the waveguide as functions of several parameters of the waveguide and propagation constant were supplied.

REFERENCES

[1] V. Krichevksy, R. Mittra, "Source Excitation of an Open, Parallel-Plate Waveguide," University of Illinois Electromagnetics Laboratory, Department of Electrical Engineering, Scientific Rep. No. 77-19, October 1977.

APPENDIX

SOURCE EXCITATION OF AN OPEN, PARALLEL-PLATE WAVEGUIDE PROGRAM

A complete program for source excitation of an open, parallel-plate waveguide program is presented. The computer program provides three-dimensional data-storage for the real and imaginary parts of five components of the EM field. Data were obtained for $\frac{x}{L}$ between 0.1 - 0.9 with step 0.1; $\frac{y}{H}$ between 0.0 - 0.9 with step 0.1; and $\tilde{\beta}$ - propagation constant between 0.0 - 0.93 with step 0.005 plus (•) 0.80009. These data were used to plot EM field components as functions of the propagation constant. The program can be readily modified to obtain data for plotting the EM-field component as a function of the x-coordinate.

THIS PAGE IS BEST QUALITY PRACTICABLE
FROM COPY FURNISHED TO DDC

```
      PROGRAM AFIELD(INPUT,OUTPUT,TAPE3,TAPE1=INPUT)
      COMPLEX BBK,BBAL,T1,F1,F2,EX0,EY0,EZ0,HX0,HZ0,CONST,AA,BB
      DIMENSION XX(9),YY(10),BETAB(188),REX0(10,9,188),AMEX0(10,9,188),
     $REY0(10,9,188),AMEY0(10,9,188),REZ0(10,9,188),AMEZ0(10,9,188),
     $RHX0(10,9,188),AMHX0(10,9,188),RHZ0(10,9,188),AMHZ0(10,9,188)
      READ(1,2)W,YBRI,YBRS,YBRF,XBRI,XBRS,XBRF
    2 FORMAT(F7.5,6(F7.3))
      M=1000
      PI=3.141592654
      CONST=CMPLX(0.,1.)
      CON=2.11593152
      BETAB(1)=0.
      DO 70 I=1,160
      BETAB(I+1)=BETAB(I)+0.005
   70 CONTINUE
      BETAB(162)=0.80009
      BETAB(163)=0.805
      DO 75 I=1,25
   75 BETAB(I+163)=BETAB(I+162)+0.005
      CONTINUE
      DO 98 N=1,161
      BETA=BETAB(N)
      K=N
      A=10.*PI*SQRT(1.-BETA**2)
      B=A*W/PI
      ALFA1=SQRT(B**2-1.)
      DD=PI*ALFA1/W
      CALL BE1(A,B,BBK,PI,M,CON,ALFA1)
      CALL BE2(A,B,BBAL,PI,M,CON,ALFA1)
      CALL TE1(A,B,T1,BBK,PI)
      CALL F12(A,B,T1,ALFA1,BBK,BBAL,F1,F2)
      X=XBRI
      J=1
   30 Y=YBRI
      I=1
   20 EX0=(PI*ALFA1/(10.*W**2))*F2*SIN(PI*Y)*SIN(DD*X)
      EY0=10.*PI*(F1*COS(A*X)+(1.-(1./(100.*W**2)))*F2*COS(PI*Y)*
     $COS(DD*X)-CEXP(CMPLX(0.,A*X))/(2.*A))
      EZ0=-CONST*BETA*(PI/W)*F2*SIN(PI*Y)*COS(DD*X)
      HX0=-BETA*10.*PI*(F1*COS(A*X)+F2*COS(PI*Y)*COS(DD*X)-(1./(2.*A))*
     $CEXP(CMPLX(0.,A*X)))
      HZ0=CONST*A*F1*SIN(A*X)+CONST*DD*F2*COS(PI*Y)*SIN(DD*X)-
     $0.5*CEXP(CMPLX(0.,A*X))
      REX0(I,J,K)=REAL(EX0)
      AMEX0(I,J,K)=AIMAG(EX0)
      REY0(I,J,K)=REAL(EY0)
```

THIS PAGE IS BEST QUALITY PRACTICABLE
FROM COPY FURNISHED TO DDC

```
      AMEYO(I,J,K)=AIMAG(EYO)
      REZO(I,J,K)=REAL(EZO)
      AMEZO(I,J,K)=AIMAG(EZO)
      RHXO(I,J,K)=REAL(HXO)
      AMHXO(I,J,K)=AIMAG(HXO)
      RHZO(I,J,K)=REAL(HZO)
      AMHZO(I,J,K)=AIMAG(HZO)
      Y=Y+YBRS
      I=I+1
      IF(Y.LE.YBRF) GO TO 20
      X=X+XBRS
      J=J+1
      IF(X.LE.XBRF) GO TO 30
   98 CONTINUE
      DO 99 L=162,188
      BETA=BETAB(L)
      K=L
      A=10.*PI*SQRT(1.-BETA**2)
      X=XBRI
      J=1
      B=A*W/PI
      CALL BE(A,B,BB,PI,M)
      X=XBRI
   17 AA=CEXP(CMPLX(0.,A*X))
      EYO=-0.5*(AA-BB*COS(A*X))/SQRT(1.-BETA**2)
      HXO=-BETA*EYO
      HZO=0.5*(-SIGN(1.,X)*AA+CONST*BB*SIN(A*X))
      DO 18 I=1,10
      REXO(I,J,K)=0.
      AMEXO(I,J,K)=0.
      REZO(I,J,K)=0.
      AMEZO(I,J,K)=0.
      REYO(I,J,K)=REAL(EYO)
      AMEYO(I,J,K)=AIMAG(EYO)
      RHXO(I,J,K)=REAL(HXO)
      AMHXO(I,J,K)=AIMAG(HXO)
      RHZO(I,J,K)=REAL(HZO)
   18 AMHZO(I,J,K)=AIMAG(HZO)
      X=X+XBRS
      J=J+1
      IF(X.LE.XBRF) GO TO 17
   99 CONTINUE
      WRITE(3,101) REXO,AMEXO,REYO,AMEYO,REZO,AMEZO,RHXO,AMHXO,RHZO,AM
     $HZO
  101 FORMAT(10F8.5)
      DY=0.1
      DX=0.1
      YY(1)=0.
      DO 50 I=1,9
      YY(I+1)=YY(I)+DY
   50 CONTINUE
```

THIS PAGE IS BEST QUALITY PRACTICABLE
FROM COPY FURNISHED TO DDC

```
      XX(1)=0.1
      DO 60 I=1,8
      XX(I+1)=XX(I)+DX
   60 CONTINUE
      WRITE(3,101) YY,XX,BETAB
      STOP
      END
      SUBROUTINE BE1(A,B,BBK,PI,M,CON,ALFA1)
      COMPLEX F,BBK
      AM1=0.
      DO 10 I=2,M
      AM1=AM1+B/I-ASIN(B/I)
   10 CONTINUE
      F=CEXP(CMPLX(-B*PI/2.,B*(CON-ALOG(B))-PI/2.+A+AM1))
      BBK=(ALFA1+B)*F
      RETURN
      END
      SUBROUTINE BE2(A,B,BBAL,PI,M,CON,ALFA1)
      COMPLEX F,BBAL,D
      AM1=0.
      DO 10 I=2,M
      AM1=AM1+ALFA1/I-ASIN(ALFA1/SQRT(I**2-1.))
   10 CONTINUE
      F=CEXP(CMPLX(-ALFA1*PI/2.,ALFA1*(CON-ALOG(B))+AM1+ALFA1*A/B))
      D=CMPLX(1.,-ALFA1)
      BBAL=F*D*SQRT(2.)*ALFA1/B
      RETURN
      END
      SUBROUTINE TE1(A,B,T1,BBK,PI)
      COMPLEX T1,BBK,D1
      D=B*SQRT(PI)/SQRT(A*2.)
      D1=CMPLX(1.+D,-D)
      T1=BBK**2*D1
      RETURN
      END
      SUBROUTINE F12(A,B,T1,ALFA1,BBK,BBAL,F1,F2)
      COMPLEX T1,BBK,BBAL,F1,F2,D1
      D1=ALFA1*(1.+T1)*(BBAL**2*(4.*T1*B/(1.+T1)-(ALFA1+B)**2/ALFA1)/
     $(2.*ALFA1)-1.)
      F1=(BBK**2/((1.+T1)*A))*(1.+2.*B*BBAL**2/D1)
      F2=2.*B*BBK*BBAL/(A*D1)
      RETURN
      END
      SUBROUTINE BE(A,B,BB,PI,M)
      COMPLEX T,F,BB
      CONST=1.115931516
      AM1=0.
      DO 10 I=1,M
      AM1=AM1+B/I-ASIN(B/I)
   10 CONTINUE
      T=CEXP(CMPLX(-B*PI,2.*(B*(CONST-ALOG(B))+A+AM1)))
      F1=SQRT(PI)*B/SQRT(2.*A)
      F=CMPLX(1.+F1,-F1)
      BB=2.*T/(1.+T*F)
      RETURN
      END
```

Attachment B

SUPPLEMENT TO ELECTROMAGNETICS LABORATORY REPORT NO. 78-4

(Source Excitation of an Open, Parallel-Plate Waveguide. Numerical Results)

by

V. Krichevsky

UNCLASSIFIED

SECURITY CLASSIFICATION OF THIS PAGE (When Data Entered)

REPORT DOCUMENTATION PAGE		READ INSTRUCTIONS BEFORE COMPLETING FORM
1. REPORT NUMBER	2. GOVT ACCESSION NO.	3. RECIPIENT'S CATALOG NUMBER
4. TITLE (and Subtitle) SUPPLEMENT TO ELECTROMAGNETICS LABORATORY REPORT NO. 78-4 (Source Excitation of an Open, Parallel-Plate Waveguide, Numerical Results)		5. TYPE OF REPORT & PERIOD COVERED Scientific Report 6. PERFORMING ORG. REPORT NUMBER EM 78-13; UILU-ENG-78-2555
7. AUTHOR(s) V. Krichevsky		8. CONTRACT OR GRANT NUMBER(s) AFOSR 76-3066
9. PERFORMING ORGANIZATION NAME AND ADDRESS Electromagnetics Laboratory Department of Electrical Engineering University of Illinois, Urbana, Illinois 61801		10. PROGRAM ELEMENT, PROJECT, TASK AREA & WORK UNIT NUMBERS Project-Task 2301/A3 P. R. No. N/A
11. CONTROLLING OFFICE NAME AND ADDRESS Air Force Office of Scientific Research Building 410 Bolling AFB, Washington, DC 20332		12. REPORT DATE October 1978 13. NUMBER OF PAGES 25
14. MONITORING AGENCY NAME & ADDRESS(if different from Controlling Office)		15. SECURITY CLASS. (of this report) Unclassified 15a. DECLASSIFICATION DOWNGRADING SCHEDULE

16. DISTRIBUTION STATEMENT (of this Report)

Distribution of this document is unlimited.

17. DISTRIBUTION STATEMENT (of the abstract entered in Block 20, if different from Report)

18. SUPPLEMENTARY NOTES

19. KEY WORDS (Continue on reverse side if necessary and identify by block number)

EM Field
Open Parallel-Plate Waveguide
Source Excitation Problem
Numerical Results

20. ABSTRACT (Continue on reverse side if necessary and identify by block number)

In this work we investigate numerically the problem of the source excitation of an open, parallel-plate waveguide. The following assumptions are made for the source current 1) the current is oriented in the y-direction, 2) it is located at $x = 0$, 3) there is no variation in the y-direction, 4) and the current has exp (i3z) behavior along the longitudinal z-direction. We provide graphical output for the EM-field components as functions of a longitudinal propagation constant and transverse coordinates and then discuss these results. (ABSTRACT for 78-4)

DD FORM 1 JAN 73 1473

UNCLASSIFIED

SECURITY CLASSIFICATION OF THIS PAGE (When Data Entered)

UILU-ENG-78-2555

Electromagnetics Laboratory Report No. 78-13

SUPPLEMENT TO ELECTROMAGNETICS LABORATORY REPORT NO. 78-4 (SOURCE EXCITATION OF AN OPEN, PARALLEL-PLATE WAVEGUIDE. NUMERICAL RESULTS)

by

V. Krichevsky

Scientific Report

October 1978

Supported by

Grant No. 76-3066B
Air Force Office of Scientific Research
Bolling AFB, Washington, D.C. 20332

Electromagnetics Laboratory
Department of Electrical Engineering
Engineering Experiment Station
University of Illinois at Urbana-Champaign
Urbana, Illinois 61801

SUPPLEMENT TO ELECTROMAGNETICS LABORATORY
REPORT NO. 78-4

In Electromagnetics Laboratory Report No. 78-4, we have calculated the electromagnetic fields as functions of β, the normalized propagation constant in the z-direction. The parameters chosen for the computation in the report were:

$$\frac{H}{L} = 0.16670, \quad \frac{L}{\lambda_0} = 5, \quad \text{where} \quad \lambda_0 = \frac{2\pi}{\omega\sqrt{\varepsilon\mu}} .$$

At the request of Dr. D. Giri of SAI, we have now derived additional numerical results for the following choice of parameters, which correspond to those of the experimental parallel-plate structure being investigated at Harvard.

$L = 12.5$ m

$H = 12.75$ m

$f = 25$ Mny ($\lambda_0 = 12$m)

$$\frac{H}{L} = 1.020 \; ; \quad \frac{L}{\lambda_0} = 1.041667$$

The propagation constant in the x-direction can be written in the form:

$$\alpha_n = \frac{\pi}{H} \left(\frac{kH}{\pi} - m^2 \right)^{1/2}, \quad m = 0,1,2,\ldots$$

where $k = k_0 \sqrt{1 - \beta^2}$, $k_0 = \frac{2\pi}{\lambda_0}$

$$kL \leq k_0 L = 2\pi \frac{L}{\lambda} = 6.544985.$$

The asymptotic analysis presented in our report 78-4 was based on the assumption (kL>>1). Consequently, great care should be exercised when the range of application of these formulas is extended below kL = 10.

It is not difficult to prove that in the range $0 < \tilde{\beta} < 0.337916$, only three modes are above cut-off in the x-direction. Furthermore, two modes are propagating in the range $0.337916 < \tilde{\beta} < 0.882353$ and only one mode can propagate in the range $\tilde{\beta} > 0.882353$. The application of the formulas and computer programs developed in Report No. 78-4, though not the theory itself, is restricted to the range where two modes can propagate in the x-direction. For this reason, we develop the numerical results only for the region $\tilde{\beta} \geq 0.34$, and specifically for the range

$$0.34 \leq \tilde{\beta} \leq 0.9.$$

We would like to mention that it is possible to develop the necessary formulas and numerical results for the region $0 < \tilde{\beta} < 0.34$ using the theory given in the Electromagnetics Report No. 77-19.

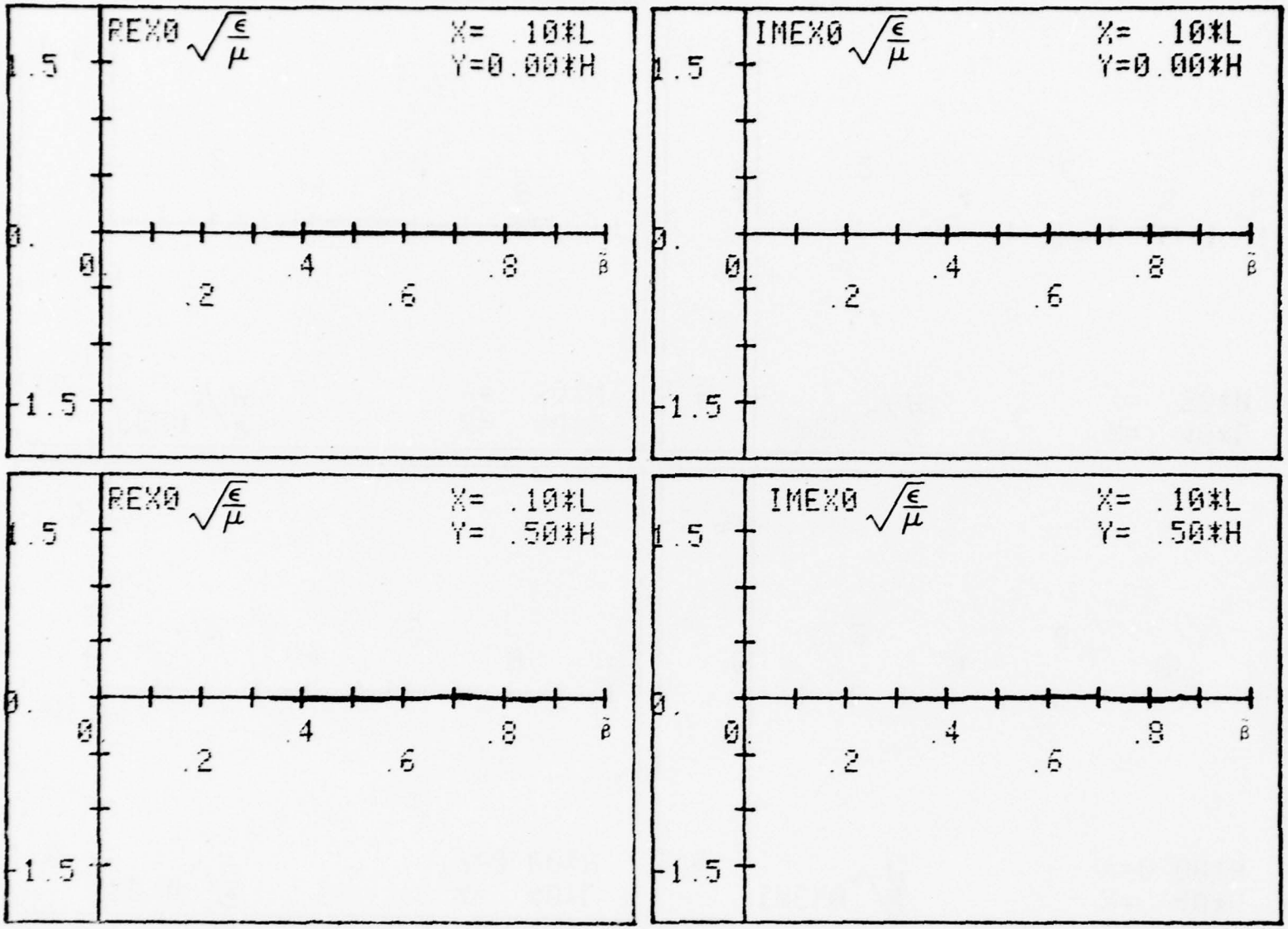

Figure 1. Real and imaginary parts of E_x as functions of $\tilde{\beta}$ for parameters given in the lower half of Page 1. The x,y values of the observation point are shown in the inset.

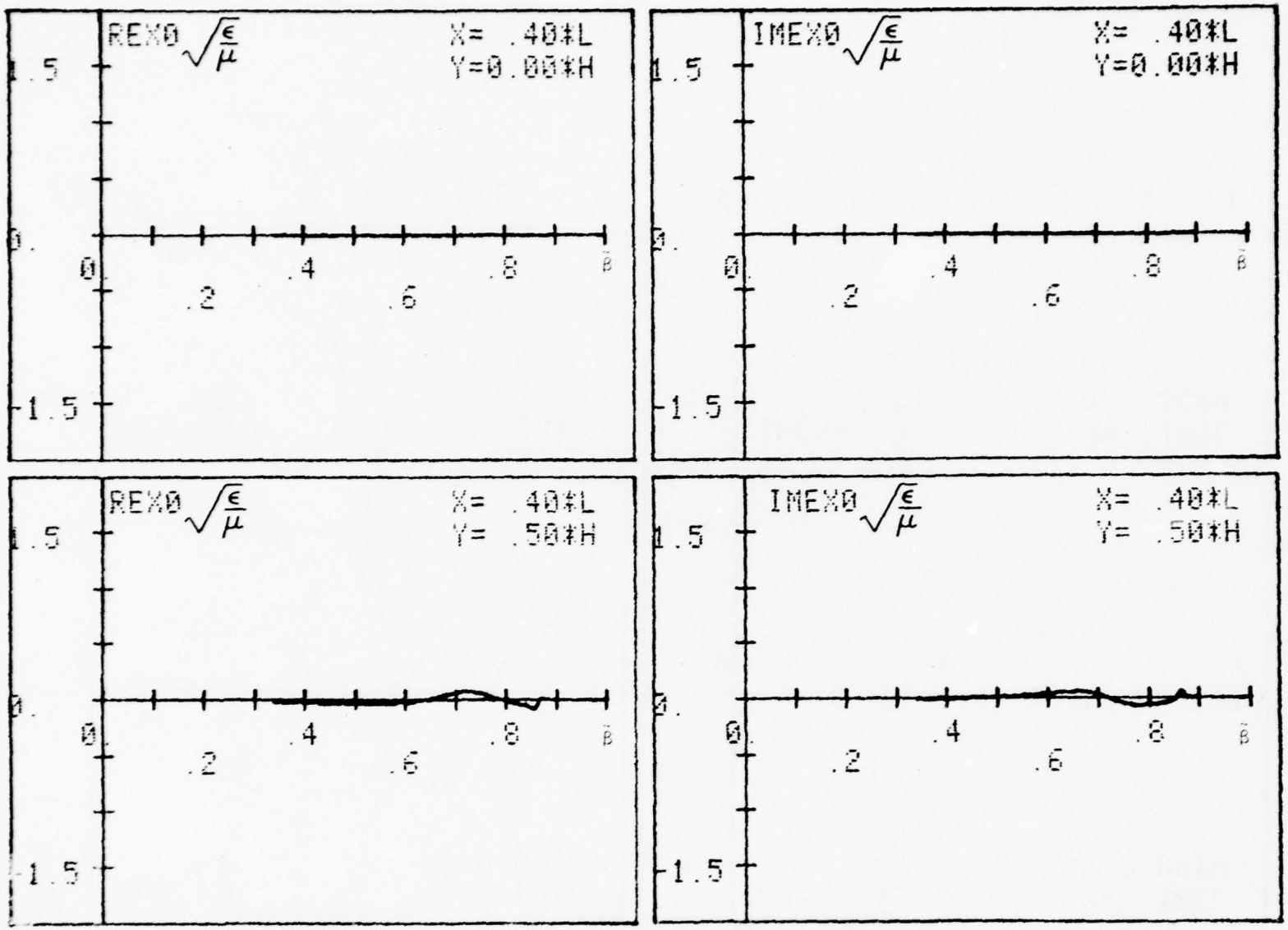

Figure 2. Real and imaginary parts of E_x as functions of β for parameters given in the lower half of Page 1. The x,y values of the observation point are shown in the inset.

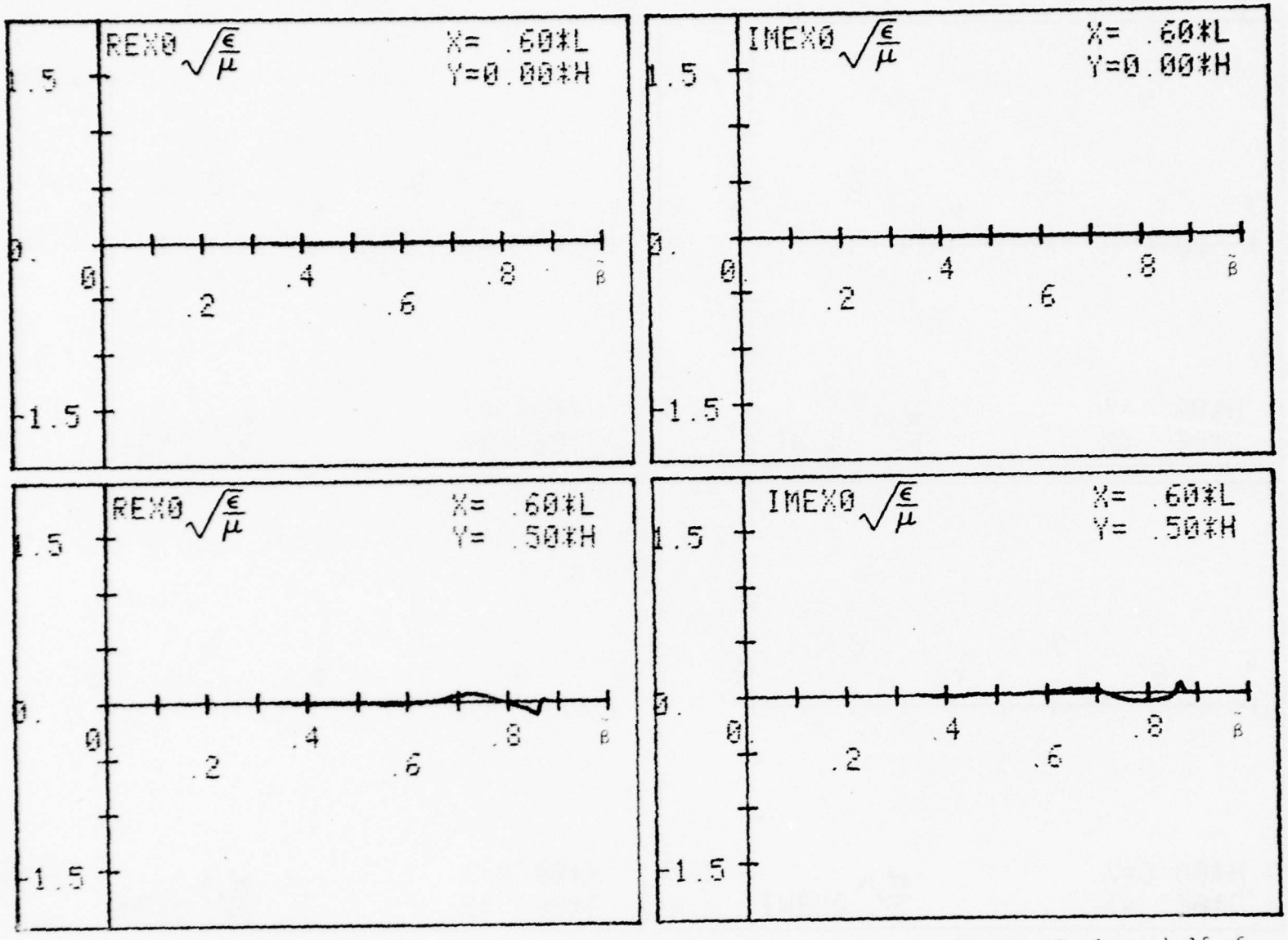

Figure 3. Real and imaginary parts of E_x as functions of β for parameters given in the lower half of Page 1. The x,y values of the observation point are shown in the inset.

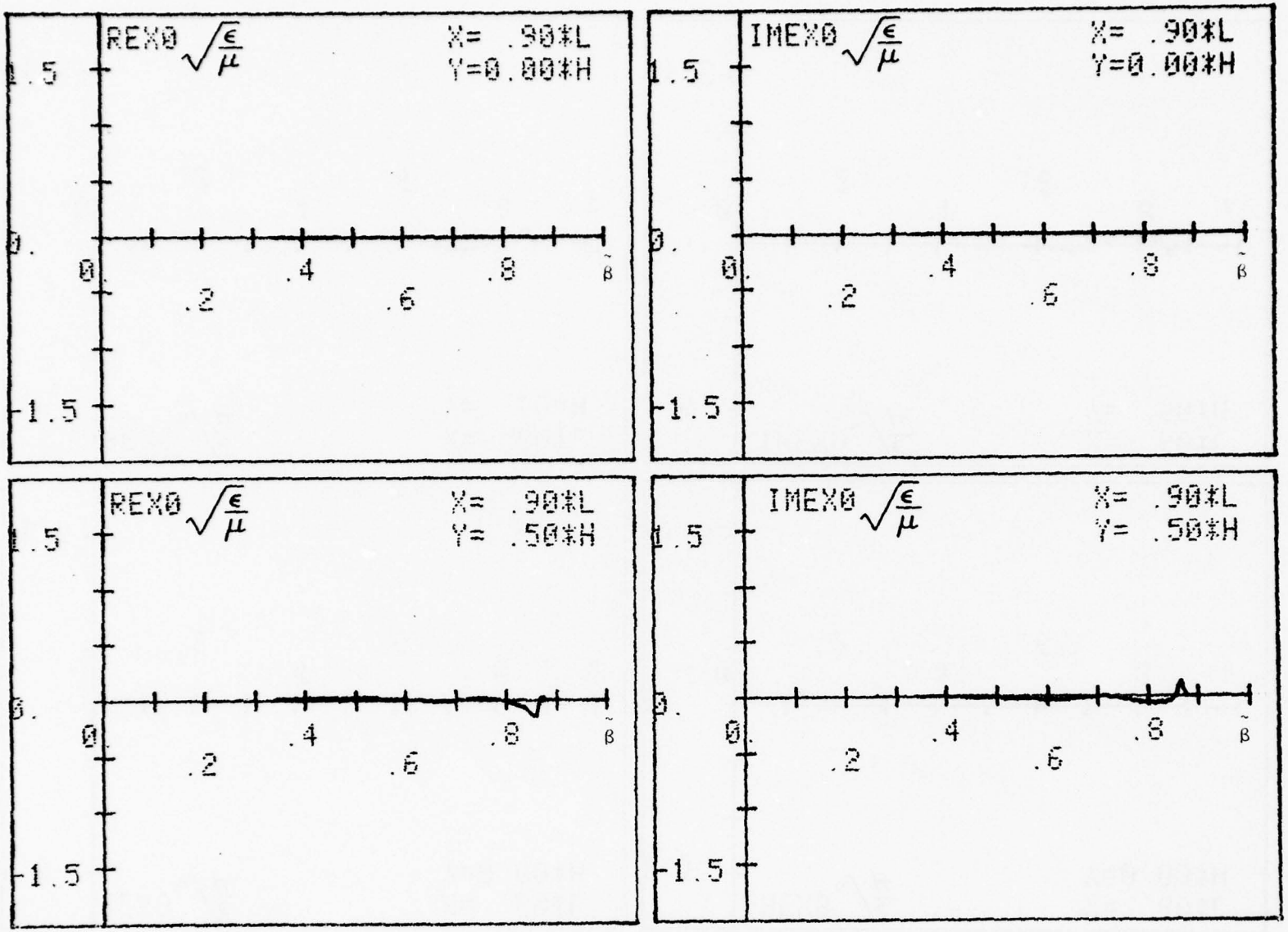

Figure 4. Real and imaginary parts of $E_x^{\tilde{e}}$ as functions of β for parameters given in the lower half of Page 1. The x,y values of the observation point are shown in the inset.

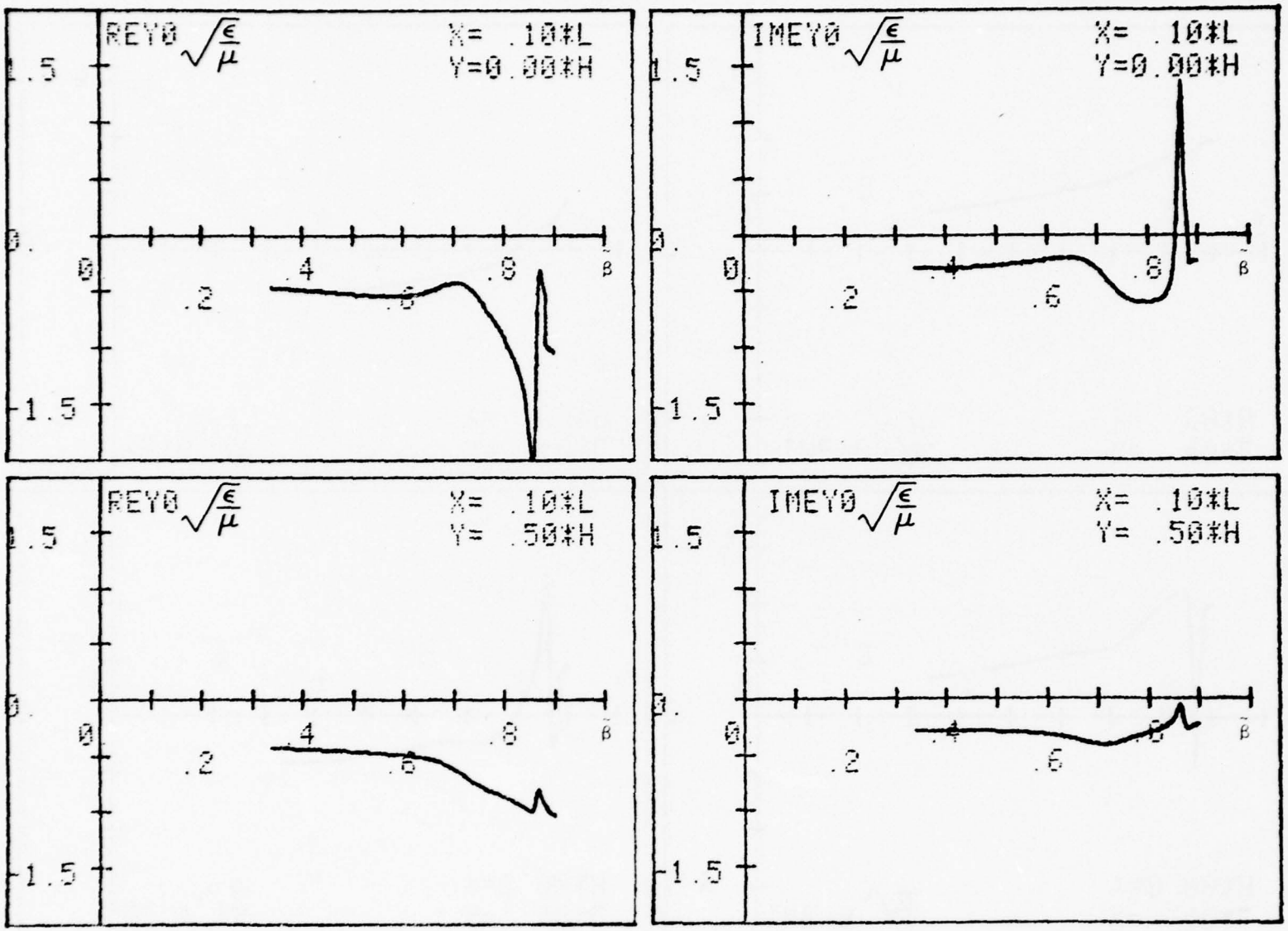

Figure 5. Real and imaginary parts of E_x as functions of β for parameters given in the lower half of Page 1. The x,y values of the observation point are shown in the inset.

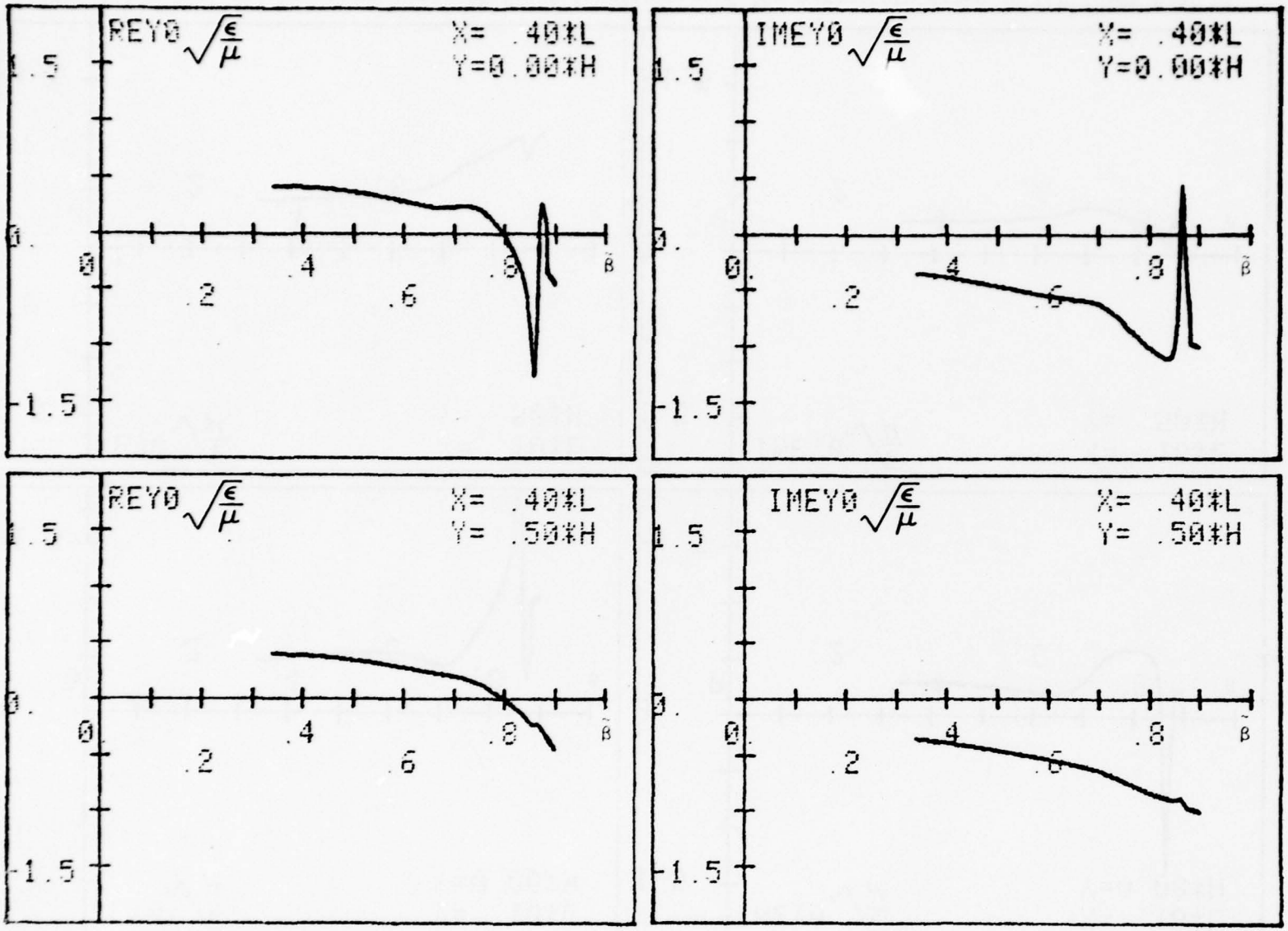

Figure 6. Real and imaginary parts of E_x as functions of β for parameters given in the lower half of Page 1. The x,y values of the observation point are shown in the inset.

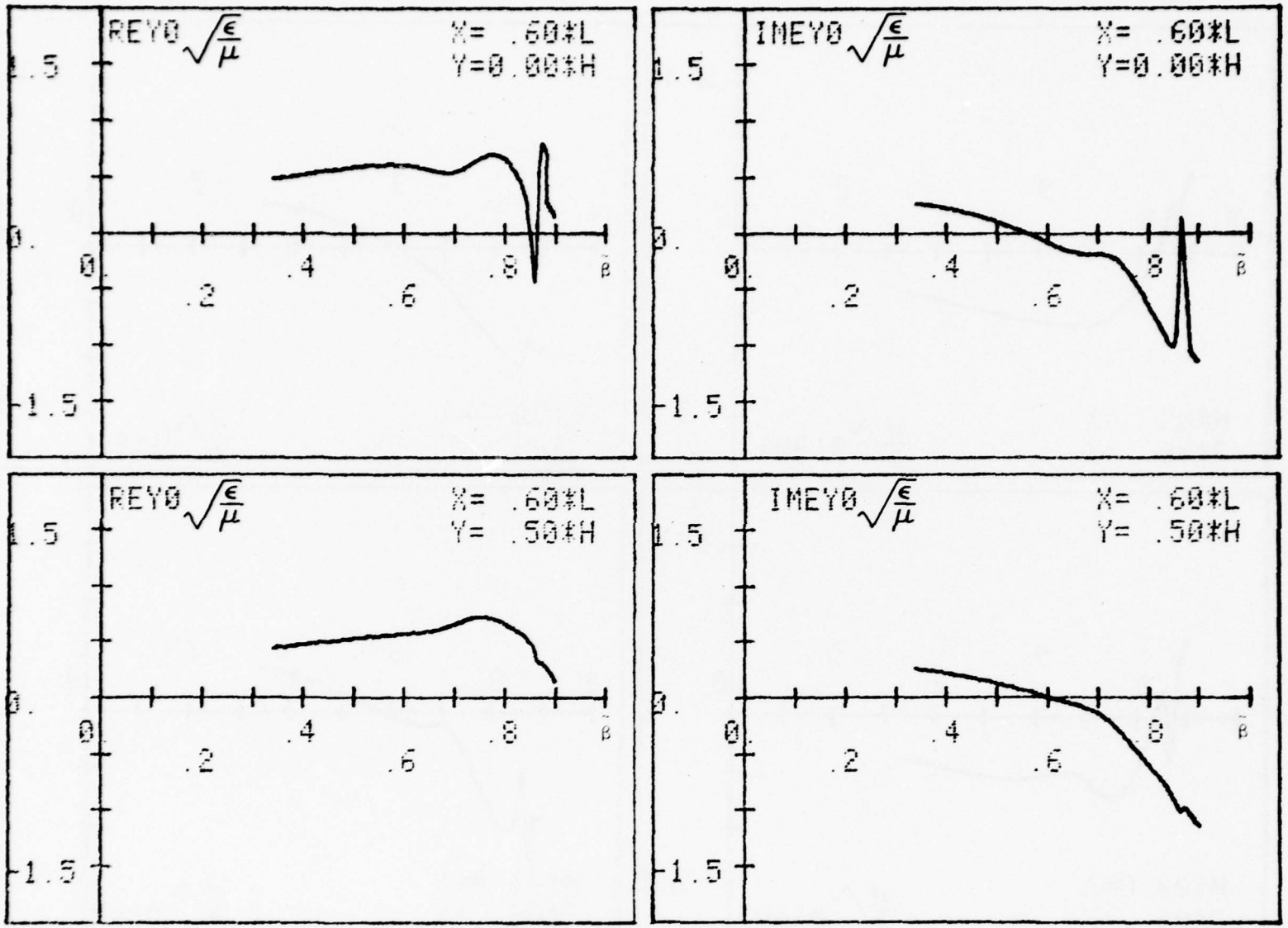

Figure 7. Real and imaginary parts of E_x as functions of $\tilde{\beta}$ for parameters given in the lower half of Page 1. The x,y values of the observation point are shown in the inset.

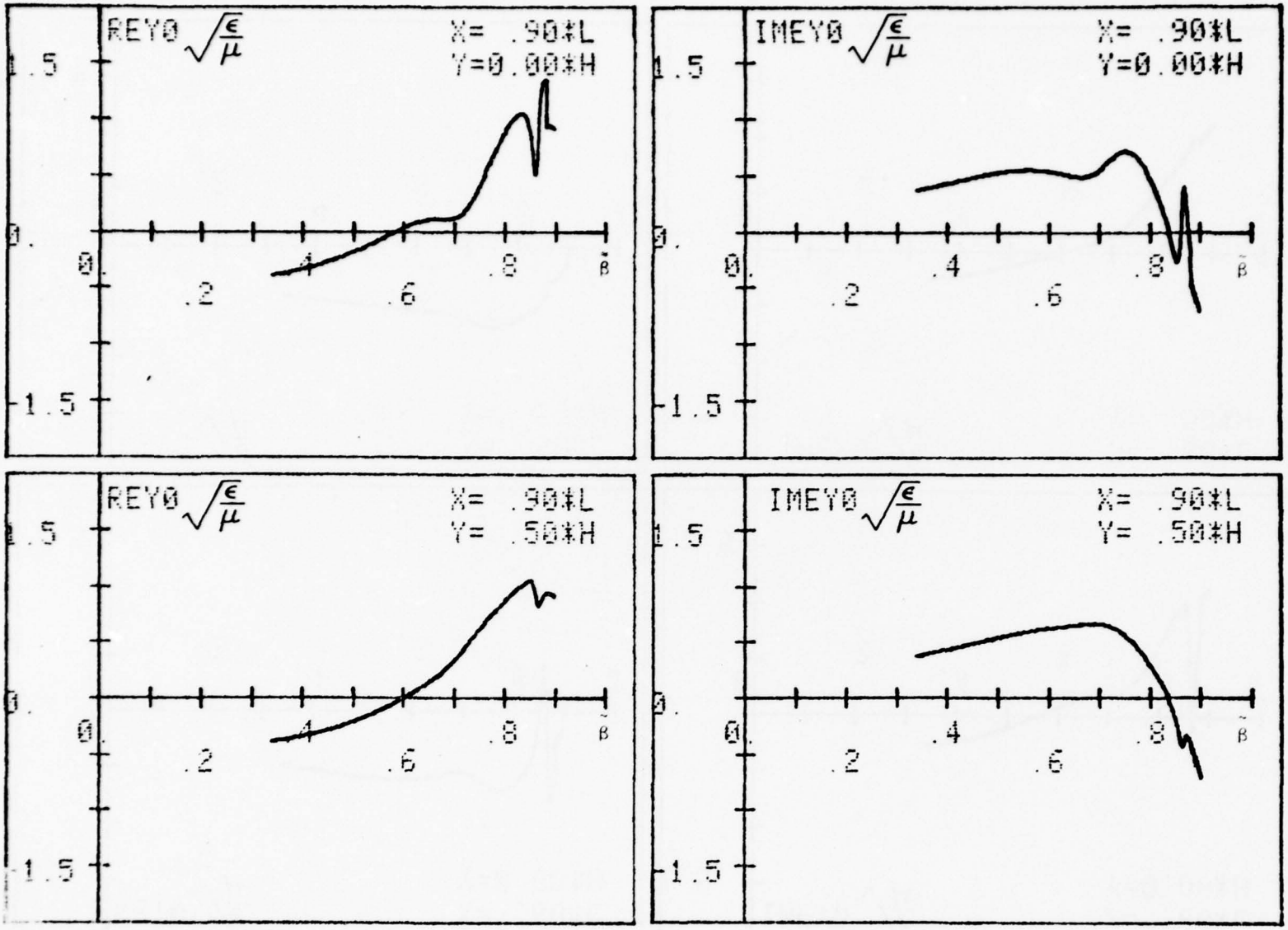

Figure 8. Real and imaginary parts of E_x as functions of $\tilde{\beta}$ for parameters given in the lower half of Page 1. The x,y values of the observation point are shown in the inset.

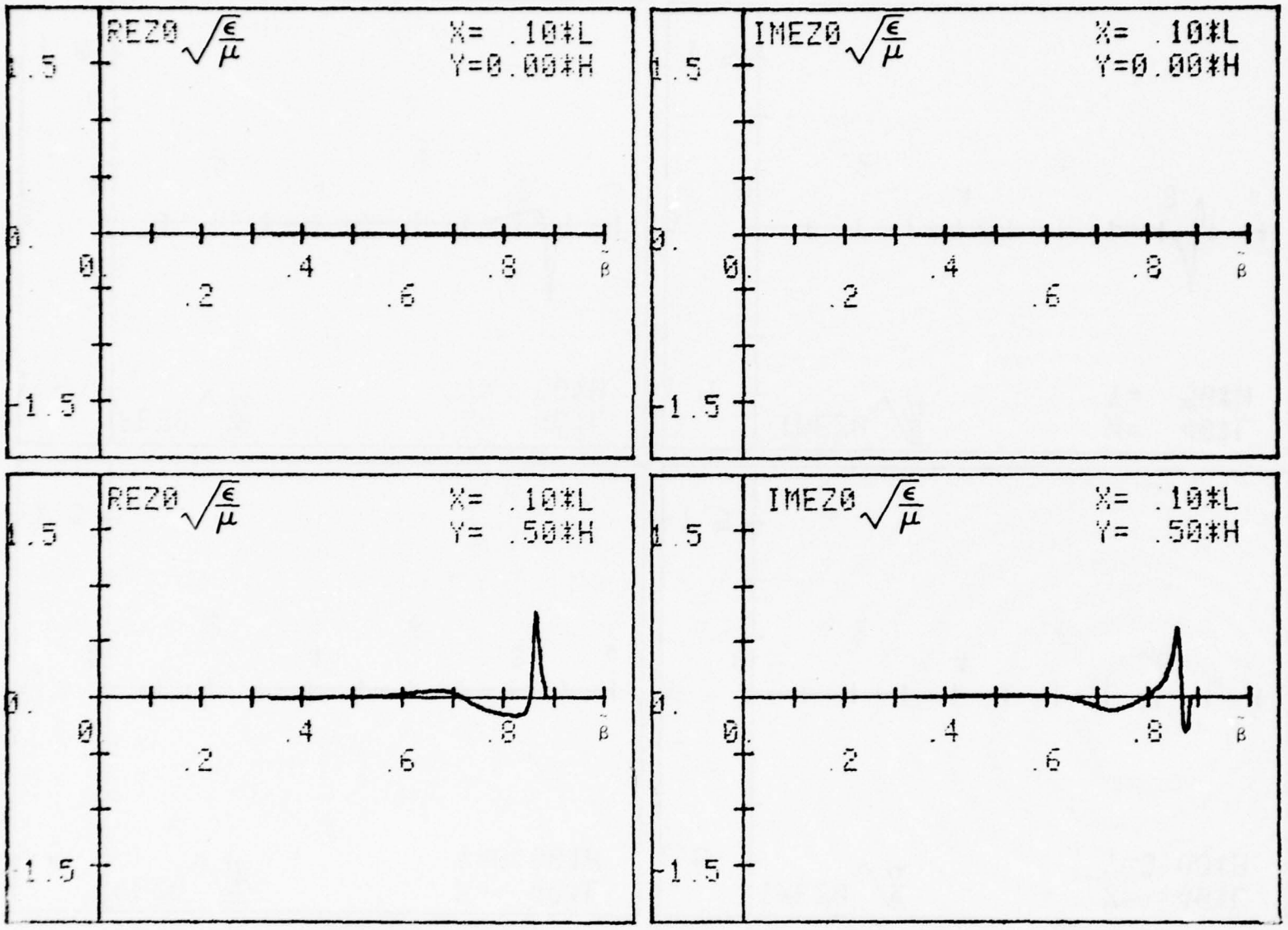

Figure 9. Real and imaginary parts of $E_{\tilde{x}}$ as functions of β for parameters given in the lower half of Page 1. The x,y values of the observation point are shown in the inset.

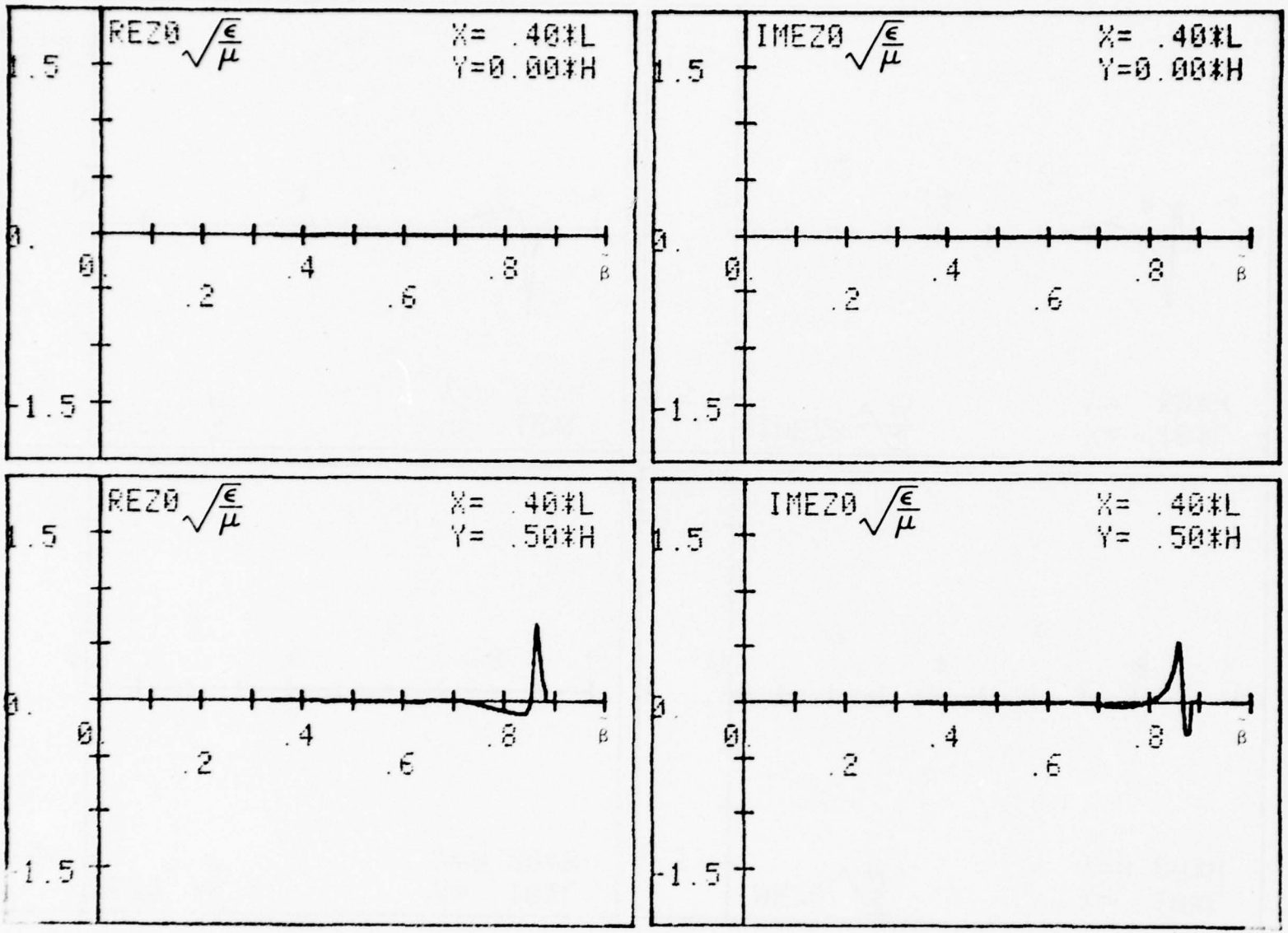

Figure 10. Real and imaginary parts of E_z as functions of β for parameters given in the lower half of Page 1. The x,y values of the observation point are shown in the inset.

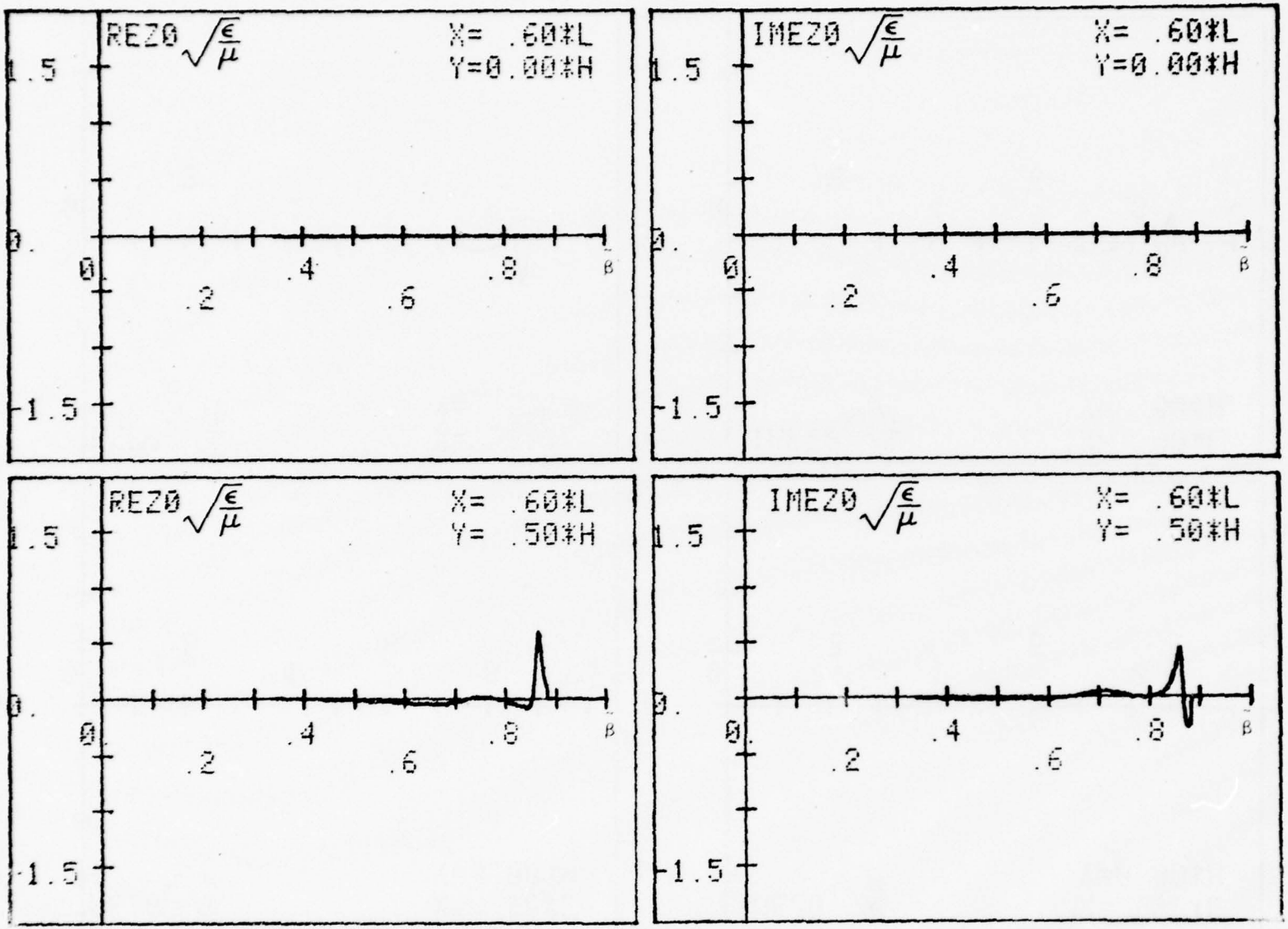

Figure 11. Real and imaginary parts of E_x as functions of β for parameters given in the lower half of Page 1. The x,y values of the observation point are shown in the inset.

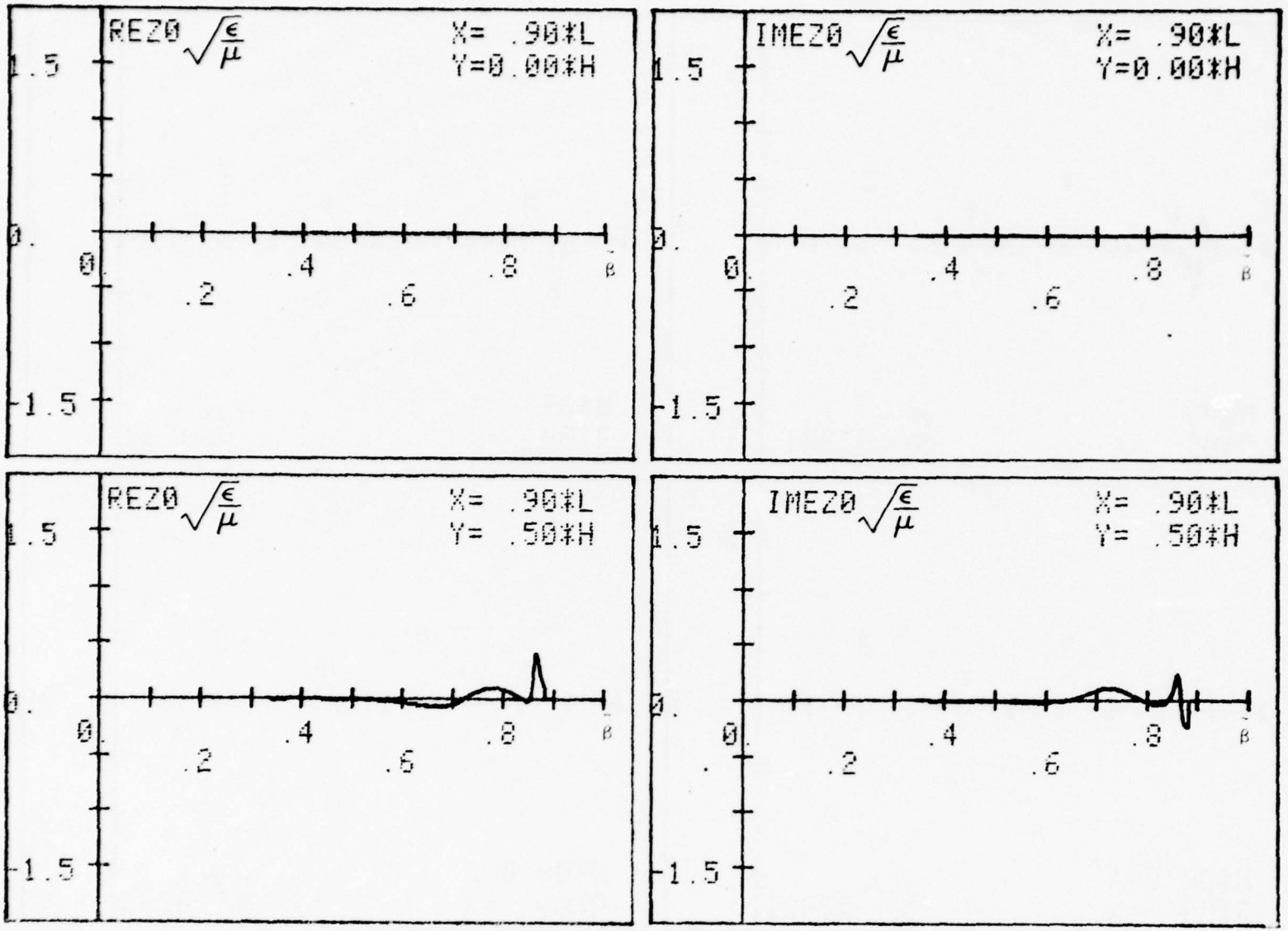

Figure 12. Real and imaginary parts of E_x as functions of β for parameters given in the lower half of Page 1. The x,y values of the observation point are shown in the inset.

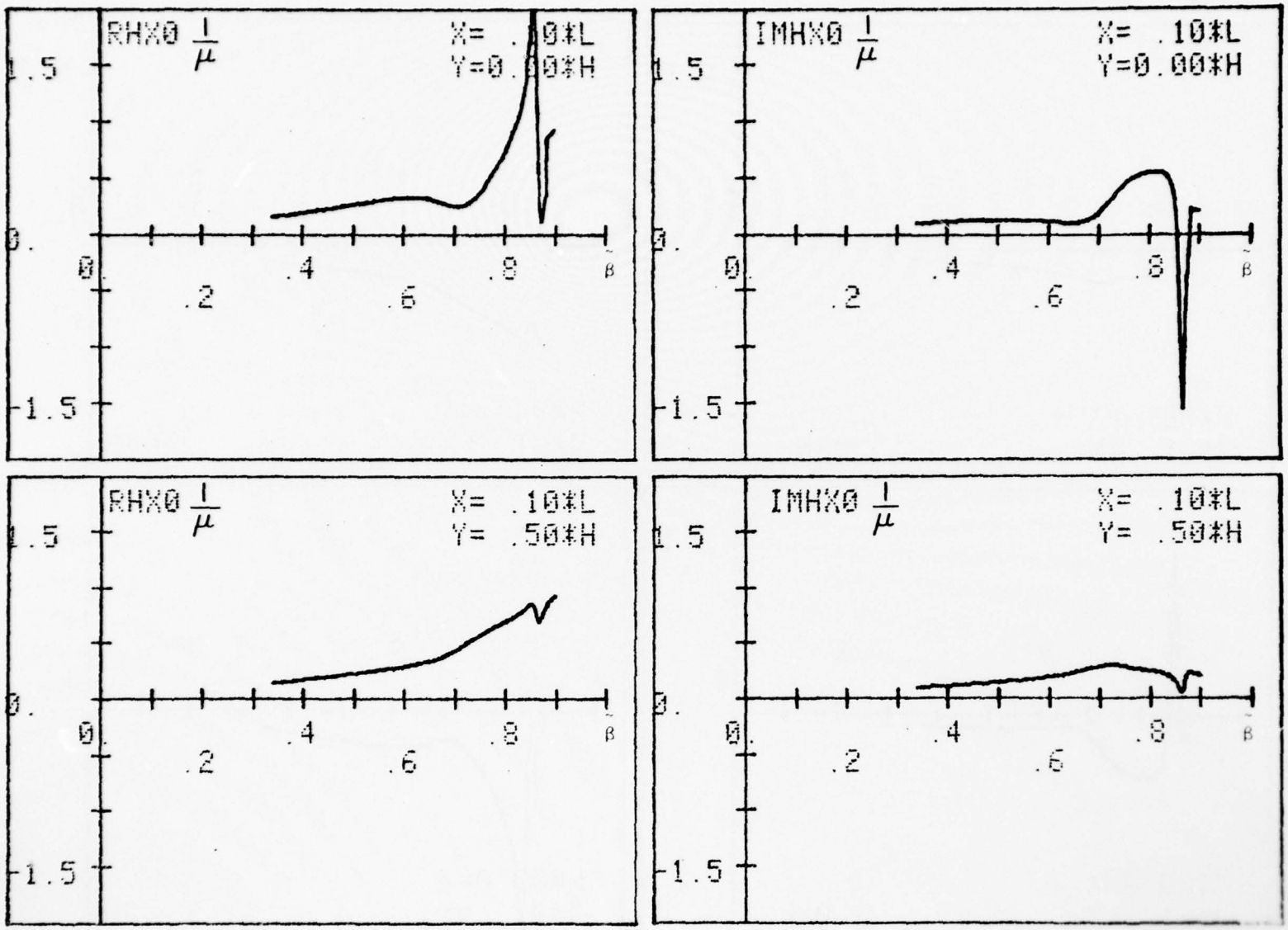

Figure 13. Real and imaginary parts of E_x as functions of β for parameters given in the lower half of Page 1. The x,y values of the observation point are shown in the inset.

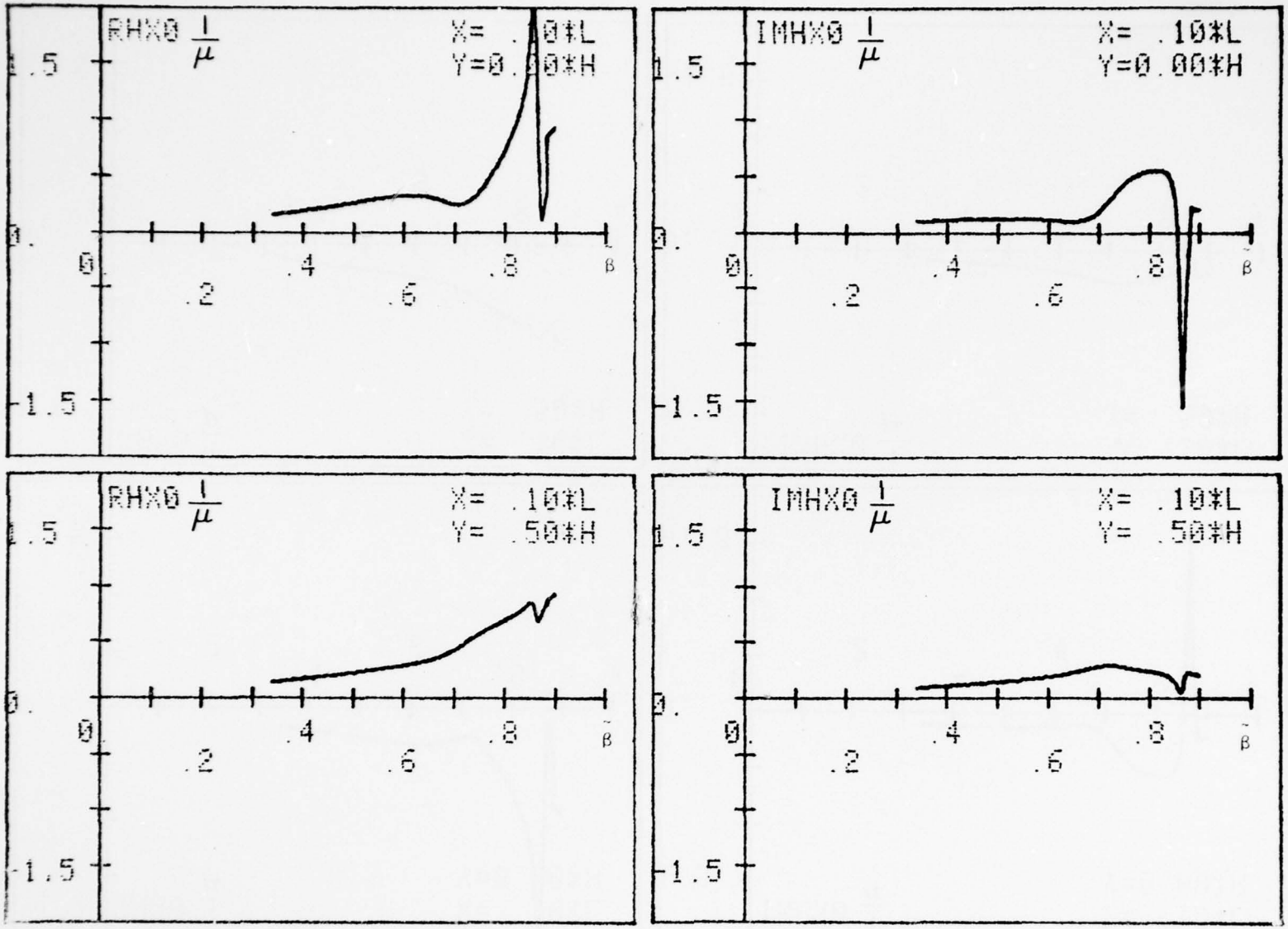

Figure 14. Real and imaginary parts of E_x as functions of β for parameters given in the lower half of Page 1. The x,y values of the observation point are shown in the inset.

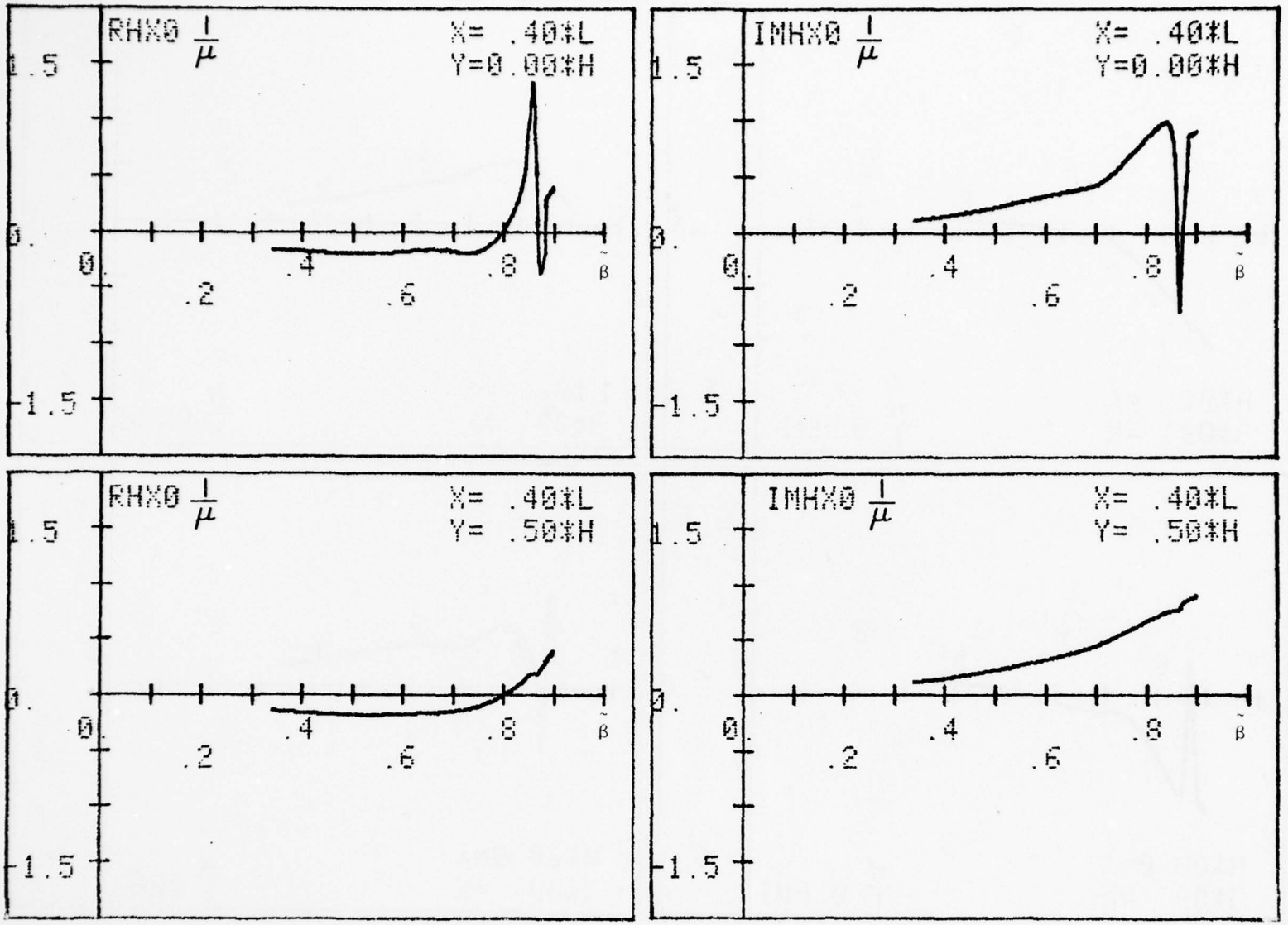

Figure 15. Real and imaginary parts of E_x as functions of $\tilde{\beta}$ for parameters given in the lower half of Page 1. The x,y values of the observation point are shown in the inset.

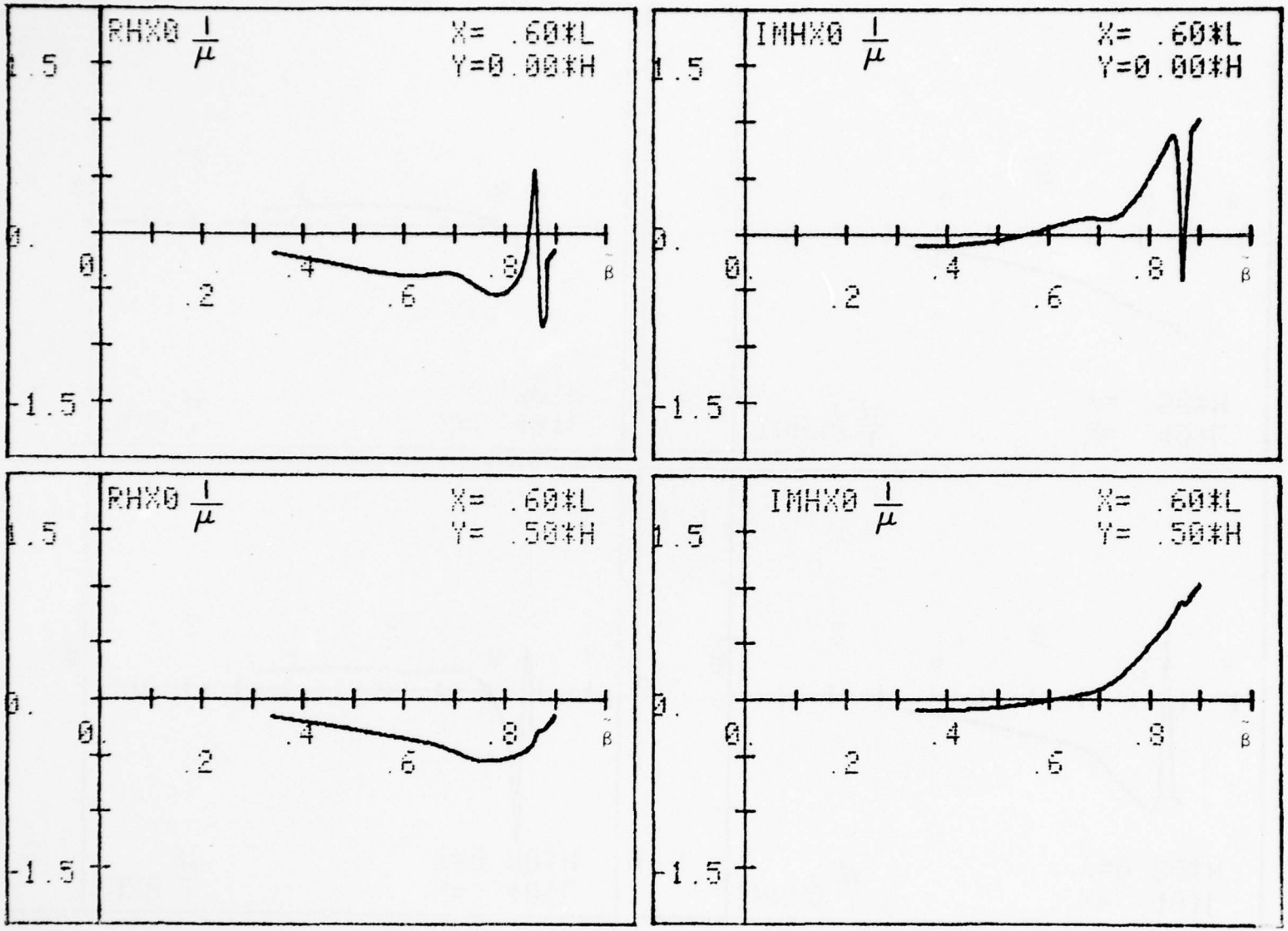

Figure 16. Real and imaginary parts of E_x as functions of β for parameters given in the lower half of Page 1. The x,y values of the observation point are shown in the inset.

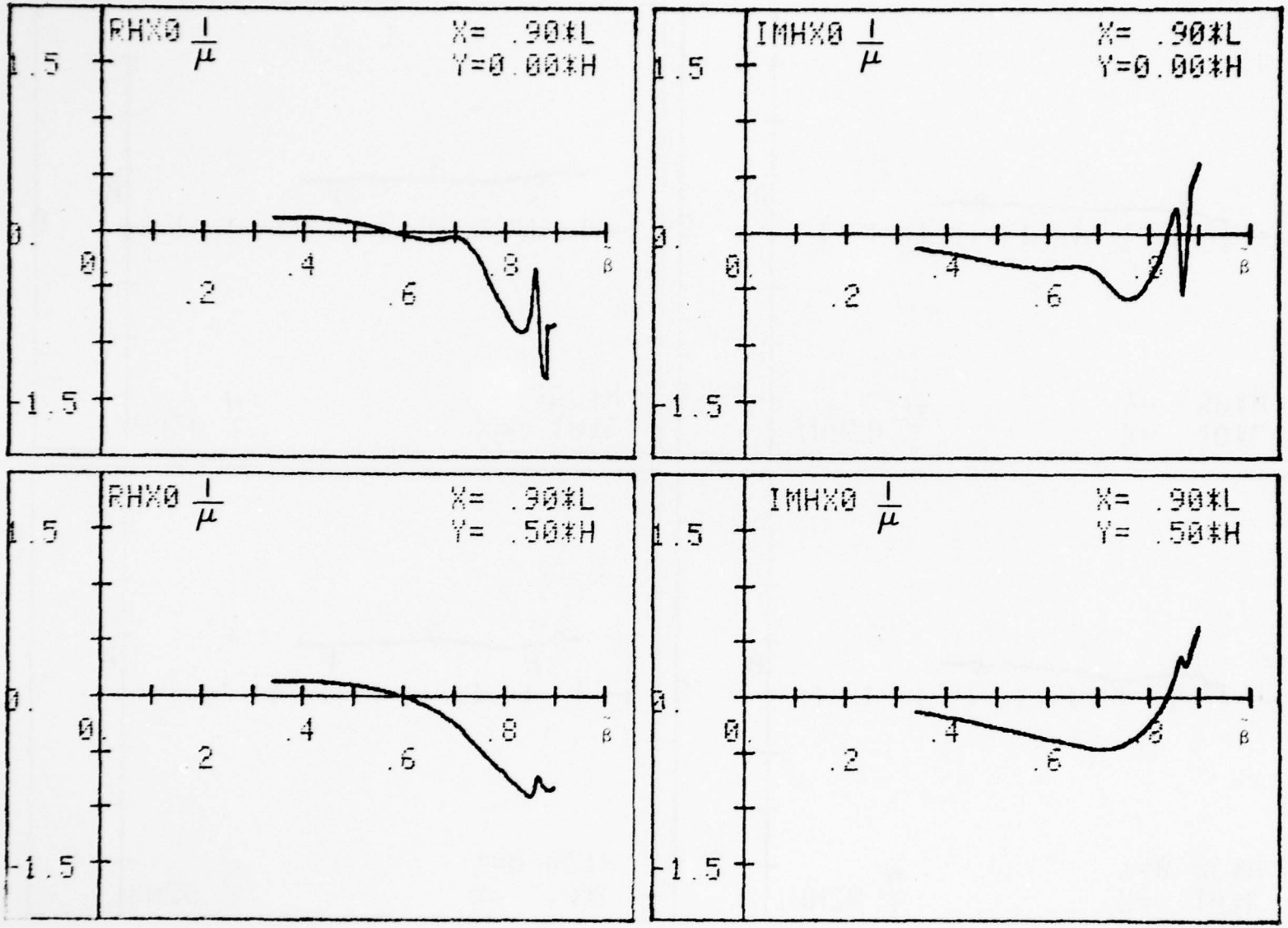

Figure 17. Real and imaginary parts of E_x as functions of β for parameters given in the lower half of Page 1. The x,y values of the observation point are shown in the inset.

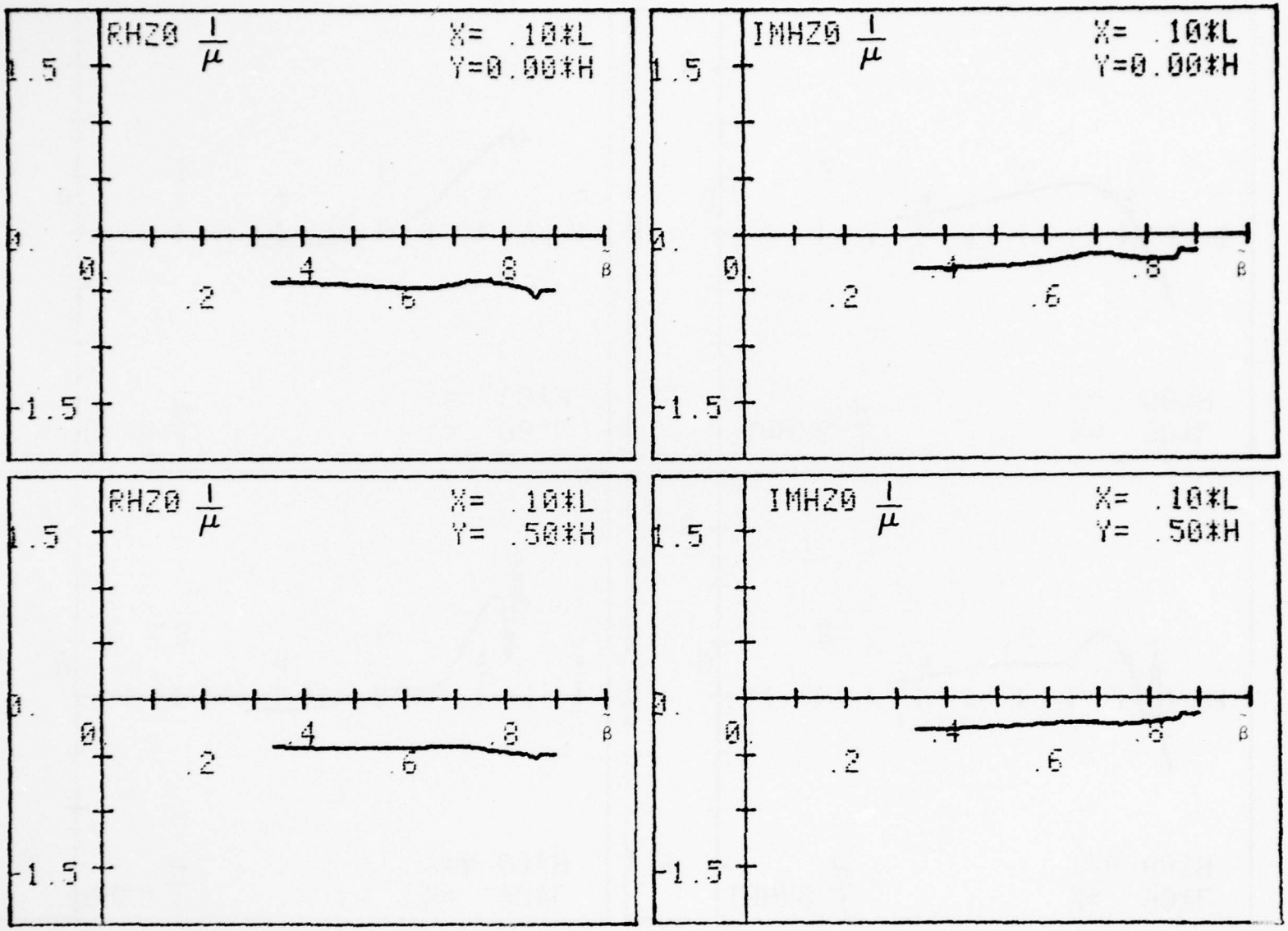

Figure 18. Real and imaginary parts of E_x as functions of β for parameters given in the lower half of Page 1. The x,y values of the observation point are shown in the inset.

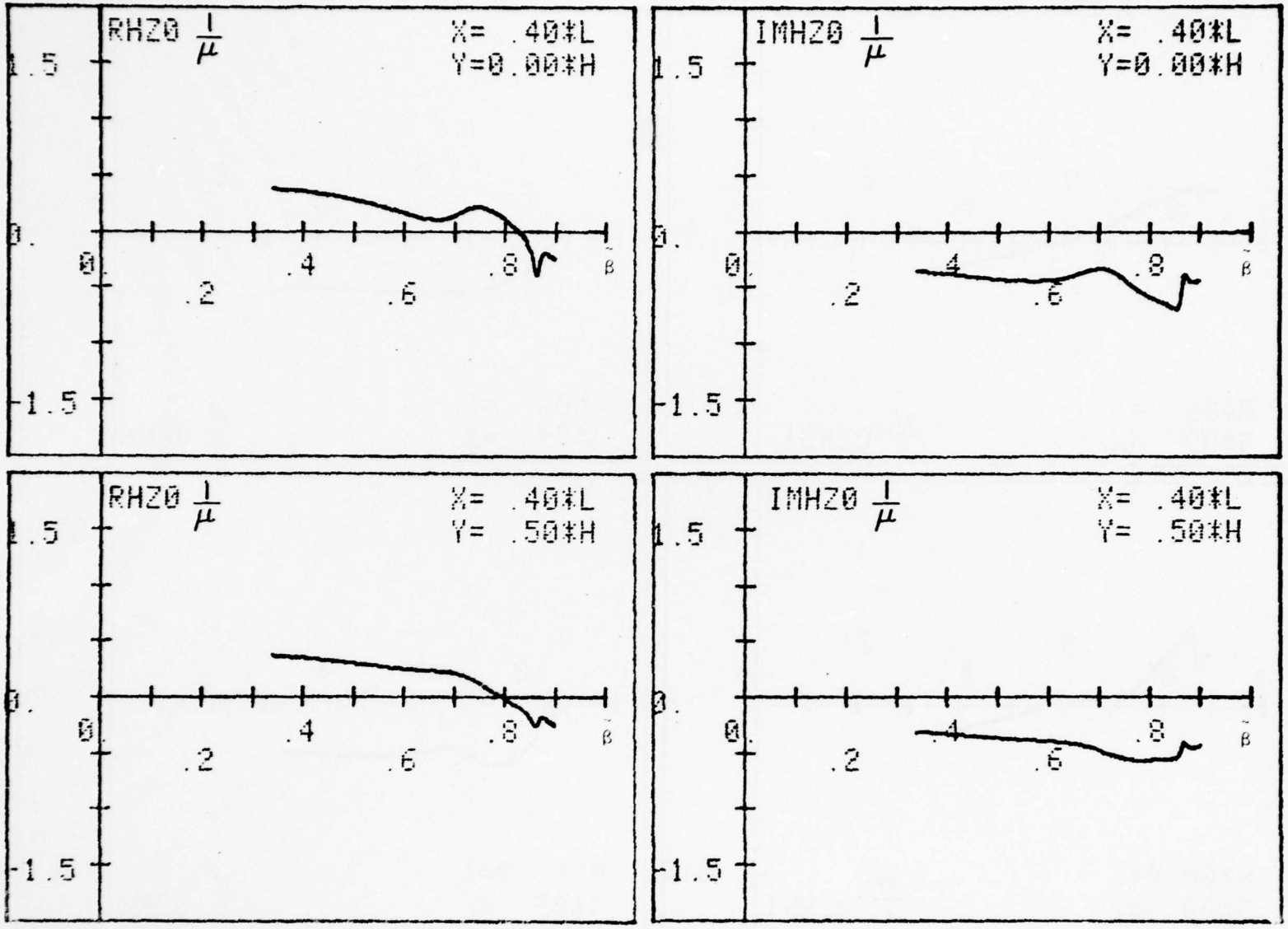

Figure 19. Real and imaginary parts of E_x as functions of β for parameters given in the lower half of Page 1. The x,y values of the observation point are shown in the inset.

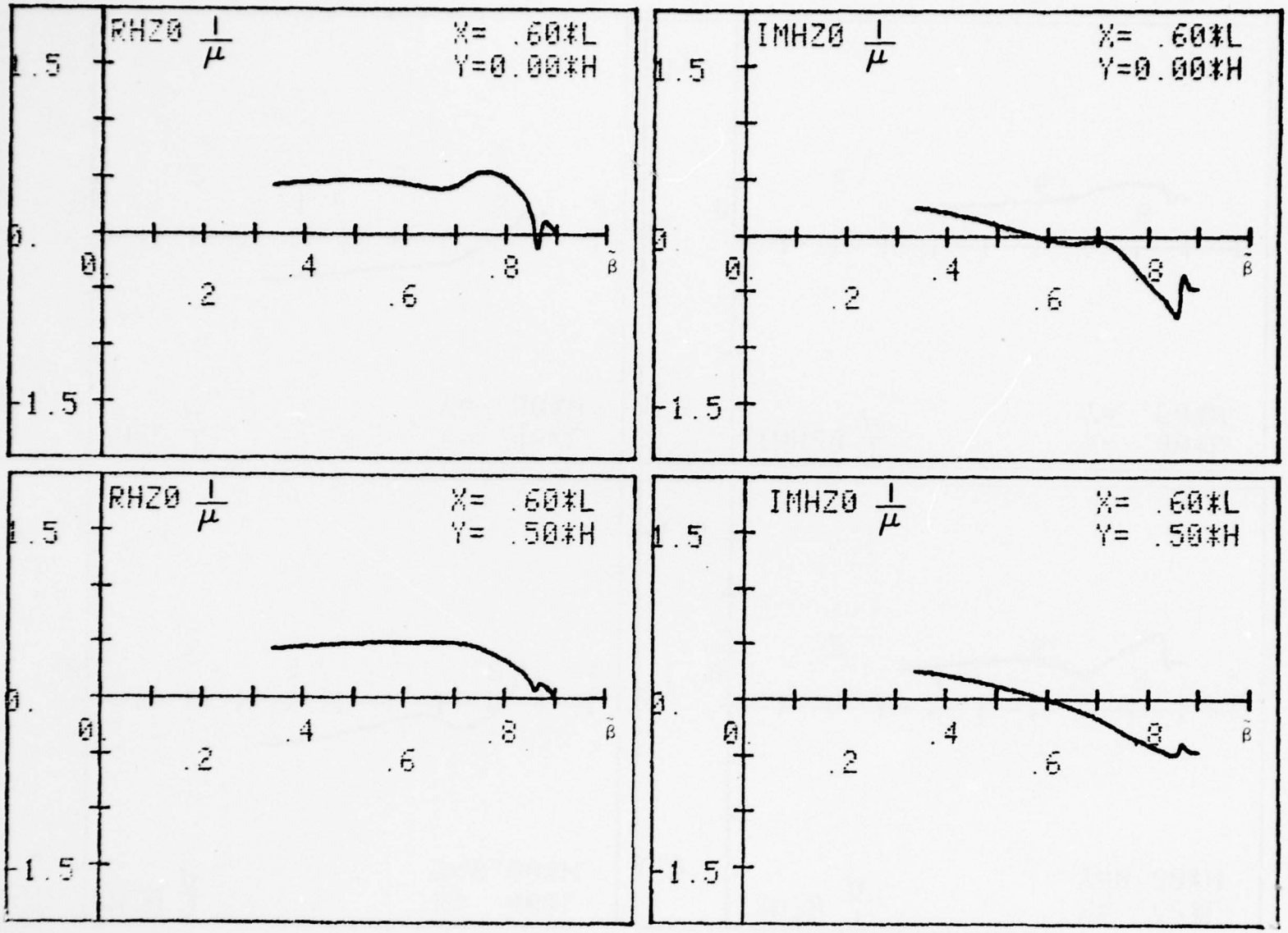

Figure 20. Real and imaginary parts of E_x as functions of $\tilde{\beta}$ for parameters given in the lower half of Page 1. The x,y values of the observation point are shown in the inset.

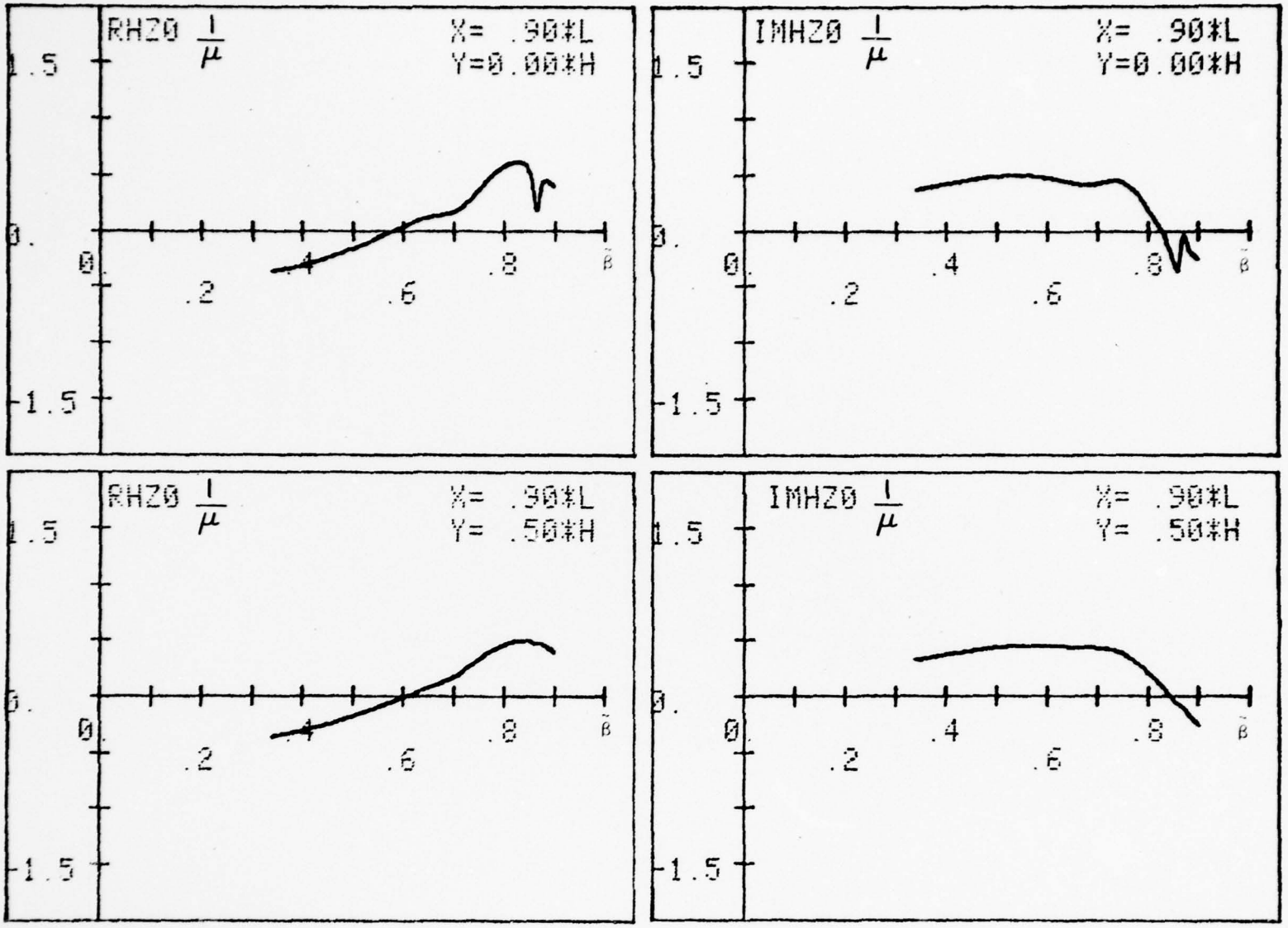

Figure 21. Real and imaginary parts of E_x as functions of β for parameters given in the lower half of Page 1. The x,y values of the observation point are shown in the inset.

ATTACHMENT C

THE SOURCE EXCITATION OF A FINITE-WIDTH PARALLEL-PLATE WAVEGUIDE

by

Chich-Hsing Tsao

Edward Yung

Raj Mittra

UNCLASSIFIED

SECURITY CLASSIFICATION OF THIS PAGE (When Data Entered)

REPORT DOCUMENTATION PAGE		READ INSTRUCTIONS BEFORE COMPLETING FORM
1. REPORT NUMBER	2. GOVT ACCESSION NO.	3. RECIPIENT'S CATALOG NUMBER
4. TITLE (and Subtitle) THE SOURCE EXCITATION OF A FINITE-WIDTH, PARALLEL-PLATE WAVEGUIDE		5. TYPE OF REPORT & PERIOD COVERED Technical Report 6. PERFORMING ORG. REPORT NUMBER EM 79-5; UIUL-ENG-79-2545
7. AUTHOR(s) Chich-Hsing Tsao, Edward Yung, and Raj Mittra		8. CONTRACT OR GRANT NUMBER(s) AFOSR 76-3066
9. PERFORMING ORGANIZATION NAME AND ADDRESS Electromagnetics Laboratory Department Of Electrical Engineering University of Illinois, Urbana, Illinois 61801		10. PROGRAM ELEMENT, PROJECT, TASK AREA & WORK UNIT NUMBERS Project-Task 2301/A3 P. R. No. N/A
11. CONTROLLING OFFICE NAME AND ADDRESS Air Force Office Of Scientific Research Building 410 Bolling AFB, Washington, DC 20332		12. REPORT DATE February 1979 13. NUMBER OF PAGES 46
14. MONITORING AGENCY NAME & ADDRESS(if different from Controlling Office)		15. SECURITY CLASS. (of this report) UNCLASSIFIED 15a. DECLASSIFICATION/ DOWNGRADING SCHEDULE

16. DISTRIBUTION STATEMENT (of this Report)

Distrubution of this document is unlimited.

17. DISTRIBUTION STATEMENT (of the abstract entered in Block 20, if different from Report)

18. SUPPLEMENTARY NOTES

19. KEY WORDS (Continue on reverse side if necessary and identify by block number)

Finite-Width Parallel-Plate Waveguide Method of Moments

20. ABSTRACT (Continue on reverse side if necessary and identify by block number)

The fields excited by a vertical current sheet source inside a parallel-plate waveguide are studied in this work. The analytical expressions for the fields have been derived, and the results of the numerical evaluation are presented. The field distributions have been obtained as functions of the longitudinal propagation constant and the transverse coordinates of the guide. The numerical results are presented in graphical forms, and the computer program used to obtain the results is contained in the Appendix.

DD FORM 1 JAN 73 1473 EDITION OF 1 NOV 65 IS OBSOLETE

UNCLASSIFIED

SECURITY CLASSIFICATION OF THIS PAGE (When Data Entered)

UIUL-ENG-79-2545

Electromagnetics Laboratory Report No. 79-5

THE SOURCE EXCITATION OF A FINITE-WIDTH, PARALLEL-PLATE WAVEGUIDE

by

Chich-Hsing Tsao

Edward Yung

Raj Mittra

Technical Report

February 1979

Supported by

Grant No. 76-3066
Air Force Office of Scientific Research
Bolling AFB, Washington, D. C. 20332

Electromagnetics Laboratory
Department of Electrical Engineering
Engineering Experiment Station
University of Illinois at Urbana-Champaign
Urbana, Illinois 61801

ABSTRACT

The fields excited by a vertical current sheet source inside a parallel-plate waveguide are studied in this work. The analytical expressions for the fields have been derived, and the results of the numerical evaluation are presented. The field distributions have been obtained as functions of the longitudinal propagation constant and the transverse coordinates of the guide. The numerical results are presented in graphical forms, and the computer program used to obtain the results is contained in the Appendix.

TABLE OF CONTENTS

		Page
I.	INTRODUCTION	1
II.	STATEMENT OF THE PROBLEM	3
III.	INCIDENT FIELD	5
IV.	SCATTERED FIELD	8
V.	NUMERICAL COMPUTATION	10
VI.	NUMERICAL RESULTS AND DISCUSSION	18
VII.	REFERENCES	28
	APPENDIX	29

LIST OF FIGURES

Figure		Page
1.	Geometry of the problem	4
2(a).	Expansion functions for J_x^s	11
2(b).	Expansion functions for J_z^s	11
3(a).	$\|J_x^s\|$ as a function of x coordinate	19
3(b).	$\|J_z^s\|$ as a function of x coordinate	20
4(a).	$\|E_x\|$ as a function of β/k for x/L = 0.5, y/H = 0.47	21
4(b).	$\|E_y\|$ as a function of β/k for x/L = 0.5, y/H = 0.47	22
4(c).	$\|E_z\|$ as a function of β/k for x/L = 0.5, y/H = 0.47	23
5(a).	$\|E_x\|$ as a function of x coordinate for y/H = 0.47	25
5(b).	$\|E_y\|$ as a function of x coordinate for y/H = 0.47	26
5(c).	$\|E_z\|$ as a function of x coordinate for y/H = 0.47	27

AD-A067 230 ILLINOIS UNIV AT URBANA-CHAMPAIGN ELECTROMAGNETICS LAB F/G 20/14
EXCITATION OF MODAL FIELDS IN PARALLEL-PLATE TRANSMISSION LINE.(U)
FEB 79 R MITTRA, S W LEE AFOSR-76-3066

UNCLASSIFIED UIEM-79-4 AFOSR-TR-79-0430 NL

2 OF 2
AD A067230

END
DATE FILMED
6-79
DDC

I. INTRODUCTION

The finite-width parallel-plate waveguide is used as an EMP simulator for guiding electromagnetic waves. There have been a number of studies devoted to the analysis of the guide. Rushdi et al. [1] and Marin [2], [3] decompose the field in the guide into two components (for the $\exp(j\omega t)$ time convention):

$$\vec{E}(\vec{r}) = \vec{E}_1 + \vec{E}_2$$

where

$$\vec{E}_1 = \sum_n \vec{A}_n(x,y)e^{-j\gamma_n z} \quad ,$$

$$\vec{E}_2 = \int\int_\Gamma \vec{B}(\alpha,\beta)e^{-j(\alpha x+\beta y+\gamma z)}d\alpha d\beta \quad .$$

The first term $\vec{E}_1$ describes the contribution from the discrete spectrum, i.e., the so-called "leaky-wave" contribution. The second term $\vec{E}_2$ is a superposition of plane waves, the contribution from the continuous spectrum. In references [1] - [3], only $\vec{E}_1$ is studied in detail. This information is useful, of course, only if $\vec{E}_2$ is negligible (for certain guide geometries and source configurations). To test this assumption, we can either evaluate $\vec{E}_2$ directly or calculate the total field $\vec{E}$ instead. We take the second approach. In references [4], [5], Krichevsky and Mittra determine $\vec{E}$ due to a current sheet in the guide by the Wiener-Hopf technique. Their results, however, are valid only if the cross-section of the guide is large in terms of wavelength. In the present report, we again calculate $\vec{E}$ by a different technique moment method which is suitable for a guide with small-to-moderate cross-section.

To calculate the field, we can first write the current source in the form of

$$\vec{J}(\vec{r}) = \int A(\beta)\tilde{\vec{J}}(x,y)e^{-j\beta z}d\beta \quad .$$

We can then calculate the field due to the integrand in the above equation for different β values, and obtain the total field by superposition. In this report, we investigate the electromagnetic fields due to the current source in the form of $\vec{J}(x,y)e^{-j\beta z}$ for different values of the longitudinal propagation constant β. The step involving the integration over the spectral variable β is not carried out in that work.

II. STATEMENT OF THE PROBLEM

The geometry of the problem is shown in Fig. 1, the open parallel waveguide of width 2L, height 2H is infinitely long in the z-direction, and is excited by a y-direction oriented current source J^i defined as:

$$\vec{J}^i = \hat{y} J^i(x,y) e^{-j\beta z}$$

$$= \hat{y}\delta(x - x_o) \begin{Bmatrix} \sin \alpha_p y \\ \cos \alpha_p y \end{Bmatrix} \text{rect}\left(\frac{y}{2h_o}\right) e^{-j\beta z} \quad , \tag{1}$$

where

$$\alpha_p = \frac{p\pi}{2h_o} \quad ; \quad p = 1, 2, 3, \cdots \tag{2}$$

and δ is the Dirac delta function. Rect is the rectangular function defined as:

$$\text{rect}\ (t) = \begin{cases} 1 & ; \quad |t| \leq 1/2 \\ 0 & ; \quad \text{elsewhere} \end{cases} . \tag{3}$$

In Equation (1) and all the following equations in this report, we have adopted a convention in which all equations are given in both cases of odd and even mode current excitation with the upper equation for the odd case, the lower, the even case.

The total electromagnetic field can be decomposed into two parts: $\vec{E}^t = \vec{E}^i + \vec{E}^s$, $\vec{H}^t = \vec{H}^i + \vec{H}^s$. $\vec{E}^i$ and $\vec{H}^i$ are the incident fields produced by the current source in free space with the waveguide removed. $\vec{E}^s$ and $\vec{H}^s$ are the scattered fields generated by the induced current on the waveguide when illuminated by $\vec{E}^i$ and $\vec{H}^i$. The incident field is first examined in the next section.

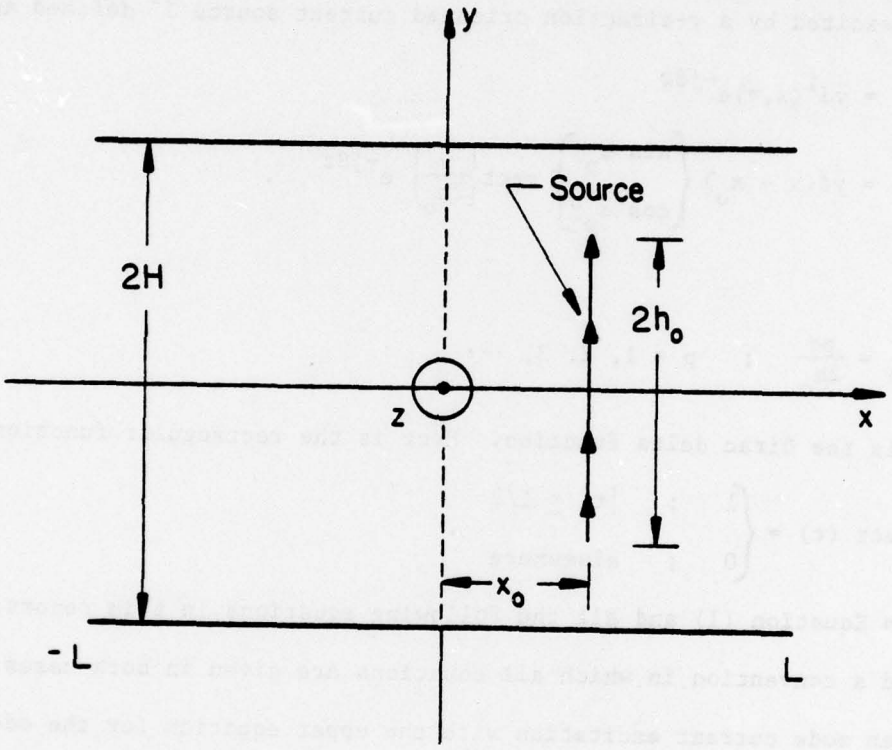

Figure 1. Geometry of the problem.

III. INCIDENT FIELD

The incident fields $\vec{E}^i$ and $\vec{H}^i$ can be computed via the $\hat{y}$-oriented magnetic vector potential $\vec{A}^i$ produced by the impressed current source.

$$\vec{A}^i = \hat{y}A^i(x,y)e^{-j\beta z} \quad .$$

The z-direction variation for all fields is $e^{j\beta z}$. Therefore, it is suppressed in the subsequent equations. Also, the subscript p in α will be omitted in the following equations for convenience of notation.

The vector potential $\vec{A}^i$ satisfies the Helmholtz equation:

$$\left(\frac{\partial^2}{\partial x^2} + \frac{\partial^2}{\partial y^2} + k_t^2\right)A^i(x,y) = -\mu J^i(x,y) \quad , \tag{5}$$

where $k_t^2 = k^2 - \beta^2 \neq 0$, (6)

in which $k = \omega\sqrt{\mu\varepsilon}$ is the wavenumber. The solution to (5) is

$$A^i(x,y) = \frac{\mu}{4j}\int_{-h_o}^{h_o}\begin{Bmatrix}\sin \alpha y' \\ \cos \alpha y'\end{Bmatrix} G(x,y\ ;\ x_o,y')dy' \quad , \tag{7}$$

where G is the Green's function defined as

$$G(x,y\ ;\ x',y') = \begin{cases} H_0^{(2)}(k_t s) & ;\quad k^2 > \beta^2 \\ \frac{j2}{\pi} K_0(k_t s) & ;\quad k^2 < \beta^2 \end{cases} \quad , \tag{8}$$

and $s = \sqrt{(x - x')^2 + (y - y')^2}$. (9)

$H_0^{(2)}$ and K_0 are zero-order Hankel's function of the second kind and modified Bessel's function of the second kind, respectively.

$\vec{E}^i$ and $\vec{H}^i$ can be derived from A^i by using the following equations

$$E_x^i(x,y) = \frac{1}{j\omega\mu\varepsilon}\frac{\partial}{\partial x}\frac{\partial A^i(x,y)}{\partial y} \quad , \tag{10a}$$

$$E_y^i(x,y) = \frac{1}{j\omega\mu\varepsilon}\left(\frac{\partial^2}{\partial y^2} + k^2\right)A^i(x,y) \quad , \tag{10b}$$

$$E_z^i(x,y) = \frac{-j\beta}{j\omega\mu\varepsilon}\frac{\partial A^i(x,y)}{\partial y} \quad , \tag{10c}$$

$$H_x^i(x,y) = \frac{(-j\beta)}{\mu}A^i(x,y) \quad , \tag{10d}$$

$$H_y^i(x,y) = 0 \quad , \tag{10e}$$

$$H_z^i(x,y) = \frac{1}{\mu}\frac{\partial A^i(x,y)}{\partial x} \quad . \tag{10f}$$

Now, we define $B^i(x,y) \equiv \frac{\partial A^i(x,y)}{\partial x}$.

From Equation (7), we have

$$B^i(x,y) = -\frac{\mu}{4j}\left\{\begin{Bmatrix}\sin \alpha h_o \\ \cos \alpha h_o\end{Bmatrix}\left[G(x,y\ ;\ x_o,h_o) \pm G(x,y\ ;\ x_o,-h_o)\right]\right.$$
$$\left. \mp \alpha \int_{-h_o}^{h_o}\begin{Bmatrix}\cos \alpha y' \\ \sin \alpha y'\end{Bmatrix} G(x,y\ ;\ x_o,y')dy'\right\} \quad . \tag{11}$$

The partial derivatives of A^i and B^i are obtained from

$$\frac{\partial A^i(x,y)}{\partial x} = \frac{\mu}{4j}(x - x_o)\int_{-h_o}^{h_o}\begin{Bmatrix}\sin \alpha y' \\ \cos \alpha y'\end{Bmatrix} G'(x,y\ ;\ x_o,y')dy' \quad , \tag{12}$$

$$\text{where } G'(x,y\ ;\ x',y') = \begin{cases} -\frac{k_t}{s}H_1^{(2)}(k_t s) & ;\ k^2 > \beta^2 \\ -\frac{k_t}{s}\frac{js}{\pi}K_1(k_t s) & ;\ k^2 < \beta^2 \end{cases} \quad . \tag{13}$$

$H_1^{(2)}$ and K_1 are, respectively, the first-order Hankel's function of the second kind and modified Bessel's function of the second kind.

Also, we have

$$\frac{\partial B^i(x,y)}{\partial x} = -\frac{\mu}{4j}(x - x_o)\left\{\begin{Bmatrix}\sin \alpha h_o \\ \cos \alpha h_o\end{Bmatrix}[G'(x,y\ ;\ x_o,h_o) \pm G'(x,y\ ;\ x_o,-h_o)]\right.$$

$$\left. \mp \alpha \int_{-h_o}^{h_o} \begin{Bmatrix}\cos \alpha y' \\ \sin \alpha y'\end{Bmatrix} G'(x,y\ ;\ x_o,y')\,dy'\right\} . \qquad (14)$$

$$\frac{\partial B^i(x,y)}{\partial y} = -\frac{\mu}{4j}\left\{\begin{Bmatrix}\sin \alpha h_o \\ \cos \alpha h_o\end{Bmatrix}[(y - h_o)G'(x,y\ ;\ x_o,h_o)\right.$$

$$\pm (y + h_o)G'(x,y\ ;\ x_o,-h_o)]$$

$$\pm \alpha \begin{Bmatrix}\cos \alpha h_o \\ \sin \alpha h_o\end{Bmatrix}[G(x,y\ ;\ x_o,h_o) \mp G(x,y\ ;\ x_o,-h_o)]$$

$$\left. + \alpha^2 \int_{-h_o}^{h_o} \begin{Bmatrix}\sin \alpha y' \\ \cos \alpha y'\end{Bmatrix} G(x,y\ ;\ x_o,y')\,dy'\right\} . \qquad (15)$$

Substituting Equations (7), (11), (12), (14), (15) together with Equations (8) and (13) into Equation (10), we can obtain $\vec{E}^i$ and $\vec{H}^i$.

IV. SCATTERED FIELD

In this section we examine the scattered fields $\vec{E}_s$ and $\vec{H}_s$. Since the induced current $\vec{J}^s$ on the waveguide has two components,

$$\vec{J}^s = \hat{x}J_x^s(x) + \hat{z}J_z^s(x) \quad ; \tag{16}$$

the magnetic vector potential $\vec{A}^s$ due to the induced current $\vec{J}^s$ also has two components,

$$\vec{A}^s = \hat{x}A_x^s(x,y) + \hat{z}A_z^s(x,y) \quad . \tag{17}$$

Both A_x^s and A_z^s satisfy the Helmholtz equation:

$$\left(\frac{\partial^2}{\partial x^2} + \frac{\partial^2}{\partial y^2} + k_t^2\right)A_u^s(x,y) = -\mu J_u^s(x) \quad , \tag{18}$$

where u = x or z, and the solutions are

$$A_x^s(x,y) = \frac{\mu}{4j}\int_{-L}^{L} J_x^s(x')[G(x,y\ ;\ x',h) \pm G(x,y\ ;\ x',-h)]dx' \quad , \tag{19}$$

$$A_z^s(x,y) = \frac{\mu}{4j}\int_{-L}^{L} J_z^s(x')[G(x,y\ ;\ x',h) \pm G(x,y\ ;\ x',-h)]dx' \quad . \tag{20}$$

$\vec{E}^s$ and $\vec{H}^s$ can be derived from $\vec{A}^s$ by using the equations given below

$$E_x^s(x,y) = -j\omega A_x^s(x,y) + \frac{1}{j\omega\mu\varepsilon}\left[\frac{\partial^2}{\partial x^2}A_x^s(x,y) - j\beta\frac{\partial}{\partial x}A_z^s(x,y)\right] \quad , \tag{21a}$$

$$E_y^s(x,y) = \frac{1}{j\omega\mu\varepsilon}\left[\frac{\partial^2}{\partial x\partial y}A_x^s(x,y) - j\beta\frac{\partial}{\partial y}A_z^s(x,y)\right] \quad , \tag{21b}$$

$$E_z^s(x,y) = -j\omega A_z^s(x,y) + \frac{(-j\beta)}{j\omega\mu\varepsilon}\left[\frac{\partial}{\partial x}A_x^s(x,y) - j\beta A_z^s(x,y)\right] \quad , \tag{21c}$$

$$H_x^s(x,y) = \frac{1}{\mu}\frac{\partial}{\partial y}A_z^s(x,y) \quad , \tag{21d}$$

$$H_y^s(x,y) = \frac{1}{\mu}\left[-j\beta A_x^s(x,y) - \frac{\partial}{\partial x}A_z^s(x,y)\right] \quad , \tag{21e}$$

$$H_z^s(x,y) = -\frac{1}{\mu}\frac{\partial}{\partial y}A_x^s(x,y) \quad . \tag{21f}$$

Note that J_x^s and J_z^s are still unknown quantities; however, they can be determined by enforcing the boundary condition that the total tangential electric field be zero on the surface of the waveguide, viz.,

$$E_x^i(x,h) + E_x^s(x,h) = 0 \quad ; \quad |x| \leq L \quad , \tag{22}$$

$$E_z^i(x,h) + E_z^s(x,h) = 0 \quad ; \quad |x| \leq L \quad . \tag{23}$$

Due to the symmetry of the problem, we do not have to enforce the boundary condition on the lower plate ($y = -h$). Equations (22) and (23) can be explicitly written as

$$\left(\frac{\partial}{\partial x^2} + k^2\right) A_x^s(x,h) - j\beta \frac{\partial}{\partial x} A_z^s(x,h) = -j\omega\mu\epsilon E_x^i(x,h) \quad ; \quad |x| \leq L \quad , \tag{24}$$

$$(-\beta^2 + k^2) A_z^s(x,h) - j\beta \frac{\partial}{\partial x} A_x^s(x,h) = -j\omega\mu\epsilon E_z^i(x,h) \quad ; \quad |x| \leq L \quad . \tag{25}$$

We then substitute Equations (19) and (20) into Equations (24) and (25) and numerically solve for J_x^s and J_z^s to obtain $\vec{E}_s$ and $\vec{H}_s$.

V. NUMERICAL COMPUTATION

To solve Equations (24) and (25) numerically, we first transform them into finite difference equations:

$$A_x^s(x + \Delta,h) + (k^2\Delta^2 - 2)A_x^s(x,h) + A_x^s(x - \Delta,h)$$

$$- j \frac{\beta\Delta}{2} [A_z^s(x + \Delta,h) - A_z^s(x - \Delta,h)] = -j \frac{k^2\Delta^2}{\omega} E_x^i(x,h) \quad ; \quad |x| \leq L \quad , \tag{26}$$

and $-j \frac{\beta\Delta}{2} [A_x^s(x + \Delta,h) - A_x^s(x - \Delta,h)] + k_t^2\Delta^2 A_z^s(x,h)$

$$= -j \frac{k^2\Delta^2}{\omega} E_z^s(x,h) \quad ; \quad |x| \leq L \quad , \tag{27}$$

where Δ is a finite increment in x. Equations (26) and (27) can be solved by the method of moments. We expand J_x^s and J_z^s in sets of N subdomain basis functions as shown in Figures 2a and 2b. We write

$$J_x^s(x) = \sum_{n=1}^{N} a_n \, \text{rect}\left(\frac{x - x_n}{\Delta}\right) \tag{28}$$

where $x_n = n\Delta - L$ (29)

$$\Delta = \frac{2L}{N + 1} \quad , \tag{30}$$

and (28) satisfies the end condition

$$J_x^s(\pm L) = 0 \quad . \tag{31}$$

$$J_z^s(x) = \sum_{n=1}^{N} b_n P_n(x) \quad , \tag{32}$$

where $P_1(x) = \frac{\sqrt{\Delta}}{\sqrt{L + x}} \quad ; \quad -L \leq x \leq x_1 + \frac{\Delta}{2} \quad , \tag{33a}$

$$P_n(x) = \text{rect}\left(\frac{x - x_n}{\Delta}\right) \quad ; \quad n = 2, 3, \cdots (N - 1) \quad , \tag{33b}$$

$$P_N(x) = \frac{\sqrt{\Delta}}{\sqrt{L - x}} \quad ; \quad x_N - \frac{\Delta}{2} \leq x \leq L \quad . \tag{33c}$$

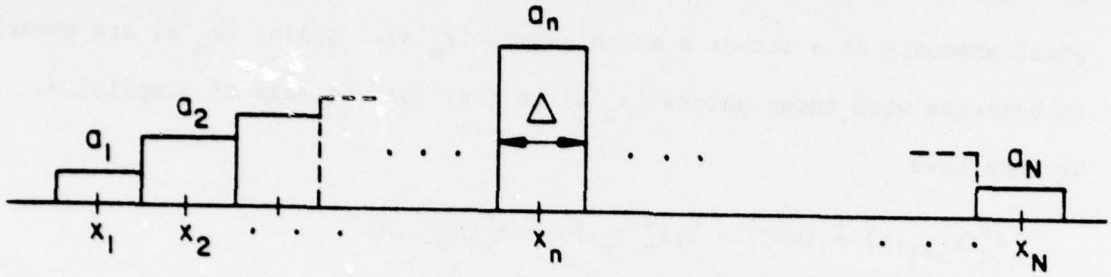

(a)

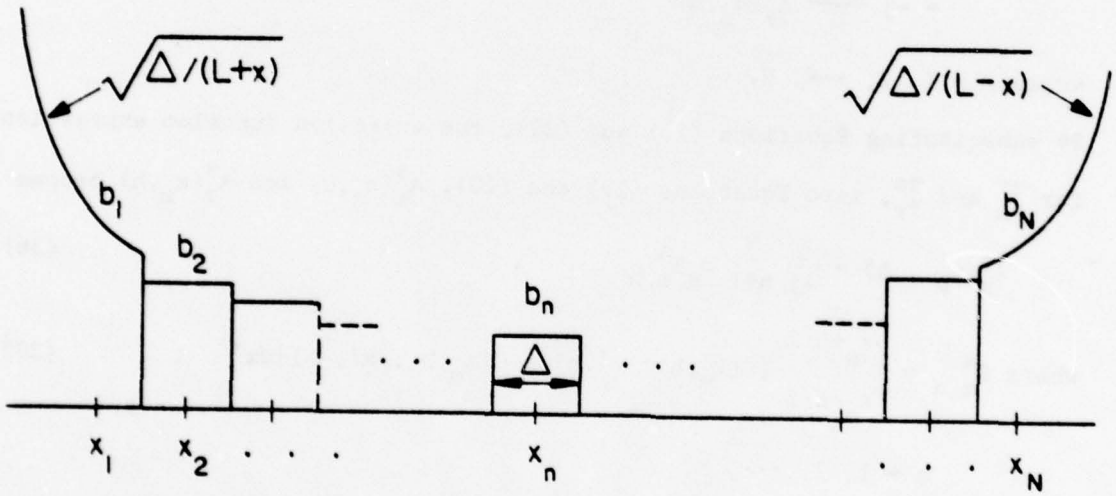

(b)

Figure 2. Expansion functions for (a) J_x^s and (b) J_z^s .

It should be pointed out that the Δ's in Equations (28) and (32) are not necessarily the same as those in Equations (26) and (27); we have chosen the same symbol for the sake of convenience. Next, we enforce (26) and (27) simultaneously at a set of N match points $\{x_m$'s$\}$. Again, $\{x_m$'s$\}$ are chosen to coincide with those points $\{x_n$'s$\}$ in (29) for the sake of simplicity. We then have

$$A_x^s(x_{m+1},h) + (k^2\Delta^2 - 2)A_x^s(x_m,h) + A_x^s(x_{m-1},h)$$

$$-j\frac{\beta\Delta}{2}\left[A_z^s(x_{m+1},h) - A_z^s(x_{m-1},h)\right] = -j\frac{k^2\Delta^2}{\omega}E_x^i(x_m,h) \qquad (34)$$

and $$-j\frac{\beta\Delta}{2}\left[A_x^s(x_{m+1},h) - A_x^s(x_{m-1},h)\right] + k_t^2\Delta^2 A_z^s(x_m,h)$$

$$= -j\frac{k^2\Delta^2}{\omega}E_z^i(x_m,h) \qquad (35)$$

where $m = 1, 2, \cdots, N$.

By substituting Equations (28) and (32), the expansion function expressions for $\overset{+}{J}{}_x^s$ and $\overset{+}{J}{}_z^s$, into Equations (19) and (20), $A_x^s(x_m,h)$ and $A_z^s(x_m,h)$ become

$$A_x^s(x_m,h) = \frac{\mu}{4j}\sum_{n=1}^{N} a_n S_{m,n}^a \quad , \qquad (36)$$

where $$S_{m,n}^a = \int_{x_n-\Delta/2}^{x_n+\Delta/2}\left[G(x_m,h\,;\,x',h) \pm G(x_m,h\,;\,x',-h)\right]dx' \quad ; \qquad (37)$$

$$n = 1, 2, \cdots, N,$$

$$m = 0, 1, \cdots, (N+1),$$

and $$A_z^s(x_m,h) = \frac{\mu}{4j}\sum_{n=1}^{N} b_n S_{m,n}^b \quad , \qquad (38)$$

where $$S_{m,1}^b = \int_{-L}^{x_1+\Delta/2}\sqrt{\frac{\Delta}{L+x'}}\left[G(x_m,h\,;\,x',h) \pm G(x_m,h\,;\,x',-h)\right]dx' \quad , \qquad (39a)$$

$$S_{m,n}^b = S_{m,n}^a \quad ; \quad n = 2, 3, \cdots, (N-1), \qquad (39b)$$

$$S^b_{m,N} = \int_{x_N-\Delta/2}^{L} \sqrt{\frac{\Delta}{L - X'}}\,[G(x_m,h\ ;\ x',h) \pm G(x_m,h\ ;\ x',-h)]dx' \qquad (39c)$$

$$m = 0,\ 1,\cdots,\ (N+1)\ .$$

Substituting Equations (36) through (39) into Equations (34) and (35), we arrive at

$$\begin{bmatrix} [S^a_{m+1,n} + (k^2\Delta^2 - 2)S^a_{m,n} + S^a_{m-1,n}] & [-j\frac{\beta\Delta}{2}(S^b_{m+1,n} - S^b_{m-1,n})] \\ [-j\frac{\beta\Delta}{2}(S^a_{m+1,n} - S^a_{m-1,n})] & [k_t^2\Delta^2 S^b_{m,n}] \end{bmatrix} \begin{bmatrix} [a_n] \\ [b_n] \end{bmatrix}$$

$$= -\Delta^2\frac{4j}{\mu}\begin{bmatrix} [\frac{\partial}{\partial x}B^i(x_m,h)] \\ [-j\beta B^i(x_m,h)] \end{bmatrix} \qquad (40)$$

The above equation can be readily solved for a_n and b_n. The unknowns A^s_x and A^s_z can then be calculated using Equations (36) through (39), and the scattered field can be determined from Equation (21) and, therefore, the total field. The equations for calculating $S^a_{m,n}$'s and $S^b_{m,n}$'s are given in the following:

(A) Evaluation of $S^a_{m,n}$'s

(i) If $m = n$,

$$S^a_{m,n} = I_0 \pm \text{image} \qquad (41)$$

$$\text{where image} = \int_{x_n-\Delta/2}^{x_n+\Delta/2} G(x_m,h\ ;\ x',-h)dx' \quad , \qquad (42)$$

$$\text{and } I_0 = \int_{x_m-\Delta/2}^{x_m+\Delta/2} G(x_m,h\ ;\ x',h)dx' \qquad (43)$$

$$= 2\int_{x_m}^{x_m+\Delta/2} G(x_m,h\ ;\ x',h)dx' \qquad (44)$$

$$= \begin{cases} 2 \int_{x_m}^{x_m+\Delta/2} H_0^{(2)}[k_t(x' - x_m)]dx' \; ; \; k^2 > \beta^2 \\ \frac{4j}{\pi} \int_{x_m}^{x_m+\Delta/2} K_0[k_t(x' - x_m)]dx' \; ; \; k^2 < \beta^2 \end{cases} \tag{45}$$

$$= \begin{cases} \frac{2}{k_t} \int_0^{k_t\Delta/2} H_0^{(2)}(t)dt \; ; \; k^2 > \beta^2 \\ \frac{4j}{\pi k_t} \int_0^{k_t\Delta/2} K_0(t)dt \; ; \; k^2 < \beta^2 \end{cases} . \tag{46}$$

Since simple algorithms have been developed to evaluate the integrals of $H_0^{(2)}$ and K_0 from zero to any positive number [6], Equation (46) can be evaluated efficiently and accurately.

(ii) If $m \neq n$,

$$S^a_{m,n} = \begin{cases} \int_{x_n-\Delta/2}^{x_m} G(x_m,h \; ; \; x',h)dx' - \int_{x_n+\Delta/2}^{x_m} G(x_m,h \; ; \; x',h)dx' \pm \text{image} \; ; \; m > n \\ \int_{x_m}^{x_n+\Delta/2} G(x_m,h \; ; \; x',h)dx' - \int_{x_m}^{x_n-\Delta/2} G(x_m,h \; ; \; x',h)dx' \pm \text{image} \; ; \; m < n \end{cases} \tag{47}$$

where the image is given in Equation (42).

(B) Evaluation of $S^b_{m,n}$'s

First consider $S^b_{m,1}$, which is expressed as:

$$S^b_{m,1} = I_1 + I_2 \quad , \tag{48}$$

$$\text{where } I_1 = \int_{-L}^{-L+\Delta/2} \sqrt{\frac{\Delta}{L + x'}} \, [G(x_m,h \; ; \; x',h) \pm G(x_m,h \; ; \; x',-h)]dx' \tag{49}$$

$$\text{and } I_2 = \int_{x_1-\Delta/2}^{x_1+\Delta/2} \sqrt{\frac{\Delta}{L + x'}} \, [G(x_m,h \; ; \; x',h) \pm G(x_m,h \; ; \; x',-h)]dx' . \tag{50}$$

(i) If $m \neq 0$,

$$I_1 = \int_{-L}^{-L+\Delta/2} \left\{ \sqrt{\frac{\Delta}{L + x'}} \left[G(x_m, h \; ; \; x', h) \pm G(x_m, h \; ; \; x', -h) \right] \right.$$

$$\left. - \sqrt{\frac{\Delta}{L + x'}} \left[G(x_m, h \; ; \; -L, h) \pm G(x_m, h \; ; \; -L, -h) \right] \right\} dx'$$

$$+ \left[G(x_m, h \; ; \; -L, h) \pm G(x_m, h \; ; \; -L, -h) \right] \int_{-L}^{-L+\Delta/2} \sqrt{\frac{\Delta}{L + x'}} \, dx' \tag{51}$$

where $\int_{-L}^{-L+\Delta/2} \sqrt{\frac{\Delta}{L + x'}} \, dx'$ can be evaluated analytically,

which is $\int_{-L}^{-L+\Delta/2} \sqrt{\frac{\Delta}{L + x'}} \, dx' = \sqrt{2}\,\Delta$. (51a)

(ii) If $m = 0$,

first, the small argument behavior of function G is obtained:

$$\lim_{x' \to -L} G(-L, h \; ; \; x', h) = - \frac{2j}{\pi} \ell n \left[\frac{\gamma k_t (L + x')}{2} \right] \quad , \tag{52}$$

where $\gamma = 0.5772156649$. Then, in evaluating I_1 in Equation (49), the singularity at $x' = -L$ is first subtracted from, then added to the integrand, and by using Equation (52), we have

$$I_1 = \int_{-L}^{-L+\Delta/2} \sqrt{\frac{\Delta}{L + x'}} \left\{ G(-L, h \; ; \; x', h) \pm G(-L, h \; ; \; x', -h) \right.$$

$$\left. + \frac{2j}{\pi} \ell n \left[\frac{\gamma k_t (L + x')}{2} \right] \right\} dx'$$

$$- \frac{2j}{\pi} \int_{-L}^{-L+\Delta/2} \sqrt{\frac{\Delta}{L + x'}} \left\{ \ell n (L + x') + \ell n \left(\frac{\gamma k_t}{2} \right) \right\} dx' \quad . \tag{53}$$

The first integral in the above equation is amenable to numerical integration, and the second integral can be evaluated analytically:

$$- \frac{2j}{\pi} \int_{-L}^{-L+\Delta/2} \sqrt{\frac{\Delta}{L + x'}} \, \ell n \left[\frac{\gamma k_t (L + x')}{2} \right] dx'$$

$$= - \frac{2j}{\pi} \sqrt{2} \, \Delta \left\{ \ell n \left[\frac{\gamma k_t \Delta}{4} \right] - 2 \right\} \quad . \tag{54}$$

On the other hand, I_2 can be evaluated as

$$I_2 = \int_{x_1 - \Delta/2}^{x_1 + \Delta/2} \left\{ \sqrt{\frac{\Delta}{L + x'}} \, [G(x_m, h \; ; \; x', h) \pm G(x_m, h \; ; \; x', -h)] \right.$$

$$\left. - \, [G(x_m, h \; ; \; x', h) \pm G(x_m, h \; ; \; x', -h)] \right\} dx' + S^a_{m,1} \quad , \tag{55}$$

$$m = 0, \, 1, \, \cdots, \, (N+1) \quad .$$

Substituting the above expressions for I_1 and I_2 into Equation (48), we then obtain $S^b_{m,1}$. Following similar procedures, we obtain the equations for $S^b_{m,N}$:

$$S^b_{m,N} = I_3 + I_4 \quad ,$$

where $I_3 = \int_{L-\Delta/2}^{L} \left\{ \sqrt{\frac{\Delta}{L - x'}} \, [G(x_m, h \; ; \; x', h) \pm G(x_m, h \; ; \; x', -h)] \right.$

$$\left. - \sqrt{\frac{\Delta}{L - x'}} \, [G(x_m, h \; ; \; L, h) \pm G(x_m, h \; ; \; L, -h)] \right\} dx'$$

$$+ \, [G(x_m, h \; ; \; L, h) \pm G(x_m, h \; ; \; L, -h)] \sqrt{2} \, \Delta \quad , \tag{56}$$

$$\text{when } m = 0, \, 1, \, \cdots, \, N$$

$$\text{or } I_3 = \int_{L-\Delta/2}^{L} \sqrt{\frac{\Delta}{L - x'}} \left\{ G(L, h \; ; \; x', h) \pm G(L, h \; ; \; x', -h) \right.$$

$$\left. + \frac{2j}{\pi} \, \ell n \, \frac{\gamma k_t (L - x')}{2} \right\} dx' - \frac{2j}{\pi} \sqrt{2} \, \Delta \left\{ \ell n \left[\frac{\gamma k_t \Delta}{4} \right] - 2 \right\} \quad ; \tag{57}$$

$$\text{when } m = N + 1,$$

$$\text{and } I_4 = \int_{x_N-\Delta/2}^{x_N+\Delta/2} \left\{ \sqrt{\frac{\Delta}{L - x'}} \left[G(x_m,h \; ; \; x',h) \pm G(x_m,h \; ; \; x',-h) \right] \right.$$

$$\left. - \left[G(x_m,h \; ; \; x',h) \pm G(x_m,h \; ; \; x',-h) \right] \right\} dx' + S^a_{m,N} \quad ; \qquad (58)$$

$$m = 0, \; 1, \; \cdots \; (N + 1) \quad .$$

Using the equations obtained above to compute $S^a_{m,n}$'s and $S^b_{m,n}$'s in Equation (40) and inversing the matrix, we then are able to determine the a_n's and b_n's.

VI. NUMERICAL RESULTS AND DISCUSSION

The results evaluated by the methods discussed in the last section are now presented in graphical form. The physical dimensions of the waveguide and the current source for which we perform the computation are (see Fig. 1 and Equations (1) and (2))

$L = 12.5$ m

$H = 12.75$ m

$h_o = 5$ m

$x_o = 0$ m

$p = 1$.

The frequency used is 25 MHz, and the current source is of even mode.

The magnitudes of the induced-current components, $|\vec{J}_x^s|$ and $|\vec{J}_x^s|$, are plotted in Figs. 3(a) and 3(b) as functions of the transverse coordinate of the waveguide. They are presented for different β/k values in the range between 0.86 and 0.99.

The plots of the magnitudes of the electrical field components, $|\vec{E}_x|$, $|\vec{E}_y|$, and $|\vec{E}_z|$, consist of two parts.

(A) Field components as functions of β/k:

E_x , E_y , and E_z are plotted for β/k in the range between 0 and 0.999 in Figs. 4(a), 4(b) and 4(c), when $x = 0.5L$, $y = 0.47H$.

It is observed from these plots that for most values of β/k between 0 and 1, $|\vec{E}_x|$, $|\vec{E}_y|$, and $|\vec{E}_z|$ are relatively small and vary rather slowly with respect to β/k; however, for β/k in the region between 0.7 and 1, the magnitude of the field component is found to have a sharp peak. Therefore, the major contributions to the total fields should come from this portion of the spectrum.

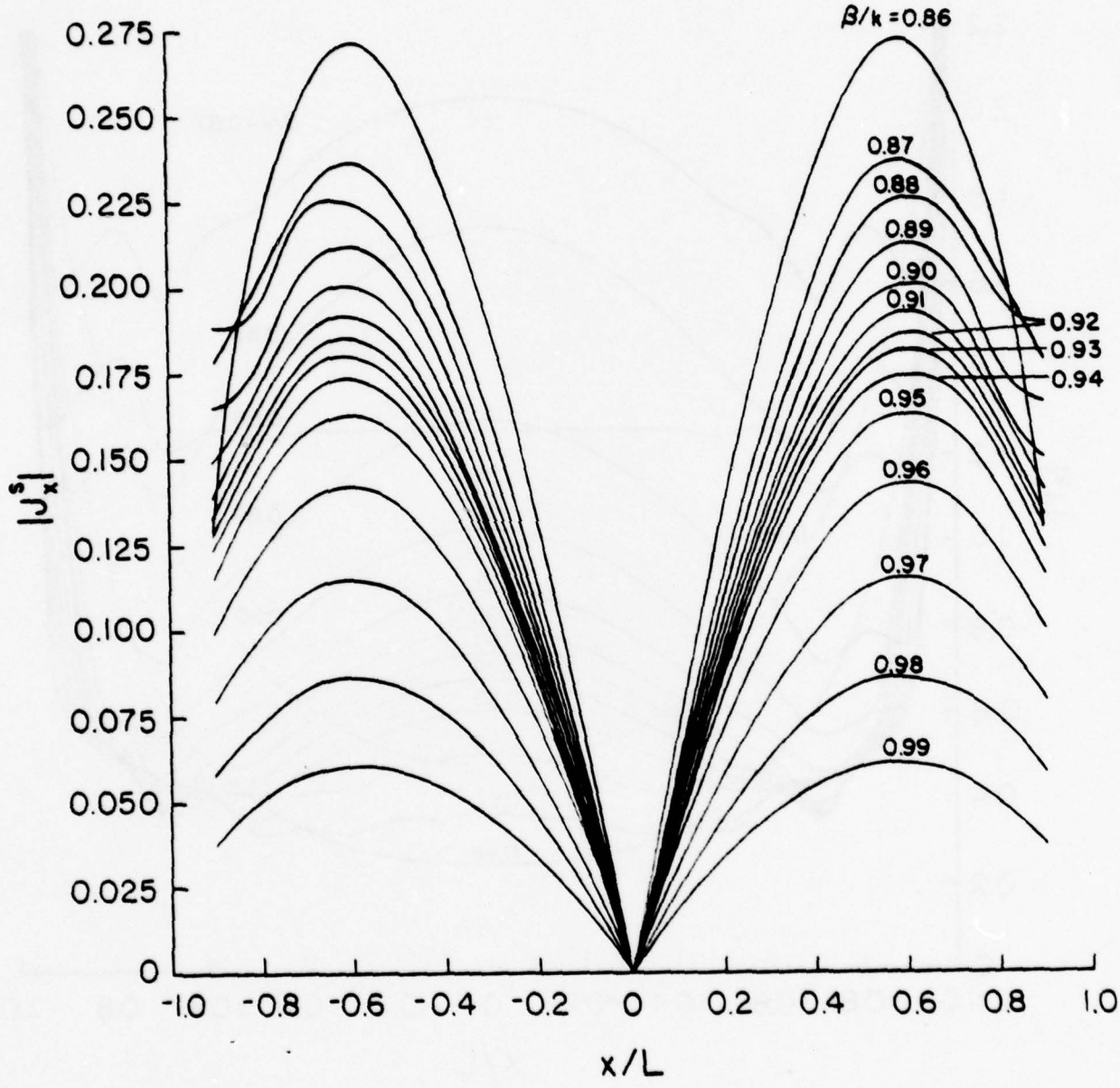

Figure 3(a). $|J_x^s|$ as a function of x coordinate.

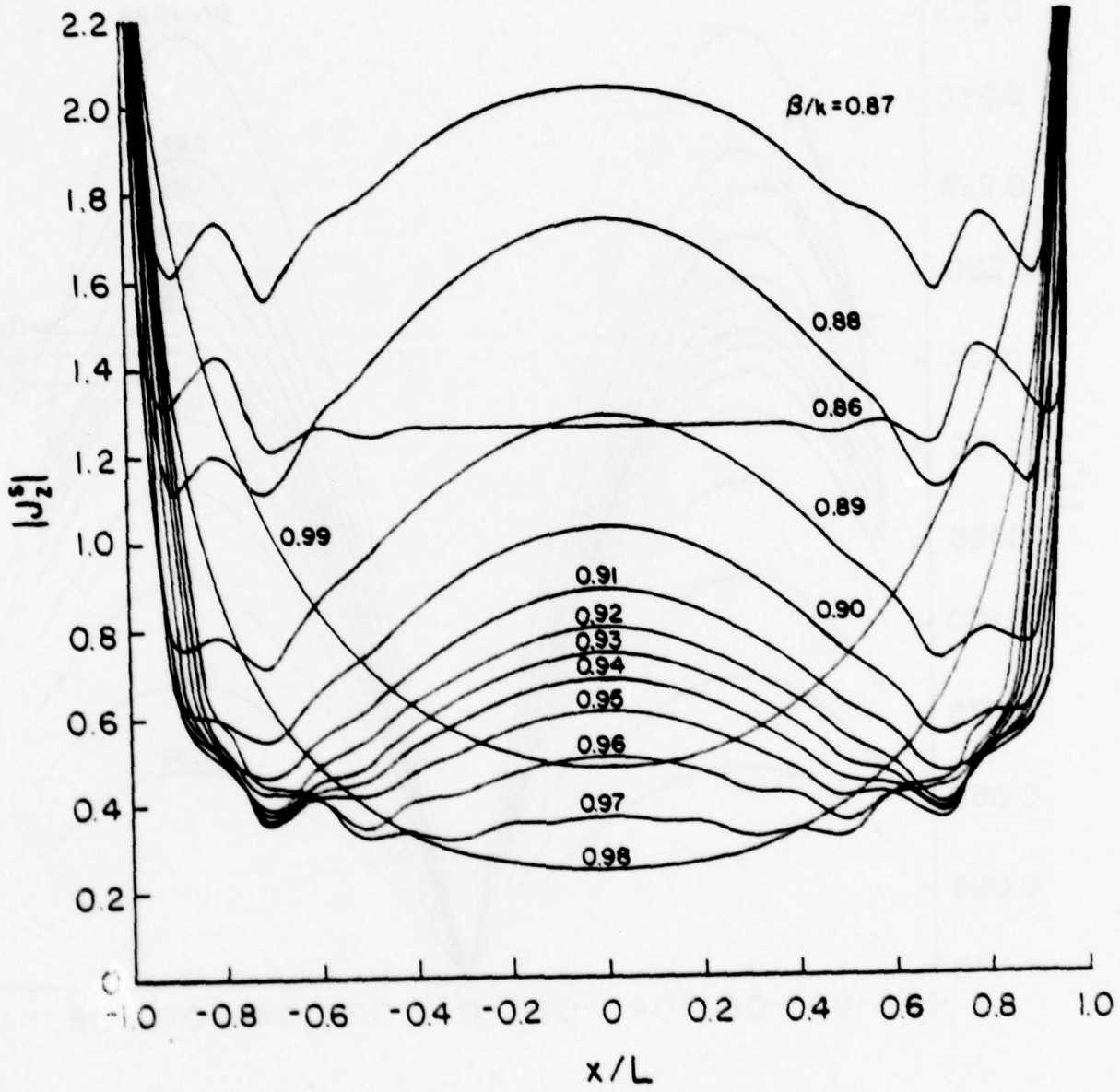

Figure 3(b). $|J_z^s|$ as a function of x coordinate

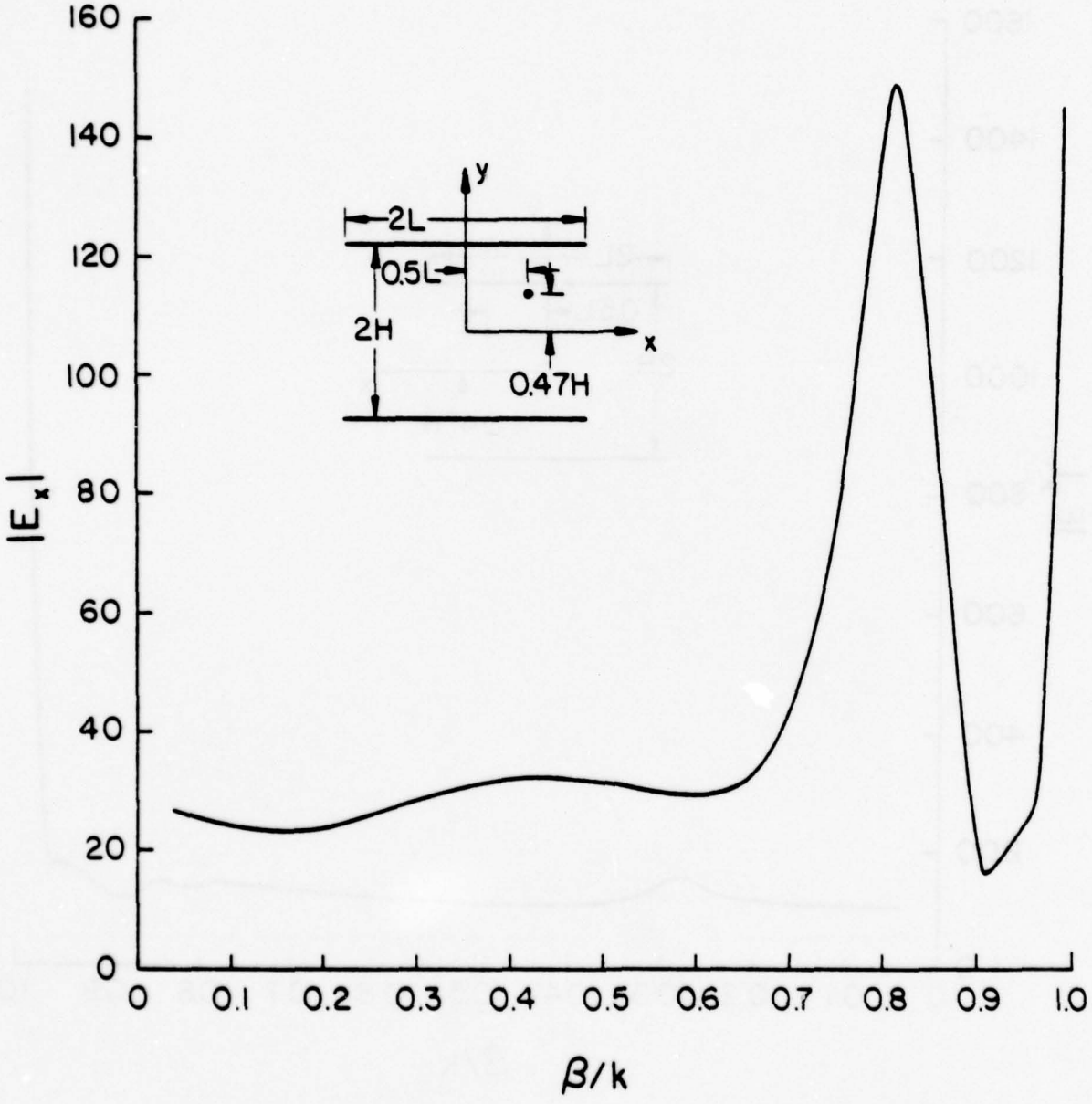

Figure 4(a). $|E_x|$ as a function of β/k for x/L = 0.5, y/H = 0.47.

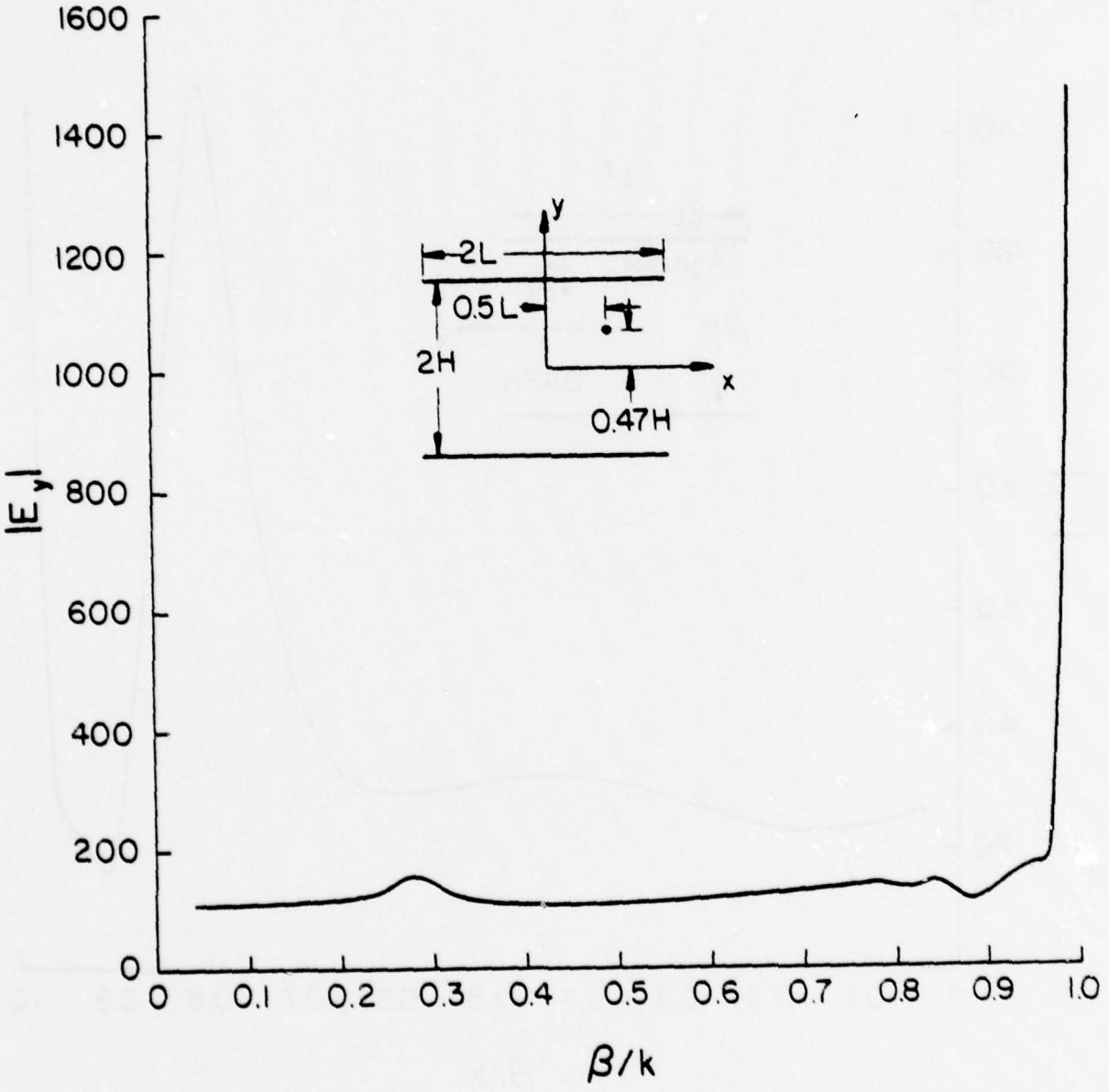

Figure 4(b). $|E_y|$ as a function of β/k for x/L = 0.5, y/H = 0.47.

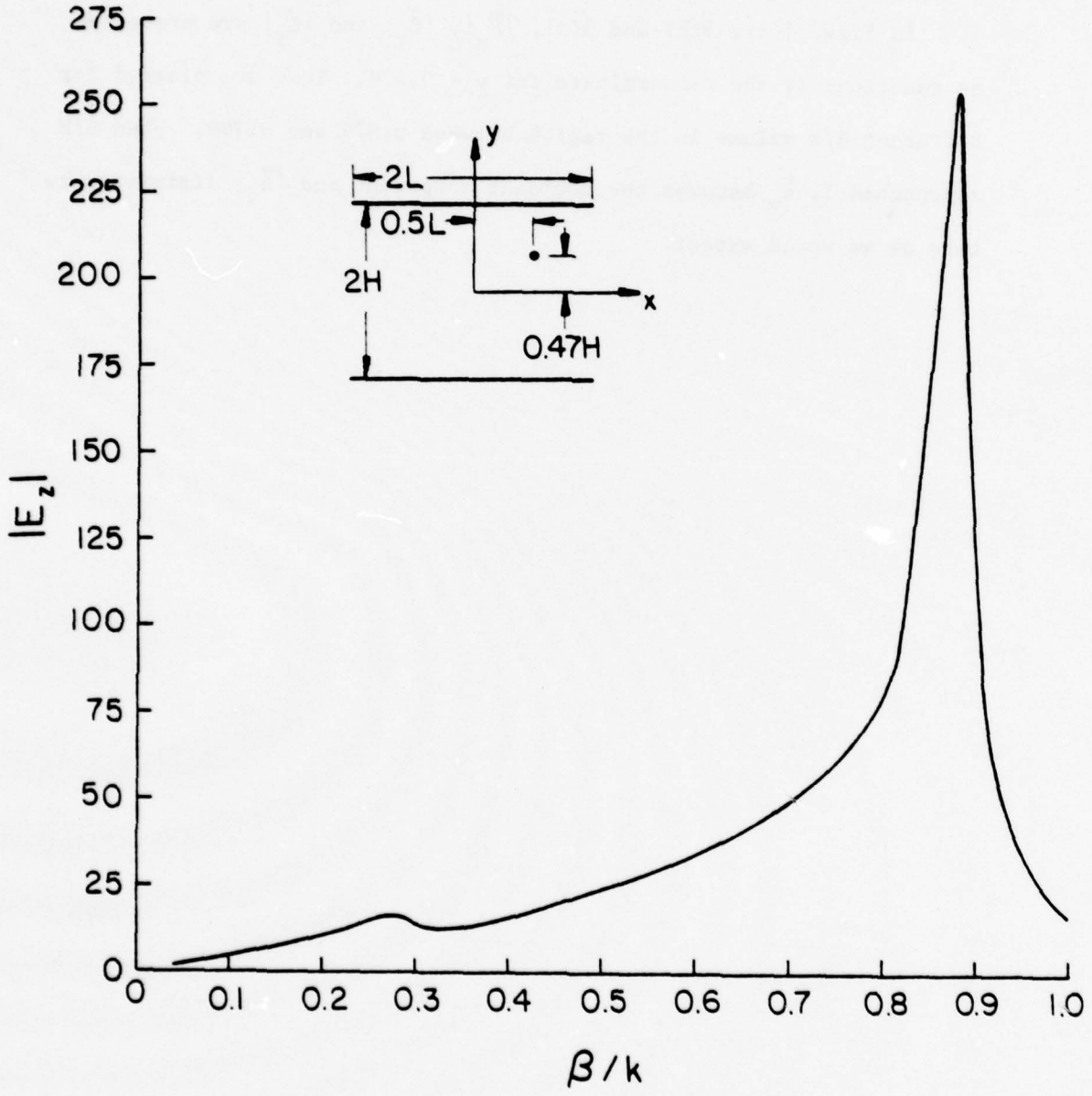

Figure 4(c). $|E_z|$ as a function of β/k for x/L = 0.5, y/H = 0.47.

(B) Field components as functions of the transverse coordinate of the waveguide.

In Figs. 5(a), 5(b) and 5(c), $|\vec{E}_x|$, $|\vec{E}_y|$ and $|\vec{E}_z|$ are presented as functions of the x-coordinate for y = 0.47H. They are plotted for different β/k values in the region between 0.879 and 0.999. When β/k approaches 1, $\vec{E}_y$ becomes the dominant component and $|\vec{E}_z|$ diminishes to zero as we would expect.

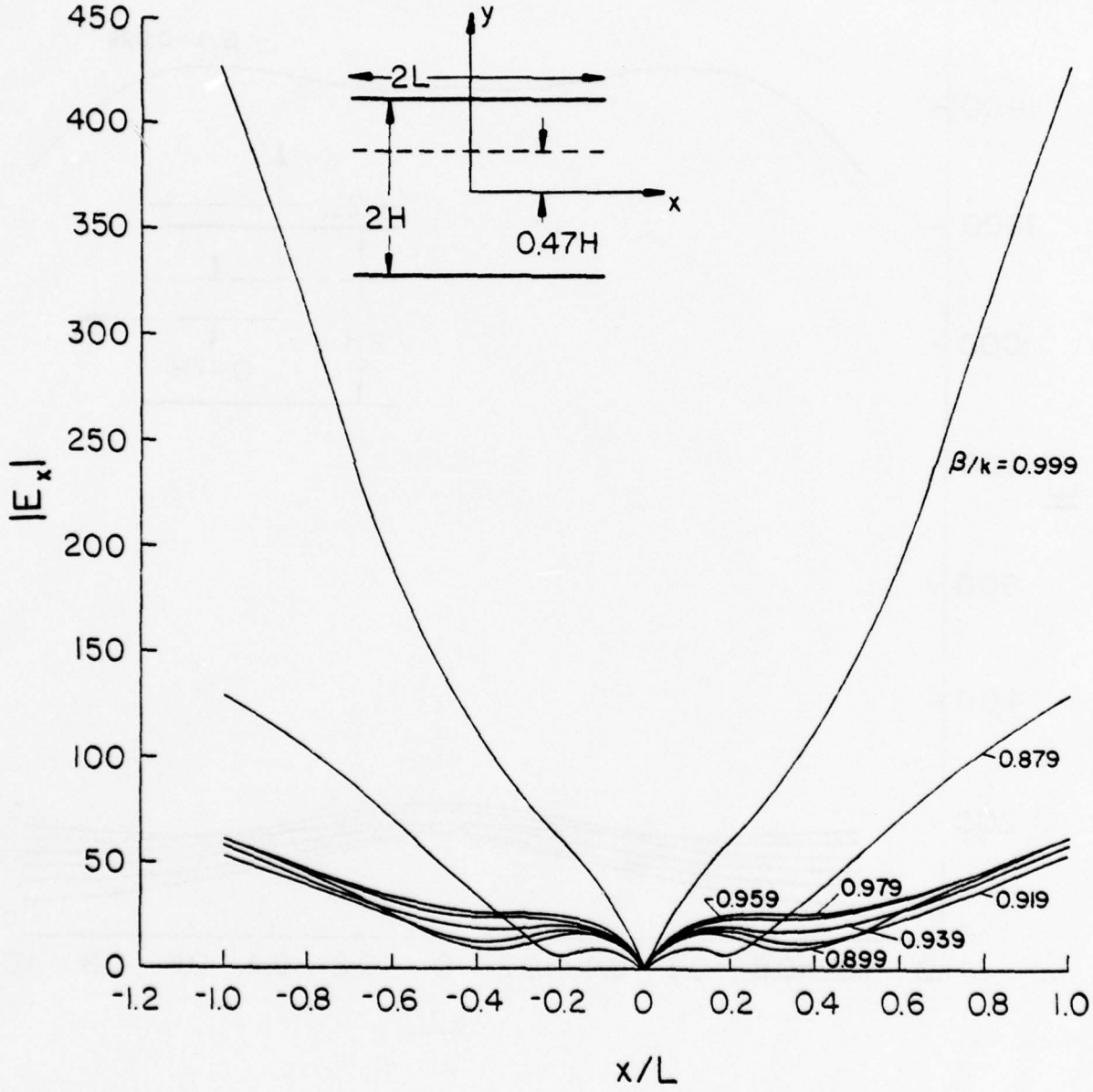

Figure 5(a). $|E_x|$ as a function of x coordinate for y/H = 0.47.

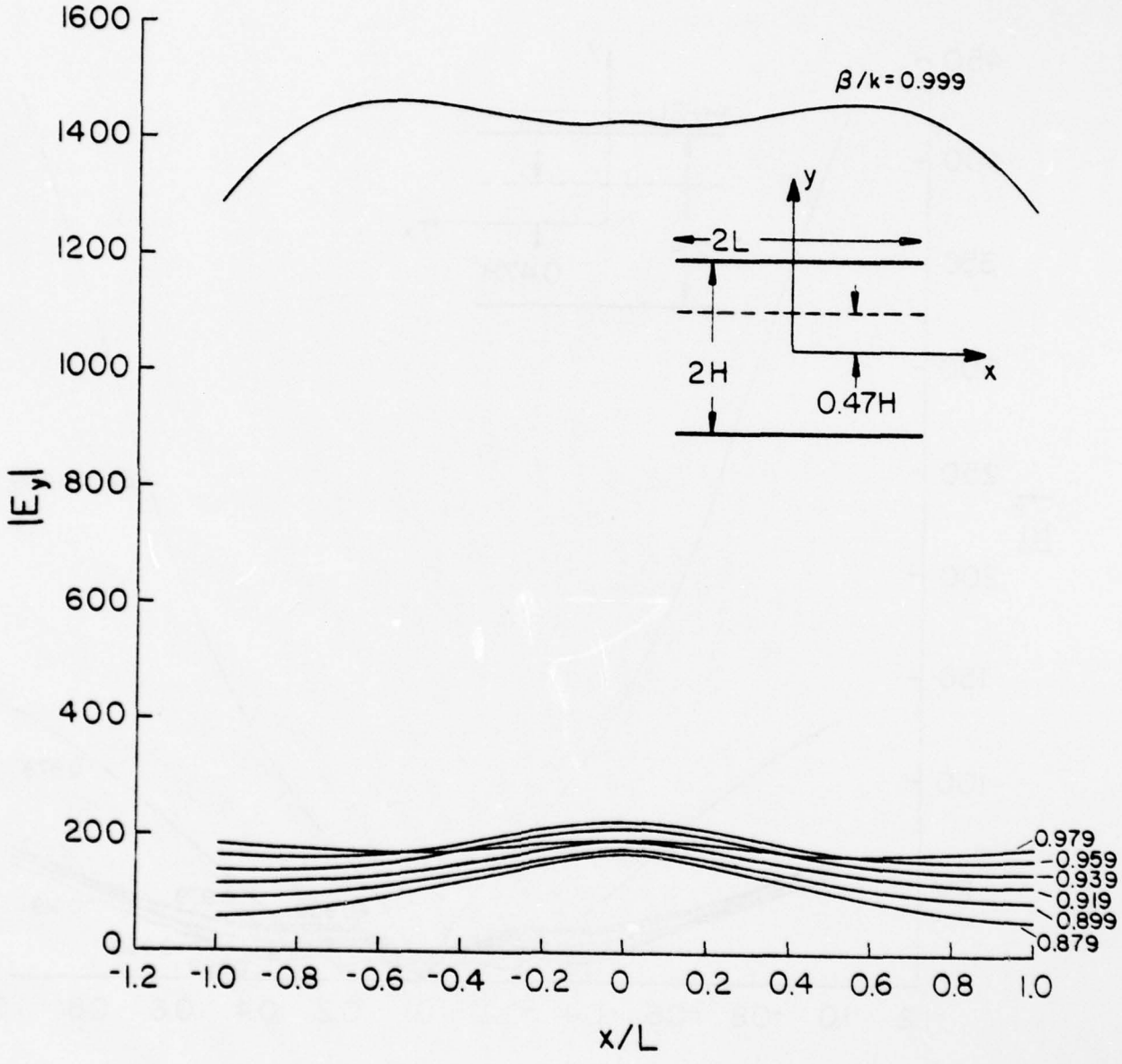

Figure 5(b). $|E_y|$ as a function of x coordinate for y/H = 0.47.

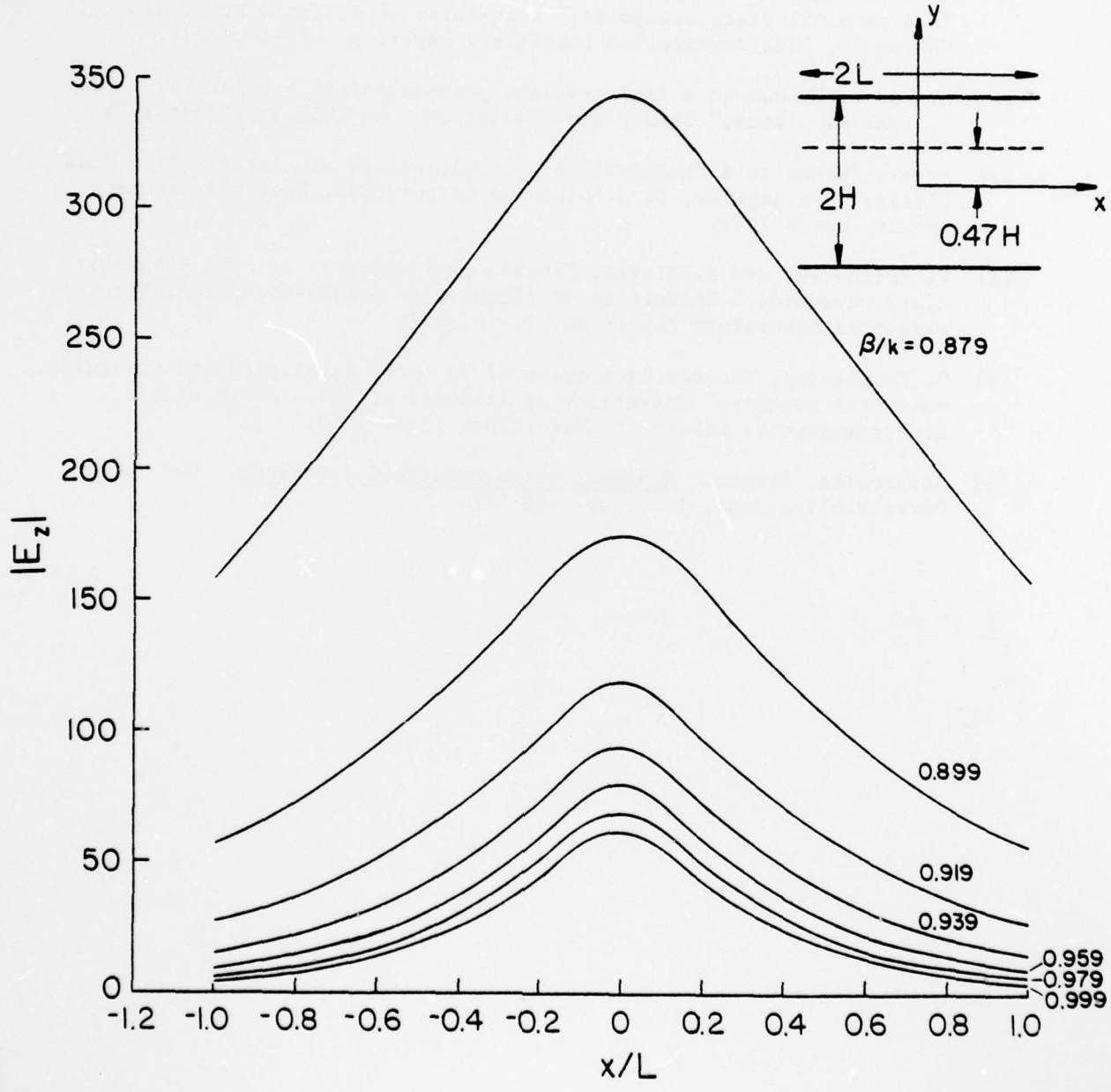

Figure 5(c). $|E_z|$ as a function of x coordinate for y/H = 0.47.

VII. REFERENCES

[1] A. M. Rushdi, R. Menendez and R. Mittra, "A study of the leaky modes in a parallel-plate waveguide," University of Illinois at Urbana-Champaign, Electromagnetics Laboratory Report no. 77-16, 1977.

[2] L. Marin, "Modes on a finite-width, parallel-plate simulator: I. Narrow plates," Sensor and Simulation Note 201, September 1974.

[3] -----, "Modes on a finite-width, parallel-plate simulator. II: Wide plates," Los Angeles, C. A. Dikewood Corporation, Westwood Research Brahch, March 1977.

[4] V. Krichevsky and R. Mittra, "Source excitation of an open parallel-plate waveguide," University of Illinois at Urbana-Champaign, Electromagnetics Laboratory Report no. 77-19, 1977.

[5] V. Krichevsky, "Source excitation of an open, parallel-plate waveguide, numerical results," University of Illinois at Urbana-Champaign, Electromagnetics Laboratory Report no. 78-4, 1978.

[6] Abramowitz, Stegun, Handbook of Mathematical Functions. New York: Dover Publications, Inc., pp. 480-491.

APPENDIX

A computer program for determining the magnitude of all six components of the EM field is presented here. Data were obtained for x/L between 0 - 1 with step 0.05, β between 0.879 - 0.999 with step 0.02, and y at any given value. The program can be readily modified to obtain the real and imaginary parts of all field components as functions of the x-coordinate and β.

THIS PAGE IS BEST QUALITY PRACTICABLE
FROM COPY FURNISHED TO DDC

```
      SUBROUTINE SETUP ( INPUT, OUTPUT, TAPE3 )
      COMPLEX FLOT(5),FLOS(5),FLO
      COMPLEX SI(61,62), JX, JY, SA, SB,BI,BIK,POLAR,CONM
      COMPLEX FA(62,22), FB(33,22)
      LOGICAL ODD,EVEN
      COMMON /FREQ   / AK,BETA,AKT,INDEX,PI
      COMMON /GUIDE  / M,AL,XA(23),XB(23),DEL,NC
      COMMON /SOURCE/ MO,XO,NO,ALPHA,SINA,COSA
      COMMON /LOGIC  / ODD,EVEN
      COMMON /ARRAY  / JX(21),JY(21)
      COMMON XFS(14),YFS(14)
      COMMON XV(15),YV(15)
      DATA ZERO/0.0/,ONE/1.0/,TWO/2.0/,HALF/0.5/
     $DATA DOTS/*LINE*,*LINE*,*LINE*,*LINE*,*LINE*,*LINE*,
     $*LINE*/

      PRINT *,'ENTER L, M, MO, (O'
      READ *,AL,M,NC,I
      PRINT *,'ENTER NO, AVELENGTH, MODE( 2 FOR EVEN, 1 FOR ODD )'
      READ *,NP,AL,LOC
      PRINT *,'ENTER NC, YO'
      READ *,NC,YO
      PRINT *,'ENTER 1 FOR COMPUTING EX, 2 FOR EY, 3 FOR EZ,
     *, 4 FOR HX, 5 FOR HY, 6 FOR HZ'
      READ *,NFC
      DO 300 I=1,7
      BETA=0.3*3.0+0.02*I
      ODD=LOC.EQ.1
      AK=2.*PI/AL

      IF(MO.EQ.   M) STOP
      IF(XO.LT.  AL) STOP
      IF(XO.LT.-AL) STOP
      BETA=BETA*BETA
      IF(BETA.EQ.1.) STOP
      IF(BETA.GT.1.) GOTO 1100
      INDEX=1
      AKT=AK*SQRT(1.-BETA2)
      GOTO 1200
1100  INDEX=2
      AKT=AK*SQRT(BETA2-1.)
1200  BETA=BETA*AK
      DEL=2.*AL/FLOAT(NC*2)
      N2=NC*2
      NT=NC*NC
      N8=NT*2
      XA(1)=AL-DEL/2.

      DO 1300 N=2,N8
      XA(N)=XA(N-1)-DEL
1300  XB(N)=XB(N-1)-DEL
      IF(MO.EQ.0.) XO=AL/2.
      SINA=SIN(ALPHA)
      COSA=COS(ALPHA)
      ALPHA=ALPHA/PI
      EVEN=.NOT.ODD

      DO 2001 M=1,N8
      FA(M,1)=SA(M-1,1)
2001  FB(M,1)=SB(M-1,1)
      DO 2002 N=2,NC
      DO 2002 M=1,N8
2002  FA(M,N)=FA(M,1)*FA(M-N+1,1)
```

THIS PAGE IS BEST QUALITY PRACTICABLE
FROM COPY FURNISHED TO DDC

```
2002    CONTINUE
        NO=NC-1
        DO 2003 N=2,NO
        DO 2003 M=1,NA
2003    T3(M,N)=TA(M,N)
        DO 2004 M=1,NA
2004    T3(M,NC)=T3(NA-M+1,1)
        CONM=ALK*ALK*DEL*DEL-2.
        CONM=CMPLX( 1.,  -BETA*DEL/2. )
        CONM=ALK*ALK*DEL*DEL
        DO 2100 M=1,NC
        DO 2100 N=1,NC
        S(  M,    N)=TA(M+2,N)+CONM*TA(M+1,N)+TA(M,N)
        S(NC+M,   N)=CONM*( TA(M+2,N)-TA(M,N) )
        S(  M,NC+N)=CONM*( T3(M+2,N)-T3(M,N) )
2100    S(NC+M,NC+N)=S(NB+M,NB+N)+CONM*T3(M+1,N)
        CONM=CONM*2.*DEL
        DO 3003 M=1,NC
        IM=IB(M+1)
        S(  M,NB)=DEL*DEL*BIX(IM,M)
3003    S(NC+M,NB)=-CONM*BI(IM,M)

        CALL CSMCD ( S,NT,+1,+2 )
        DO 4100 M=1,NC
        XC(M)=S(M,N3)
4100    XS(M)=S(M+NC,N3)
        DO 4200 M=1,NA
        CALL FILCOS(FLOS,T3(N),YI)
        CALL FILSIN(FLOS,T3(N),YI)
        FLO=FLO(NF)*FLOS(NF)
        X(M)=(1-I)*NA+M
4200    Y(M)=T3(N)/FL
900     CONTINUE
        CALL USTART
        CALL USETUP(XSIZE,YSIZE,SW)
        CALL USETC('XLABEL',WX/2.,M)
        CALL USETC('YLABEL',0.,M)
        CALL USETC('MAJOR',NA,0.,NA,0.,M)
        CALL UGRID(0.,0.,0.,0.,0,0)
        CALL UDEMO

        STOP
        END
        REAL FUNCTION SA(M,N)
        DIMENSION XU(1),YU(1)
        COMMON /UGRID/ XL,XU,YL,YU,NC,NR
        COMMON /UGRIDC/ IGRID,IDOT,IEN
        COMMON /UPAI/ PI,TWOPI,PI2
        CALL UGRID( 2,XL,XU,YL,YU,IMAGE )
        IF(M.LE.N) SA=FO(XU(M)-XU(N))-FO(XL(M)-XU(N))
        IF(M.GT.N) SA=2.*FO(XU(M)-XU(N))
        IF(IMAGE.EQ.1) SA=SA-IMAGE
        IF(IMAGE.EQ.2) SA=SA+IMAGE
        RETURN
```

THIS PAGE IS BEST QUALITY PRACTICABLE
FROM COPY FURNISHED TO DDC

```
      COMPLEX FUNCTION S8(N,N)
      COMPLEX SA,F80,F81,F82,S,S0,S1,S2,RES1,RES2
      DOUBLE PRECISION AL,DEL,EN
      COMMON /FRED/ AK,BETA,AKT,INDEX,PI
      COMMON /JUDE/ N,AL,SA(23),SB(23),DEL,NC
      COMMON /SAM/ S0,S1,S2,EN
      DATA SA(4),SQRT2/ 0.577215664E0,1.414213562E0/
      SB=SA(N,N)
      IF(N.GT.1) GO TO 1000
      AL=ALOG(AK)
      XL=AL*DEL
      CALL F80(XL,S0,RES2)
      S=S0
      IF(CABS(S).LT.1.E-30) GO TO 2000
      CALL F81(-AL,S1,RES1)
      S=S+S1
      IF(CABS(S).LT.1.E-30) GO TO 2000
      CALL F82(-AL,S2,RES2)
      S=S+S2
 2000 S8=S
      RETURN
 1000 AL=ALOG(AK)
      XL=AL*DEL
      CALL F80(XL,S0,RES2)
      CALL F81(-AL,S1,RES1)
      S=S0+S1
      IF(CABS(S).LT.1.E-30) GO TO 3000
      CALL F82(-AL,S2,RES2)
      S=S+S2
 3000 S8=S
      RETURN
      END
      COMPLEX FUNCTION F80(XP)
      COMMON /FRED/ AK,BETA,AKT,INDEX,PI
      COMMON /JUDE/ N,AL,SA(23),SB(23),DEL,NC
      COMMON /SAM/ S0,S1,S2,EN
      DATA SQRT2/ 1.414213562E0/
      AL=XP
      ADDAL=SQRT(DEL/DEN)
      S=1.
      DO 1000 I=1,NC
      AL=AL+ADDAL
      ADDAL=ADDAL+SQRT(DEL/DEN)
      S=S+1.
      IF(CABS(1./S).LT.1.E-30) GO TO 2000
 1000 CONTINUE
 2000 F80=S
      RETURN
      END
      COMPLEX FUNCTION F81(XP)
      COMMON /FRED/ AK,BETA,AKT,INDEX,PI
      COMMON /JUDE/ N,AL,SA(23),SB(23),DEL,NC
      COMMON /SAM/ S0,S1,S2,EN
      AL=XP
      ADDAL=SQRT(DEL/(AL+XP))
      S=1.
      DO 1000 I=1,NC
      AL=AL+ADDAL
      ADDAL=ADDAL+SQRT(DEL/(AL+XP))
      S=S+1.
      IF(CABS(1./S).LT.1.E-30) GO TO 2000
 1000 CONTINUE
 2000 F81=S*CEXP(-AL)
      RETURN
      END
```

THIS PAGE IS BEST QUALITY PRACTICABLE
FROM COPY FURNISHED TO DDC

```
      Y=H
      G2=G(XP)-G(-AL)
      IF(JOD  ) FB1=G1+G2
      IF(JEVEN) FB1=G1-G2
      RADICAL=SQRT(DEL/(AL+XP))
      RETURN
      END
      COMPLEX FUNCTION FB2(XP)
      REAL*8 X,A,B
      LOGICAL JOD,JEVEN
      COMMON /GUID/ H,AL,(A(23),B(23),DEL,NC
      COMMON /LOGIC/ JOD,JEVEN
      COMMON /CARTA/ X(49),Y(49)
      RADICAL=SQRT(DEL/(AL+XP))
      Y=H
      G1=G(XP)
      G2=G(XP)
      IF(JOD  ) FB2=G1+G2
      IF(JEVEN) FB2=G1-G2
      FB2=FB2*(RADICAL-AL)
      RETURN
      END
      COMPLEX FUNCTION FO(X)
      COMMON /DEBUG/ NX,NSET,AKT,INDEX(99
      IF(INDEX.GE.99) GOTO 1000
      CALL SHOI( 1,AKT*X )
      FO=CMPLX( 1.0/AKT, 0.0 )
      GOTO 1004
1000  FO=CMPLX( 0. ,2.*ZKOI(AKT*X)/PI/AKT )
1004  RETURN
      END
      COMPLEX FUNCTION GS(YP)
      COMPLEX *
      LOGICAL JOD,JEVEN
      COMMON /GUID/ H0,XO,NP,ALPHA,SINA,COSA
      COMMON /LOGIC/ JOD,JEVEN
      IF(JOD  ) GS=SIN(ALPHA*YP)*G(YP)
      IF(JEVEN) GS=COS(ALPHA*YP)*G(YP)
      RETURN
      END
      COMPLEX FUNCTION GC(YP)
      COMPLEX *
      LOGICAL JOD,JEVEN
      COMMON /GUID/ H0,XO,NP,ALPHA,SINA,COSA
      COMMON /LOGIC/ JOD,JEVEN
      IF(JOD  ) GC=COS(ALPHA*YP)*G(YP)
      IF(JEVEN) GC=SIN(ALPHA*YP)*G(YP)
      RETURN
      END
      COMPLEX FUNCTION GPS(YP)
      COMPLEX *
      LOGICAL JOD,JEVEN
      COMMON /GUID/ H0,XO,NP,ALPHA,SINA,COSA
      COMMON /LOGIC/ JOD,JEVEN
      IF(JOD  ) GPS=SIN(ALPHA*YP)*GP(YP)
      IF(JEVEN) GPS=COS(ALPHA*YP)*GP(YP)
      RETURN
      END
      COMPLEX FUNCTION GPC(YP)
      COMPLEX *
      LOGICAL JOD,JEVEN
      COMMON /GUID/ H0,XO,NP,ALPHA,SINA,COSA
      COMMON /LOGIC/ JOD,JEVEN
```

THIS PAGE IS BEST QUALITY PRACTICABLE
FROM COPY FURNISHED TO DDC

```
      IF(ODD ) GPC=SIN(ALPHA*YP)*GP(YP)
      IF(EVEN) GPC=SIN(ALPHA*YP)*GP(YP)
      RETURN
      END
      COMPLEX FUNCTION G(XP)
      COMMON /FREQ  / AK,BETA,AKT,INDEX,PI
      COMMON /DATA  / X,YP,Y
      S=SQRT((X-XP)**2+(Y-YP)**2)
      IF(INDEX.EQ.1) G=CMPLX( EJO(AKT*S),-EYO(AKT*S) )
      IF(INDEX.EQ.2) G=CMPLX( 0.    ,2./PI*EKO(AKT*S) )
      RETURN
      END
      COMPLEX FUNCTION GP(YP)
      COMMON /FREQ  / AK,BETA,AKT,INDEX,PI
      COMMON /DATA  / X,YP,Y
      S=SQRT((X-XP)**2+(Y-YP)**2)
      IF(INDEX.EQ.1) GP=CMPLX( EJ1(AKT*S),-EY1(AKT*S) )
      IF(INDEX.EQ.2) GP=CMPLX( 0.    ,2./PI*EK1(AKT*S) )
      GP=-AKT*GP/S
      RETURN
      END
```

THIS PAGE IS BEST QUALITY PRACTICABLE
FROM COPY FURNISHED TO DDC

```
      SUBROUTINE FLD(X,Y)
      COMPLEX FLD(5),AI,AIX,BI,BIX,CJ
      COMMON /CRED  / AK,BETA,AKT,INDEX,PI
      COMMON /SOURCE/ HO,XO,NP,ALPHA,SINA,COSA
      CJ=(0.,1.)
      FLD(1)=BI(X,Y)
      FLD(2)=BIX(X,Y)+AK*AK*AI(X,Y)
      FLD(3)=-CJ*BETA*BI(X,Y)
      DO 1000 I=1,3
1000  FLD(I)=-30.*FLD(I)/AK*FLD(I)
      FLD(4)=BETA/-.*AI(X,Y)
      FLD(5)=(3.,0.)
      FLD(5)=-CJ/2.*AI(X,Y)
      RETURN
      END
      COMPLEX FUNCTION AI(X,Y)
      COMPLEX ZS,RES1,RES2
      EXTERNAL ZS
      COMMON /SOURCE/ HO,XO,NP,ALPHA,SINA,COSA
      COMMON /DATA  / YY,ZS,XX
      XX=X
      YY=Y
      XP=XO
      CALL ZOO ( ZS,-HO,0.,3,RES1 )
      CALL ZOO ( ZS, 0.,HO,4,RES2 )
      AI=RES1+RES2
      RETURN
      END
      COMPLEX FUNCTION AIX(X,Y)
      COMPLEX ZS,RES1,RES2
      EXTERNAL ZS
      COMMON /SOURCE/ HO,XO,NP,ALPHA,SINA,COSA
      COMMON /DATA  / YY,ZS,XX
      XX=X
      YY=Y
      XP=XO
      CALL ZOO ( ZS,-HO,0.,3,RES1 )
      CALL ZOO ( ZS, 0.,HO,4,RES2 )
      AIX=RES1+RES2
      AIX=(Y-(2)*AIX
      RETURN
      END
      COMPLEX FUNCTION BI(X,Y)
      COMPLEX ZS,RES1,RES2
      EXTERNAL ZS
      COMMON /SOURCE/ HO,XO,NP,ALPHA,SINA,COSA
      COMMON /DATA  / YY,ZS,XX
      XX=X
      YY=Y
      XP=XO
      CALL ZOO ( ZS,-HO,0.,3,RES1 )
      CALL ZOO ( ZS, 0.,HO,4,RES2 )
      BI=RES1+RES2
      IF(IOD.EQ.1) BI=-SINA*( G(HO)+G(-HO) )
      IF(IOD.EQ.0) BI=-ALPHA*BI-COSA*( G(HO)-G(-HO) )
      RETURN
      END
      COMPLEX FUNCTION BIX(X,Y)
      COMPLEX ZS,RES1,RES2
      EXTERNAL ZOO,EVEN
      EXTERNAL ZS
      COMMON /SOURCE/ HO,XO,NP,ALPHA,SINA,COSA
```

THIS PAGE IS BEST QUALITY PRACTICABLE
FROM COPY FURNISHED TO DDC

```
      COMMON /LOGIC / EVEN
      COMMON /DATA  / YY,XP,XX
      XX=X
      YY=Y
      XP=X0
      CALL SSS ( SSS,-H0,3,3,RES1 )
      CALL SSS ( SSS, 0.,H0,3,RES2 )
      BIY=RES1+RES2
      IF(EVEN) BIY=-AL*MA*BIY-SINA*( SP(H0)-SP(-H0) )
      IF(.NOT.EVEN) BIY=-AL*MA*BIY-COSA*( SP(H0)-SP(-H0) )
      BIY=((-XP)*BIY
      RETURN
      END
      COMPLEX FUNCTION BIY(X,Y)
      COMPLEX SSS,RES1,RES2
      LOGICAL EVEN
      EXTERNAL SSS
      COMMON /SOURCE/ H0,X0,XP,ALPHA,SINA,COSA
      COMMON /LOGIC / EVEN
      COMMON /DATA  / YY,XP,XX
      XX=X
      YY=Y
      XP=X0
      CALL SSS ( SSS,-H0,3,3,RES1 )
      CALL SSS ( SSS, 0.,H0,3,RES2 )
      BIY=RES1+RES2
      IF(.NOT.EVEN) GO TO 1300
      BIY=-SINA*( (Y-H0)*GP(H0)+(Y+H0)*GP(-H0) )
     $    -AL*MA*COSA*( G(H0)-G(-H0) )+AL*MA*AL*MA*BIY
      RETURN
1300  BIY=-COSA*( (Y-H0)*GP(H0)-(Y+H0)*GP(-H0) )
     $    -AL*MA*SINA*( G(H0)+G(-H0) )+AL*MA*AL*MA*BIY
      RETURN
      END
```

THIS PAGE IS BEST QUALITY PRACTICABLE
FROM COPY FURNISHED TO DDC

```
      SUBROUTINE VF FIELD( FLD)Y,Y )
      COMPLEX FLDS(5),CJ,AX,AZ,DXAX,DYAX,DXAZ,DYAZ,DXDXAX,DXDYAX
      COMMON /BEAM  / AK,BETA,AKT,INDEX,JJ
      COMMON /GUIDE / M,AL,XA(23),XB(23),DEL,NC
      CJ=(0.,1.)
      DO 1000 N=1,5
1000  FLDS(N)=(0.,0.)
      IF(ABS(Y-M).LT.1.E-12) RETURN
      FLDS(1)=AX*AX+AX(X,Y)*DXAX(X,Y)-CJ*BETA*DXAZ(X,Y)
      FLDS(2)=DXDYAX(X,Y)-CJ*BETA*DYAZ(X,Y)
      FLDS(3)=AX*AKT*AZ(X,Y)-CJ*BETA*DXAX(X,Y)
      DO 2000 N=1,3
2000  FLDS(N)=CJ*AKT*FLDS(N)
      FLDS(4)=DYAX(X,Y)
      FLDS(5)=-CJ*BETA*AX(X,Y)-DXAZ(X,Y)
      FLDS(5)=-DYAX(X,Y)
      DO 3000 N=1,5
3000  FLDS(N)=-CJ/4.*FLDS(N)
      RETURN
      END
      COMPLEX FUNCTION AX(X,Y)
      COMPLEX CJ,VAL1,VAL2,RES1,RES2,G
      LOGICAL ODD,EVEN
      EQUIVALENCE (
      COMMON /GUIDE / M,AL,XA(23),XB(23),DEL,NC
      COMMON /ARRAY / AA(21),JJ(21)
      COMMON /LOGIC / ODD,EVEN
      COMMON /DATA  / XX,YS,YY
      XX=X
      YY=Y
      VAL1=VAL2=(0.,0.)
      DO 1000 N=1,NC
      XL=XA(N)
      XU=XL+DEL
      YS=M
      CALL GSQ ( 2,XL,XU,3,RES2 )
      YS=-M
      CALL GSQ ( 3,XL,XU,3,RES2 )
      VAL1=VAL1+AA(N)*RES1
1000  VAL2=VAL2+JJ(N)*RES2
      IF(ODD ) AX=VAL1-VAL2
      IF(EVEN) AX=VAL1+VAL2
      RETURN
      END
      COMPLEX FUNCTION DXAX(X,Y)
      COMPLEX CJ,VAL1,VAL2,RES1,RES2,G
      LOGICAL ODD,EVEN
      COMMON /GUIDE / M,AL,XA(23),XB(23),DEL,NC
      COMMON /ARRAY / AA(21),JJ(21)
      COMMON /LOGIC / ODD,EVEN
      COMMON /DATA  / XX,YS,YY
      XX=X
      YY=Y
      VAL1=VAL2=(0.,0.)
      DO 1000 N=1,NC
      XL=XA(N)
      XU=XL+DEL
      YS=M
      RES1=G(XU)-G(XL)
      YS=-M
      RES2=G(XU)-G(XL)
      VAL1=VAL1+AA(N)*RES1
1000  VAL2=VAL2+JJ(N)*RES2
```

THIS PAGE IS BEST QUALITY PRACTICABLE
FROM COPY FURNISHED TO DDC

```
      IF(ODD ) SYAX=VAL1+VAL2
      IF(EVEN) SYAX=VAL1-VAL2
      RETURN
      END
      COMPLEX FUNCTION SYAX(X,Y)
      COMPLEX JX,JZ,VAL1,VAL2,RES1,RES2,GP
      LOGICAL ODD,EVEN
      EXTERNAL GP
      COMMON /SOLIDE / N,XL,XA(23),X3(23),DEL,NC
      COMMON /ARRAY / JX(21),JZ(21)
      COMMON /LOGIC / ODD,EVEN
      COMMON /DATA / XX,YY,YY
      XX=X
      YY=Y
      VAL1=VAL2=(0.,0.)
      DO 1000 N=1,NC
      XL=XA(N)
      XU=XL+DEL
      YY=H
      CALL CGQ ( GP,XL,XU,8,RES1 )
      YY=-H
      CALL CGQ ( GP,XL,XU,8,RES2 )
      VAL1=VAL1+JX(N)*RES1
1000  VAL2=VAL2+JX(N)*RES2
      IF(ODD ) SYAX=(Y-H)*VAL1+(Y+H)*VAL2
      IF(EVEN) SYAX=(Y-H)*VAL1-(Y+H)*VAL2
      RETURN
      END
      COMPLEX FUNCTION AII(X,Y)
      COMPLEX JX,JZ,VAL1,VAL2,RES0,RES1,RES2,G,GI
      LOGICAL ODD,EVEN
      EXTERNAL G,GI
      COMMON /SOLIDE / N,XL,XA(23),X3(23),DEL,NC
      COMMON /ARRAY / JX(21),JZ(21)
      COMMON /LOGIC / ODD,EVEN
      COMMON /DATA / XX,YY,YY
      COMMON /DATAI / NC,XN
      XX=X
      YY=Y
      VAL1=VAL2=(0.,0.)
      NC=1
      XN=-AL
      XL=XN
      XU=XA(2)
1000  YY=H
      RES0=SQRT(8.)*DEL*G(XN)
      CALL CGQ(GI,XL,XU,8,RES1)
      VAL1=VAL1+JX(NC)*(RES0+RES1)
      YY=-H
      RES0=SQRT(8.)*DEL*G(XN)
      CALL CGQ(GI,XL,XU,8,RES2)
      VAL2=VAL2+JX(NC)*(RES0+RES2)
      IF(NC.NE.1) GOTO 2000
      NC=NC
      XN=AL
      XL=XA(NC)
      XU=XN
      GOTO 1000
2000  NC=NC-1
      DO 1002 N=2,NC
      XL=XA(N)
      XU=XL+DEL
      YY=H
      CALL CGQ ( G,XL,XU,8,RES1 )
```

THIS PAGE IS BEST QUALITY PRACTICABLE
FROM COPY FURNISHED TO DDC

```
      YP=-H
      CALL CGQ ( 3,XL,XU,3,RES2 )
      VAL1=VAL1+JZ(N)*RES1
3000  VAL2=VAL2+JZ(N)*RES2
      IF(ODD ) AZ=VAL1+VAL2
      IF(EVEN) AZ=VAL1-VAL2
      RETURN
      END
      COMPLEX FUNCTION CXAZ(X,Y)
      COMPLEX JX,JZ,VAL1,VAL2,RESO,RES1,RES2,S,GP,GPX
      LOGICAL ODD,EVEN
      EXTERNAL GP,GPX
      COMMON /GUIDE / H,AL,XA(23),XB(23),DEL,NC
      COMMON /ARRAY / JX(21),JZ(21)
      COMMON /LOGIC / ODD,EVEN
      COMMON /DATA  / XX,YY,ZZ
      COMMON /DATAL / NO,XN
      XX=X
      YY=Y
      VAL1=VAL2=(0.,0.)
      NO=1
      XN=-AL
      XL=XN
      XU=XA(2)
1000  YP=H
      RESO=SQRT(S.)*DEL*(X-XN)*GP(XN)
      CALL CGQ(GPX,XL,XU,3,RES1)
      VAL1=VAL1+JZ(NO)*(RESO+RES1)
      YP=-H
      RESO=SQRT(S.)*DEL*(X-(N)*GP(XN)
      CALL CGQ(GPX,XL,XU,3,RES2)
      VAL2=VAL2+JZ(NO)*(RESO+RES2)
      IF(NO.NE.1) GOTO 2000
      NO=NC
      XN=AL
      XL=XA(NC)
      XU=XN
      GOTO 1000
2000  NO=NC-1
      DO 3000 N=2,NO
      XL=XA(N)
      XU=XL+DEL
      YP=H
      RES1=G(XU)-G(XL)
      YP=-H
      RES2=G(XU)-G(XL)
      VAL1=VAL1-JZ(N)*RES1
3000  VAL2=VAL2-JZ(N)*RES2
      IF(EVEN) CXAZ=VAL1-VAL2
      RETURN
      END
      COMPLEX FUNCTION CXBZ(X,Y)
      COMPLEX JX,JZ,VAL1,VAL2,RESO,RES1,RES2,GP,GP1
      LOGICAL ODD,EVEN
      EXTERNAL GP,GP1
      COMMON /GUIDE / H,AL,XA(23),XB(23),DEL,NC
      COMMON /ARRAY / JX(21),JZ(21)
      COMMON /LOGIC / ODD,EVEN
      COMMON /DATA  / XX,YB,YY
      COMMON /DATAL / NO,XN
      XX=X
      YY=Y
      VAL1=VAL2=(0.,0.)
```

THIS PAGE IS BEST QUALITY PRACTICABLE
FROM COPY FURNISHED TO DDC

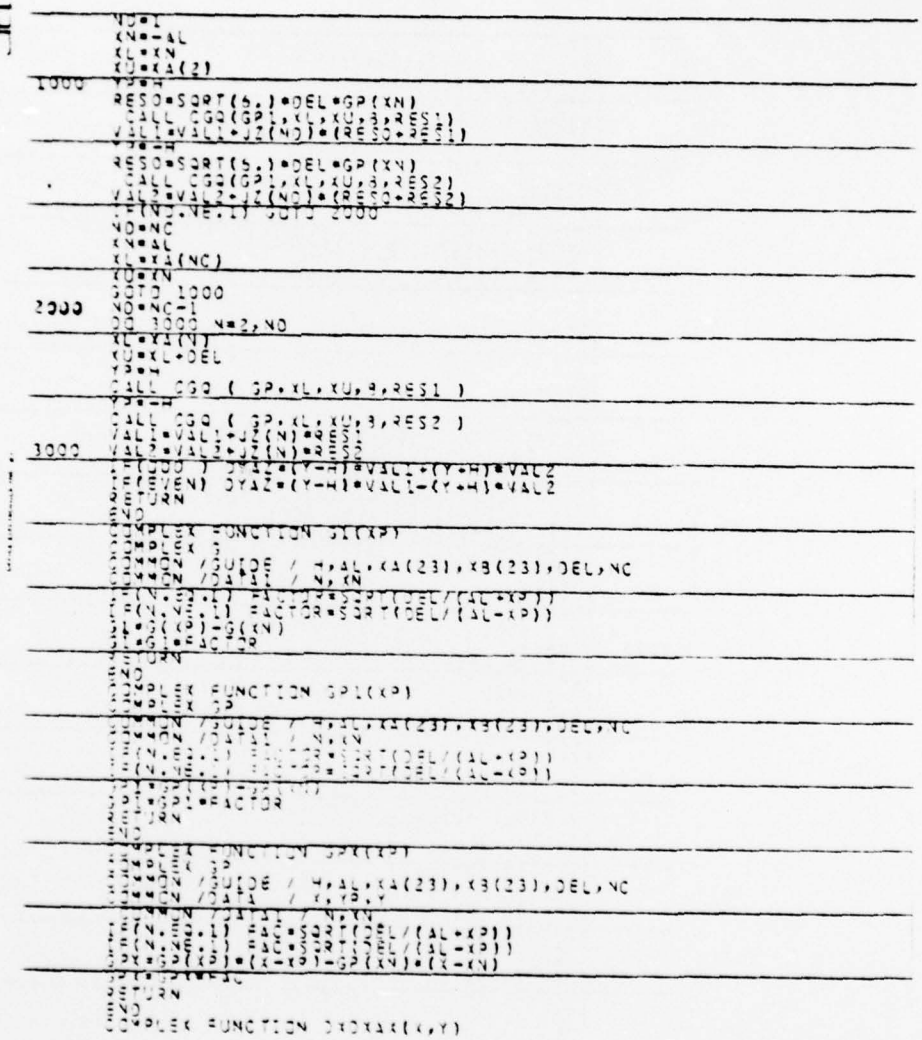

```
      NO=1
      XN=-AL
      XL=XN
      XU=XA(2)
1000  YS=+1
      RESO=SQRT(5.)*DEL*GP(XN)
      CALL CGQ(GP,XL,XU,S,RES1)
      VAL1=VAL1+WZ(NO)*(RESO+RES1)
      YS=-1
      RESO=SQRT(5.)*DEL*GP(XN)
      CALL CGQ(GP,XL,XU,S,RES2)
      VAL2=VAL2+WZ(NO)*(RESO+RES2)
      IF(NO.NE.1) GOTO 2000
      NO=NC
      XN=AL
      XL=XA(NC)
      XU=XN
      GOTO 1000
2000  NO=NC-1
      DO 3000 N=2,NO
      XL=XA(N)
      XU=XL+DEL
      YS=+1
      CALL CGQ ( GP,XL,XU,S,RES1 )
      YS=-1
      CALL CGQ ( GP,XL,XU,S,RES2 )
      VAL1=VAL1+WZ(N)*RES1
3000  VAL2=VAL2+WZ(N)*RES2
      IF(Y.GT.0.) SYAZ=(Y-H)*VAL1+(Y+H)*VAL2
      IF(Y.LT.0.) SYAZ=(Y-H)*VAL1-(Y+H)*VAL2
      RETURN
      END
      COMPLEX FUNCTION SI(XP)
      COMPLEX X
      COMMON /GUIDE / H,AL,XA(23),XB(23),DEL,NC
      COMMON /DATA1 / N,XN
      IF(N.EQ.1) SI=XP*SQRT(DEL/(AL+XP))
      IF(N.NE.1) FACTOR=SQRT(DEL/(AL-XP))
      SI=B(XP)-B(N)
      SI=SI*FACTOR
      RETURN
      END
      COMPLEX FUNCTION SPI(XP)
      COMPLEX XP
      COMMON /GUIDE / H,AL,XA(23),XB(23),DEL,NC
      COMMON /DATA1 / N,XN
      IF(N.EQ.1) FACTOR=SQRT(DEL/(AL+XP))
      IF(N.NE.1) FACTOR=SQRT(DEL/(AL-XP))
      SPI=GP(XP)-GP(XN)
      SPI=SPI*FACTOR
      RETURN
      END
      COMPLEX FUNCTION SPX(XP)
      COMPLEX XP
      COMMON /GUIDE / H,AL,XA(23),XB(23),DEL,NC
      COMMON /DATA1 / N,XN
      IF(N.EQ.1) FAC=SQRT(DEL/(AL+XP))
      IF(N.NE.1) FAC=SQRT(DEL/(AL-XP))
      SPX=GP(XP)*(X-XP)-GP(XN)*(X-XN)
      SPX=SPX*FAC
      RETURN
      END
      COMPLEX FUNCTION SYDYAZ(X,Y)
```

THIS PAGE IS BEST QUALITY PRACTICABLE
FROM COPY FURNISHED TO DDC

```
      COMPLEX VAL1,VAL2,RES1,RES2,GP,JX,JZ
      COMMON /GUIDE / H,AL,XA(23),XB(23),DEL,NC
      COMMON /ARRAY / JX(21),JZ(21)
      COMMON /LOGIC / ODD,EVEN
      COMMON /DATA / XX,YP,YY
      LOGICAL  ODD,EVEN
      XX=X
      YY=Y
      VAL1=VAL2=(0.,0.)
      DO 1000 N=1,NC
      XL=XA(N)
      XU=XL+DEL
      YP=H
      RES1=(X-XU)*GP(XU)-(X-XL)*GP(XL)
      YP=-H
      RES2=(X-XU)*GP(XU)-(X-XL)*GP(XL)
      VAL1=VAL1-JX(N)*RES1
1000  VAL2=VAL2-JX(N)*RES2
      IF(ODD) DXDYAX=VAL1+VAL2
      IF(EVEN) DXDYAX=VAL1-VAL2
      RETURN
      END
      COMPLEX FUNCTION DXDYAX(X,Y)
      COMPLEX VAL1,VAL2,RES1,RES2,GP,JX,JZ
      LOGICAL ODD,EVEN
      COMMON /GUIDE / H,AL,XA(23),XB(23),DEL,NC
      COMMON /ARRAY / JX(21),JZ(21)
      COMMON /LOGIC / ODD,EVEN
      COMMON /DATA / XX,YP,YY
      XX=X
      YY=Y
      VAL1=VAL2=(0.,0.)
      DO 1000 N=1,NC
      XL=XA(N)
      XU=XL+DEL
      YP=H
      RES1=GP(XU)-GP(XL)
      YP=-H
      RES2=GP(XU)-GP(XL)
      VAL1=VAL1-JX(N)*(Y-H)*RES1
1000  VAL2=VAL2-JX(N)*(Y+H)*RES2
      IF(ODD) DXDYAX=VAL1+VAL2
      IF(EVEN) DXDYAX=VAL1-VAL2
      RETURN
      END


FILE1  FT
FILE1  FT
FILE1  FS
```